Active Matrix Liquid Crystal Displays

Fundamentals and Applications

Willem den Boer

Newnes

BOE Ex. 1010
BOE v. Bishop Display
IPR2025-01330
Page 00001

Active Matrix Liquid Crystal Displays

Active Matrix Liquid Crystal Displays

Willem den Boer

ELSEVIER

AMSTERDAM • BOSTON • HEIDELBERG • LONDON
NEW YORK • OXFORD • PARIS • SAN DIEGO
SAN FRANCISCO • SINGAPORE • SYDNEY • TOKYO
Newnes is an imprint of Elsevier

Newnes

Newnes is an imprint of Elsevier
30 Corporate Drive, Suite 400, Burlington, MA 01803, USA
Linacre House, Jordan Hill, Oxford OX2 8DP, UK

Copyright © 2005, Elsevier Inc. All rights reserved.

No part of this publication may be reproduced, stored in a retrieval system, or transmitted in any form or by any means, electronic, mechanical, photocopying, recording, or otherwise, without the prior written permission of the publisher.

Permissions may be sought directly from Elsevier's Science & Technology Rights Department in Oxford, UK: phone: (+44) 1865 843830, fax: (+44) 1865 853333, e-mail: permissions@elsevier.co.uk. You may also complete your request on-line via the Elsevier homepage (http://elsevier.com), by selecting "Customer Support" and then "Obtaining Permissions."

∞ Recognizing the importance of preserving what has been written, Elsevier prints its books on acid-free paper whenever possible.

Library of Congress Cataloging-in-Publication Data
Application submitted.

British Library Cataloguing-in-Publication Data
A catalogue record for this book is available from the British Library.

ISBN-10: 0-7506-7813-5
ISBN-13: 978-0-7506-7813-1

For information on all Newnes publications
visit our Web site at www.books.elsevier.com

05 06 07 08 09 10 10 9 8 7 6 5 4 3 2 1

Printed in the United States of America

Working together to grow
libraries in developing countries
www.elsevier.com | www.bookaid.org | www.sabre.org
ELSEVIER BOOK AID International Sabre Foundation

Contents

Preface . . . . . *xi*

Chapter One: Introduction *1*
1.1 Historical Perspective 1
1.2 Liquid Crystal Properties 7
1.3 Polarization, Dichroism, and Birefringence 11
1.4 The Twisted Nematic Cell 14
1.5 Limitations of Passive Matrix Addressing 17
References 21

Chapter Two: Operating Principles of Active Matrix LCDs *23*
2.1 The Case for Active Matrix 23
2.2 Requirements for Active Matrix Switching Devices 24
2.3 The Thin Film Transistor 29
2.4 Thin Film Silicon Properties 32
2.5 Amorphous Silicon TFTs 34
2.6 Poly-Silicon TFTs 36
2.7 Basic Pixel Circuit and Addressing Methods 39
2.8 Diode-Based Displays 43
2.9 Plasma-Addressed LCDs 47
References 48

Chapter Three: Manufacturing of AMLCDs *49*
3.1 Basic Structure of AMLCDs 49
3.2 Thin Film Processing 50
3.3 Thin Film Properties 61
3.4 Amorphous Silicon TFT Array Processes 65
3.5 Poly-Si TFT Array Processes 69
3.6 Color Filter Array Process 73
3.7 LC Cell Assembly 74
3.8 Module Assembly 77

3.9 Yield Improvements and Considerations 79
3.10 Trends in Manufacturing 83

Chapter Four: AMLCD Electronics *87*
4.1 Drive Methods 87
4.2 Row Select and Column Data Drivers 93
4.3 Timing Controllers, Display Controllers, and Interfaces 99
4.4 Integration of Electronics on Glass 102
4.5 Backlights 105
4.6 Power Consumption 109
References 110

Chapter Five: Performance Characteristics *113*
5.1 Basics of Photometry and Colorimetry 113
5.2 Brightness and Contrast Ratio 117
5.3 Viewing Angle Behavior 121
5.4 Color and Gray Scale Performance 123
5.5 Response Time and Flicker 129
5.6 Resolution and Size 131
5.7 Image Artifacts 134
References 137

Chapter Six: Improvement of Image Quality in AMLCDs *139*
6.1 Brightness Improvements 139
6.1.1 Increased Color Filter Transmission 140
6.1.2 High-Aperture Ratio Designs 140
6.1.3 Alternative Color Filter Arrangements 144
6.1.4 Brightness Enhancement Films 145
6.2 Readability Under High Ambient Lighting Conditions 146
6.3 Color Gamut Improvements 149
6.4 Wide Viewing Angle Technologies 150
6.4.1 Compensation Films 151
6.4.2 In-Plane-Switching Mode 152
6.4.3 Vertical Alignment 157
6.4.4 A Comparison and Other Viewing Angle Improvement Methods 162
6.5 Enhancement of Video Performance 166
6.5.1 Response Time Compensation 167
6.5.2 Emulation of an Impulse-Type Display 169

6.6 Large Size 172
References 176

Chapter Seven: Special AMLCD Configurations 179
7.1 Ultra-High-Resolution Monitors and Improved Gray Scale 179
7.2 Reflective and Transflective Displays 182
7.3 Field-Sequential Color LCDs 185
7.4 Stereoscopic AMLCDs 187
7.5 Touch Screen Technologies 190
References 196

Chapter Eight: Alternative Flat Panel Display Technologies 197
8.1 Plasma Displays 199
8.2 Electroluminescent Displays 201
8.2.1 TFEL Displays 202
8.2.2 Organic LED Displays 203
8.2.3 Passive Matrix Organic LED Displays 205
8.2.4 Active Matrix Organic LED Displays 206
8.3 Electronic Paper and Flexible Displays 209
8.4 Organic Thin Film Transistors 213
8.5 Front and Rear Projection Displays 214
References 221

Chapter Nine: Active Matrix Flat Panel Image Sensors 223
9.1 Flat Panel Image Sensors 223
9.2 Direct Conversion Detectors 225
9.3 Indirect Conversion Detectors 228
9.4 Applications of Flat Panel X-Ray Sensors 233
References 234

Index 235

Preface

The meteoric rise of the active matrix LCD over less than two decades to undisputed dominance as a flat panel display has been breathtaking. The technology behind this remarkable progress will be summarized in this book. Manufacturing of AMLCDs is a more than $40 billion industry and now plays an important role in the economy of several Asian countries. This book will address the fundamentals of LCD operation and the principles of active matrix addressing. The reader will become familiar with the construction and manufacturing methods of AMLCDs, as well as with drive methods; performance characteristics; recent improvements in image quality; and applications in cellular phones, portable computers, desktop monitors, and LCD televisions.

This book is on an introductory level and intended for students, engineers, managers, educators, IP lawyers, research scientists, and technical professionals. Emphasis has been placed on explaining underlying principles in the simplest possible way without relying extensively on equations. Last, but not least, the book is intended for those inquiring minds who, for many hours every day, look at the LCD displays of notebook computers, flat panel monitors, and televisions and simply wonder how they work.

This book grew out of the course materials from seminars I presented several times at UCLA, at the gracious invitation of course organizer Larry Tannas. The course materials were further updated when the Society for Information Display kindly invited me to present Short Courses on AMLCDs at the annual SID Symposiums in 2002 and 2003.

A book like this would not have been possible without frequent interaction and discussions with colleagues in the field. Working with them has always been a great pleasure and I would like to mention specifically some of my former coworkers at OIS Optical Imaging Systems, Inc. and at Planar Systems, Inc. They include Adi Abileah, Steve Aggas, Tom Baker, Yair Baron, Bill Barrow, Mike Boyd, Young Byun, Vin Cannella, Mark Friends, Pat Green, Tieer Gu, Chris King, Terrance Larsson, Alan Lien, Darrin Lowe, Yiwei Lu, Fan Luo, Tin Nguyen, Cheng-bin Qiu, Scott Robinson, Scott Smith, Scott Thomsen, Dick Tuenge, Victor Veerasamy, Mimi Wang, Moshe Yang, Mei Yen, Zvi Yaniv, and John Zhong.

Finally, I would like to thank the Elsevier Science organization for the opportunity to write this book and for their support during its production.

Willem den Boer

IPR2025-01330 Page 00006

CHAPTER

1

Introduction

1.1 Historical Perspective

Electronic displays have, for many years, been the window to the world in television as well as the primary human interface to computers. In today's information society, they play an increasingly important and indispensable role in communication, computing, and entertainment devices.

The venerable cathode ray tube (CRT) has been around for more than 100 years and has been the workhorse for television displays and, until recently, for computer screens. As one of the few surviving electronic devices based on vacuum tubes, the CRT can boast an unrivaled success as a low-cost color display with good image quality. Its large depth, weight, and power consumption, however, have limited its use to nonportable applications.

From the early days of electronic display development, a flat panel display was considered a very attractive alternative to the bulky CRT. For decades, display engineers searched for flat panel display technologies to replace the CRT in many applications. In spite of many attempts to develop flat CRTs, plasma displays, and other low-profile displays, commercial success remained elusive for many years. Finally, by the 1990s several technologies were making significant inroads to achieve this goal. In particular, active matrix liquid crystal displays (AMLCDs) and plasma displays demonstrated large sizes and high image quality comparable to CRTs.

The success of AMLCDs, the subject of this book, is the culmination of two significant developments: liquid crystal cell technology and large-area microelectronics on glass. For more than two decades these technologies have been refined and an extensive infrastructure for manufacturing equipment and materials has been established, especially in Asia.

Liquid crystals were discovered in 1888 by the Austrian botanist Friedrich Reinitzer. He experimented with the cholesterol-type organic fluid cholesteryl benzoate and found that,

upon heating, it underwent a phase transition from a milky fluid to a mostly transparent fluid. This was later explained as a transition from an optically and electrically anisotropic fluid to an isotropic fluid. The anisotropy (i.e., the difference in dielectric constant and refractive index for different orientations of the molecules in the fluid) led to the analogy with the anisotropy of solid crystals, hence the name liquid crystal. The technological and commercial potential of liquid crystal was not realized until the 1960s, when RCA developed the first liquid crystal displays (LCDs) based on the dynamic scattering effect [1]. The twisted nematic (TN) mode of operation, on which many current LCDs are based, was first described by Schadt and Helfrich [2] in 1971 and, independently around the same time, by Fergason [3]. Twisted nematic LCDs appeared on the scene in the early 1970s in electronic wrist watches and in calculators.

LCDs quickly dominated in small portable applications due to the compatibility of the simple reflective-type LCD with low-power CMOS driving circuitry and therefore with battery operation. In addition, high-volume manufacturing led to very low cost. The market for small, direct-driven, segmented, TN LCDs in portable devices increased rapidly during the 1970s. They were initially mostly used in a reflective mode, relying on ambient light for legibility. Since each segment in a direct-driven alphanumeric display needs to be separately connected to the control electronics, the information content of this type of display is very limited, usually to one or two lines of text or numbers. Other drawbacks of the reflective mode included the difficulty of implementing color, the dependence on ambient lighting, and the parallax caused by the separation of about 0.5–1 mm between the back reflector and the LC layer.

The mass market for electronic wrist watches, calculators, and other applications, however, allowed investments in manufacturing and further development.

For displays with higher information content, the large number of picture elements (pixels) precluded the individual addressing of every pixel. This led to the development of matrix addressing in which an array of $M \times N$ pixels is addressed by applying pulses to each of its M rows and N columns. It reduces the number of interconnects to the external addressing circuitry from $M \times N$ to $M + N$. For example, a 100×100-pixel display now required $100 + 100 = 200$ interconnections instead of $100 \times 100 = 10{,}000$. Such passive matrix displays are usually operated with a one-line-at-a-time addressing method called multiplexing. The TN LCD was limited to only about 10 rows of pixels because of its gradual transmission-voltage curve. Many improvements in passive matrix addressing have been proposed and implemented over the last fifteen years, notably the super-twisted nematic (STN) LCD. However, their performance in terms of viewing angle, response time, gray scale, and contrast ratio has generally fallen short of what was possible with a single direct-driven pixel.

Early during the development of LCD technology, the limitations of direct multiplexing or passive matrix addressing were recognized. A solution was proposed by Lechner et al. [4] and by Marlowe and Nester [5]. By incorporating a switch at each pixel in a matrix display, the voltage across each pixel could be controlled independently. The same high-contrast ratio of more than 200, obtained in simple, direct-driven backlit displays, could then also be achieved in high-information-content displays.

Peter Brody and coworkers [6] constructed the first so-called active matrix LCDs (AMLCDs) with CdSe thin film transistors (TFTs) as the switching elements. The TFTs in the array act merely as ON/OFF switches and do not have an amplifying function. For an electronic engineer, the term "active matrix" may therefore be inappropriate. It is now, however, commonly used and its definition has been extended to include arrays of switching elements other than TFTs, such as diodes.

The CdSe TFTs used for the first AMLCDs turned out to be a temporary solution. Semiconductors such as CdSe are not compatible with standard processing in the microelectronic industry, which uses mainly silicon as the semiconductor material. Advanced photolithographic and etching processes have been developed over the years for silicon devices and this technology is not readily applicable to CdSe TFTs. Dr. Brody has, nonetheless, remained a strong and vocal proponent of CdSe-based AMLCDs over the years, even in the face of the overwhelming success of silicon thin film-based TFT LCDs.

Polycrystalline Si materials and devices are more familiar to semiconductor process engineers and were developed for use in AMLCDs in the early 1980s. The first LC pocket television marketed by Seiko Epson in 1983 used a poly-Si TFT active matrix [7] and was the very first commercial application of AMLCDs. The early poly-Si TFTs required high-temperature processing and therefore used expensive quartz substrates.

A color LCD was obtained by subdividing the pixel into three subpixels with red, green, and blue color filters. Since the color filters absorb a large portion of the light, these color LCDs required a backlight to operate in a transmissive rather than a reflective mode to be useful in most ambient lighting conditions.

In parallel to the early development of LC cell technology and CdSe TFTs, thin film amorphous silicon (a-Si) was investigated in the 1970s. The rationale behind this interest was initially not its potential use for LCDs, but rather its promise for low-cost solar cells. A major development occurred at the University of Dundee in Scotland in 1979, when LeComber et al [8] developed the first TFT with a-Si as the semiconductor material and suggested the active matrix LCD as one of its applications. Interestingly, a patent on the basic a-Si TFT was never filed, since this work was performed at an

academic institution. The University of Dundee had been a pioneer in the development and understanding of amorphous silicon materials under the leadership of Professor W.E. Spear and Dr. P.G. LeComber. Unfortunately, Dr. LeComber witnessed only the start of the tremendous growth in AMLCDs based on a-Si TFTs; he died at the age of 51 of a fatal heart attack while vacationing in Switzerland in 1992.

Amorphous silicon can be deposited on low-cost, large-area glass substrates at a temperature below 300°C. It was more attractive than the early polycrystalline technology for active matrix LCDs, which needed much higher process temperatures and more process steps. A pocket television with a-Si TFTs was put on the market by Matsushita in 1984 [9].

Soon after the first TFT LCD with amorphous silicon TFTs was introduced, the a-Si TFT overshadowed poly-Si TFTs as the semiconductor device of choice for AMLCDs. The first TFT LCDs had a diagonal size of 2–3 in. and were mainly used in small portable televisions. The performance of the color AMLCD was initially improved for high-end applications such as aircraft cockpit displays. In avionics, cost was a secondary concern and emphasis was placed on the highest possible performance in terms of legibility under any lighting conditions.

While a market was established, volume production capability was gradually increased at several Japanese companies. This was accompanied by a scale-up in glass substrate size from wafer-like sizes to around 300×400 mm. A significant breakthrough occurred in the late 1980s, when the first laptop computers with 10-in. diagonal size TFT LCDs were marketed by several companies, including IBM, NEC, Sharp, Toshiba, and Hitachi. This scale-up was made possible by the gradual increase in manufacturing yields by process improvement methods borrowed from the semiconductor industry. Laptop and notebook computers turned out to be the killer application for active matrix liquid crystal displays. They addressed the need of traveling businessmen for lightweight computers with high image quality, and thin and low-power flat panel displays.

By 1996 the manufacturing substrate size had grown to 550×650 mm and many improvements in processing and materials were implemented. In the mid-1990s Korean companies started mass production of AMLCD modules, followed a few years later by massive investments by several companies in Taiwan.

The late 1990s also witnessed a revival of poly-Si TFT LCDs for small displays. Several companies succeeded in producing low-temperature poly-Si TFTs processed at temperatures below 600°C, compatible with lower-cost glass. The main attraction of poly-Si TFTs is their higher current-carrying capability, allowing the integration of some of the drive electronics on the glass.

Application of a-Si TFT LCDs in notebook computers facilitated large investments in their manufacturing infrastructure. This, in turn, made possible the introduction of space- and power-saving, flat-panel desktop monitors based on AMLCD panels with improved viewing angles.

Several methods to improve the viewing angle, including compensation films and different LC modes (in-plane-switching and multi-domain vertical alignment) were introduced after 1995 and implemented in 17-in. and larger monitors. In 2003 TFT LCDs surpassed CRTs in terms of revenue for computer monitors.

Recent further improvements in brightness, color performance, viewing angle, and response time have led to the development of LCD television with superior image quality and progressively larger screens, now well beyond 40 in. in diagonal size. LCD television is the final frontier for the AMLCD and a number of companies have started production on glass substrates with 1–4 m^2 size to participate in this rapidly growing market.

Another application where AMLCDs have attained a large market share is handheld devices (i.e., in PDAs, digital cameras, camcorders, and mobile phones). With the introduction of 3G cellular phone service and built-in cameras, the demand for high-contrast, video-rate color displays have allowed the AMLCD to replace many of the poorer-performing passive matrix LCDs.

Parallel to the development of direct-view displays, microdisplays for projection have been developed since the late 1970s. It was realized early on that the LCD is a light valve that can act as an electronically controlled slide in a slide projector. Business-grade front projectors appeared on the scene in the early 1990s with three high-resolution poly-Si TFT LCDs. They are now commonplace in many meeting rooms and classrooms across the world and can weigh less than 3 lbs. Rear-projection, high-definition television based on reflective microdisplays (liquid crystal on silicon [LCOS]) have entered the marketplace as well.

Microdisplays are also used in personal viewers such as viewfinders for digital cameras and camcorders.

The success of AMLCD technology is the result of many years of close cooperation among scientists and engineers from different disciplines. They include organic chemists, physicists, optical, electrical, electronic, mechanical, packaging, and manufacturing engineers, all supported by increasing revenues from sales of LCDs.

Figure 1.1 illustrates the exponential increase in the total market for AMLCDs. The development shows a remarkable parallel with the semiconductor industry in the 1980s and 1990s, also indicated in the plot. Some fluctuations in the LCD revenue curve can

be attributed to supply-demand cycles. Based on an extrapolation of this plot, the AMLCD industry will achieve $100 billion in annual revenues around the year 2010.

The market for AMLCDs is usually subdivided into small displays with a diagonal size of less than 10 in. (in PDAs, cell phones, digital cameras, camcorders, etc.), medium displays of 10–20 in. (in notebook computers and desktop monitors), and large displays exceeding 20 in. (mostly in televisions). Figure 1.2 shows the recent rapid unit growth in all applications. Although the small displays have the largest unit sales, the larger displays obviously represent a large part of the total revenues.

AMLCDs are also increasingly used in medical, industrial, and retail applications, often with a touch panel included.

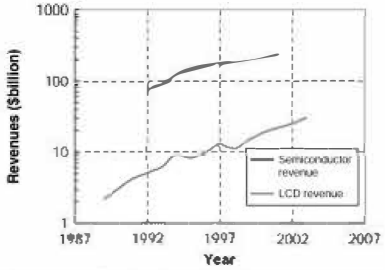

Figure 1.1: Growth of the semiconductor IC and LCD market.

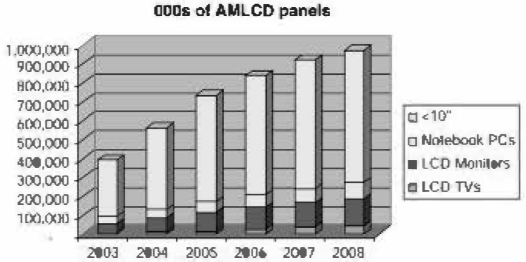

Figure 1.2: Market forecast for TFT LCDs (courtesy of Displaysearch).

The AMLCD manufacturers are supported by a large infrastructure of equipment and material suppliers, which continue to improve efficiency and reduce cost. They include color filter, polarizer, and optical film manufacturers, driver IC and controller IC vendors, packaging firms, backlight manufacturers, and suppliers of materials such as LC fluids and alignment layers.

The momentum the LCD industry has gained is difficult to supplant by alternative flat panel display technologies, even if, on paper, they may have advantages over LCDs.

1.2 Liquid Crystal Properties

After their discovery by Reinitzer in 1888, liquid crystals were, for many decades, considered interesting only from an academic point of view. Liquid crystals are an intermediate phase between crystalline solids and isotropic liquids, and combine certain characteristic properties of the crystal structure with those of a deformable fluid. Display devices utilize both their fluidity and the anisotropy associated with their crystalline character. The anisotropy causes the dielectric constant and refractive index of the LC fluid to depend on the orientation of its molecules.

Nematic liquid crystals are commercially the most interesting type. Upon heating, most crystalline solids undergo a phase transition to an isotropic liquid. The nematic intermediate phase (mesophase) occurs in certain, mostly organic, substances in a temperature range between the solid and isotropic liquid state. Figure 1.3 shows an example of the molecular structure of a liquid crystal, p-methoxybenzylidene-p-n-butylaniline (MBBA), with its nematic temperature range.

The liquid crystal (LC) molecules are generally elongated in shape and have a length of around 2 nm. Because of their "cigar" shape they tend to line up more or less parallel to each other in the lowest energy state. The average orientation axis along the molecules is a unit vector **n**, called the director. Nematic LC molecules are not polar, so there is no differentiation between **n** and **−n**. The dielectric constant and refractive index of the LC is different along the director and perpendicular to the director, as shown in Fig. 1.4, giving rise to dielectric and optical anisotropy, respectively. The dielectric anisotropy

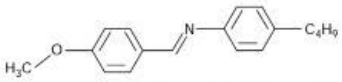

Figure 1.3: Example of molecular structure of LC – MBBA, with a nematic range of 21–48°C.

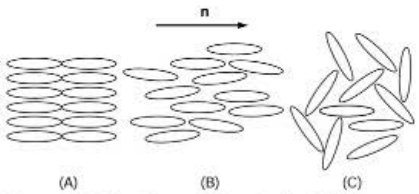

Figure 1.4: Orientation of LC molecules in (A) smectic, (B) nematic, and (C) isotropic phase.

makes it possible to change the orientation of the LC molecules in an electric field, crucial for application in electro-optical devices. The optical anisotropy leads to birefringence effects (described later in this chapter) and is essential for the modulation of polarized light in display operation.

In bulk, liquid crystal tends to form microdroplets. Within the droplets there is one director orientation, but the director can be different for adjacent droplets. Although most high-purity liquid crystals are transparent, this explains the milky appearance of bulk LC, as scattering of light occurs at the boundaries of the microdroplets.

When nematic LC is heated beyond a certain temperature, a phase transition occurs to an isotropic liquid. The nematic-isotropic transition temperature is often referred to as the clearing point or clearing temperature because of the drastic reduction in light scattering that occurs when the fluid no longer consists of microdroplets with different directors. Just below the clearing point, the optical and dielectric anisotropy of the LC fluid starts to decline, until at the clearing point there is a single dielectric constant and refractive index in the isotropic state. Above the clearing point, the LC fluid no longer has the desirable optical and dielectric anisotropy, and display operation fails.

When the temperature is lowered, the LC fluid undergoes another phase transition from the nematic to the smectic phase. In the smectic phase, the LC molecules form a layered structure and obtain a higher viscosity to become more grease-like. When approaching the smectic phase, the LC response to an electric field change becomes very sluggish, and below the transition temperature the display operation fails.

A large variety of nematic liquid crystals has been synthesized over the years, each with its own molecular formula and nematic temperature range. For MBBA in the example of Fig. 1.3, the nematic range is 21–48°C. This range is too limited for practical applications. Commercial fluids generally consist of a mixture of two or more liquid crystal components and have a much wider nematic range.

Another LC type is the cholesteric (chiral nematic) phase in which the molecular interaction causes a helical twist of the director orientation **n**, as illustrated in Fig. 1.5. The pitch (p) of the cholesteric phase is defined as the distance over which the director twists 360 degrees. In display devices based on the twisted nematic effect, small concentrations of cholesteric material are usually added to produce a preferred twist sense in the cell and avoid display artifacts.

Nematic liquid crystal is a viscous fluid with a viscosity at room temperature about ten times higher than that of water. The viscosity plays an important role in the response time of LC fluids to electric fields, and a low viscosity is required for displays operating at video rates.

The lowest energy state for bulk nematic liquid crystal occurs when there is a single director throughout the fluid (i.e., when all molecules have the same orientation). The bulk elastic properties associated with the curvature of the director **n** can be described by three elastic constants. These constants K_{11}, K_{22}, and K_{33} quantify the restoring torque opposing splay, twist, and bend deformation of the director orientation, respectively (Fig. 1.6).

The constants K_{11}, K_{22}, and K_{33} are of the order of 10^{-11} N and orders of magnitude smaller than the elastic constants in a solid-state material. This allows the LC fluid to readily deform when subjected to an electric field, which is essential for display operation. With increasing temperature, K_{11}, K_{22}, and K_{33} decrease as elasticity weakens.

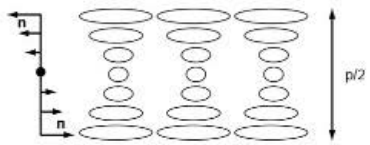

Figure 1.5: Cholesteric or chiral nematic phase.

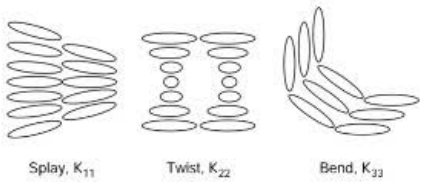

Figure 1.6: Elastic deformations in LC fluid and their associated elastic constants.

In Table 1.1 selected properties of a typical nematic liquid crystal fluid are shown. $V_{th,10}$ is the voltage at which 10% of transmittance change is obtained in display operation.

Table 1.1: Selected properties of a typical nematic liquid crystal mixture for display applications

Parameter	Symbol	Typical Value	Comments
Clearing point	T_{Clp}	80°C	Max. operating temperature
Smectic-Nematic transition	$T_{S\text{-}N}$	–40°C	Min. operating temperature
Optical anisotropy	$\Delta n = n_{\parallel} - n_{\perp}$	0.085=1.562–1.477	Determines optical behavior
Dielectric anisotropy	$\Delta\varepsilon = \varepsilon_{\parallel} - \varepsilon_{\perp}$	7=10.5–3.5	Determines behavior in electric field
Threshold voltage TN cell	$V_{th\ 10}$	1.6 V	Voltage at 10% transmission in NB mode
Elastic constants	K_{11}, K_{22}, K_{33}	10^{-11} Newton	Important for response time
Rotational viscosity at 20°C	γ_1	100 mPa-s	Important for response time

For display applications LC is sandwiched in a thin layer of 2–10 μm between two substrates, usually glass, which have conducting electrodes on their inner surfaces. Near the substrate surface the LC molecules can exhibit alignment phenomena, which can be strengthened by depositing certain organic or inorganic films on the surface and treating the surface of the film to obtain a preferred orientation of the molecules. These so-called orienting layers or alignment layers force the director to assume a single orientation at and near the entire surface. The degree of anchoring to the surface is called the anchoring strength and depends on the orienting layer, its surface treatment, and the liquid crystal.

Examples of surface alignment are shown in Fig. 1.7. Orientation perpendicular to the surface is called homeotropic alignment and anchoring of the director parallel to the surface is called homogeneous alignment. Both types of alignment are used in practical displays.

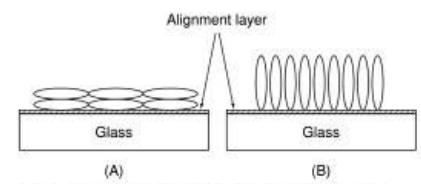

Figure 1.7: Homogeneous (A) and homeotropic (B) surface alignment.

Another important property of LC fluid, in particular for active matrix displays, is its resistivity. The LC pixel acts like a capacitance that stores the data voltage loaded once every frame time. If the pixel capacitance is leaky as a result of low resistivity of the LC fluid, the data voltage will decay during the frame time. It is then not possible to obtain a uniform, consistent, gray scale. A resistivity of 10^{11} Ωcm or higher is typically required for active matrix LCDs. The LC material therefore needs to be very pure and not contain moisture and ionic contamination, which can reduce its resistivity.

1.3 Polarization, Dichroism, and Birefringence

Most LCDs rely on the manipulation of polarized light to generate an image based on data from an electronic signal source. Before discussing LC modes of operation, it is therefore useful to address the basics of polarized light and of the optical anisotropy or birefringence allowing this manipulation.

Natural light consists of transverse electromagnetic waves which vibrate in arbitrary planes and can be described as the sum of two orthogonal waves. A polarizer (P) transmits only one of the two composing waves in one plane of vibration to obtain linearly polarized light (see Fig. 1.8). The intensity (or luminance) of the transmitted light is not more than 50% of that of the natural incident light. When a second polarizer (A, the analyzer) is placed behind P such that its plane of vibration is at an angle ϕ with that of P, the amplitude E_t of the wave transmitted through A is

$$E_t = E_i \cos\phi, \tag{1.1}$$

where E_i is the amplitude of the incident wave on A.

Since the light intensity is proportional to the square of the amplitude, the transmitted light intensity is

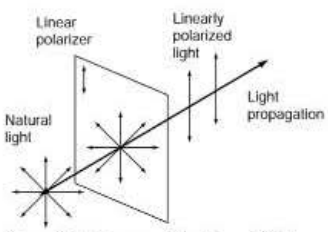

Figure 1.8: Linear polarization of light.

$$T = T_0 \cos^2\phi, \tag{1.2}$$

where T_0 is the intensity of transmitted light through the first polarizer.

For crossed ideal polarizers, $\phi = 90°$ and transmission is zero. For parallel ideal polarizers, $\phi = 0°$ and transmission is 50%.

Practical polarizers do not follow Eqs. 1.1 and 1.2 exactly. Polarizers used in LCDs usually consist of stretched polymer films, such as polyvinylacetate (PVA), doped with iodine or other specific additives. The stretching process makes the polymer optically anisotropic. The iodine doping causes strong absorption of incident light along the optical axis, so that only one linearly polarized component of the incident light is transmitted.

The optical absorption along the optical axis is referred to as dichroism.

Polarizers are characterized by their transmittance and degree of polarization (also called polarization or polarizing efficiency).

The polarization efficiency *Eff* is defined as

$$Eff = \sqrt{\frac{T_1 - T_2}{T_1 + T_2}}, \tag{1.3}$$

where T_1 is the transmission of two parallel polarizers and T_2 the transmission of two crossed polarizers.

For LCDs using two polarizers, one outside each of its glass substrates, the maximum contrast ratio CR_{max} is limited by the polarization efficiency of the polarizers:

$$CR_{max} = \frac{T_1}{T_2}. \tag{1.4}$$

The transmittance of practical single polarizers used in LCDs is typically 40–45%, so that T_1 = 32–40.5%, and polarizing efficiencies are 99.0–99.9%.

Other types of polarization are circularly and elliptically polarized light. Circularly polarized light can be thought of as a combination of two linearly polarized light waves with equal amplitudes but with a phase difference of $\pi/2$ (90 degrees). In elliptically polarized light, the amplitudes can be different as well.

All liquid crystal displays utilize the optical anisotropy $\Delta n = n_{\parallel} - n_{\perp}$ of the liquid crystal fluid, where $n_{\parallel}$ is the refractive index parallel to the director and $n_{\perp}$ is the refractive index perpendicular to the director. The optical anisotropy causes the polarization

components of light to propagate differently, giving rise to birefringence, or double refraction. Birefringence is the key physics phenomenon on which LCD operation is based. The ease with which the director orientation, and therefore the birefringence effects, can be modified in an electric field is responsible for the low-voltage and low-power operation of LCDs.

When natural light enters a slice of LC fluid with uniformly aligned directors (see Fig. 1.9), the light will emerge unchanged only if its propagation direction coincides with the director orientation. When the light is incident under an angle ψ with the director, it can be dissected into two composing linearly polarized waves with different propagation velocities. The first one is called the ordinary wave and it oscillates perpendicular to the plane formed by the director and the propagation direction. The ordinary wave propagates independent of ψ with velocity c/n_0, where c is the speed of light in vacuum and n_0 is the refractive index for the ordinary wave. In the LC fluid, $n_0 = n_\perp$. The other component is called the extraordinary wave and it oscillates in the plane formed by the director and the propagation direction. Its refractive index n_e varies between $n_{||}$ and $n_\perp$, depending on the angle ψ between the director and the propagation direction. Its velocity is c/n_e. For $\psi = 0°$ and 90°, the refractive index n_e is equal to $n_\perp$ and $n_{||}$, respectively.

The two components will propagate differently and will emerge from the LC slice with a phase change Φ with respect to each other:

$$\Phi = \frac{2\pi(n_e - n_o)d}{\lambda}, \tag{1.5}$$

where d is the thickness of the LC slice and λ is the wavelength of the light.

Since the incident natural light has a random distribution of polarization directions, the exiting light will also be randomly polarized. However, when the light entering the LC layer is polarized perpendicularly to the plane of Fig. 1.9, only the ordinary wave is propagated and the LC cell is said to be operating in the o-mode. When the

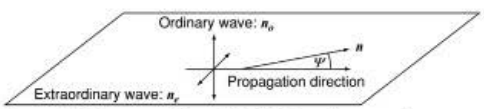

Figure 1.9: Decomposition of light into ordinary and extraordinary components, which causes birefringence in optically anisotropic media.

light entering the LC layer is polarized parallel to the plane of Fig. 1.9, only the extra-ordinary wave is propagated and the LC cell is said to be operating in the e-mode.

As an example of how the polarization of light is changed by the LC layer, consider linearly polarized light with wavelength λ perpendicularly entering an LC layer with uniform, homogeneous alignment ($\psi = 90°$) and thickness $d = 1/4\ \lambda/\Delta n$. In this case $n_e = n_{||}$ and the LC slice acts, for all practical purposes, as a quarter-wavelength plate: when the polarization angle is at 45 degrees with the plane of Fig. 1.9, it converts linearly polarized light into circularly polarized light, because one of the two composing waves is retarded by $\Phi = 90°$ (see Eq. 1.5). However, when the orientation of the LC fluid could be changed to homeotropic ($\psi = 0°$) by applying an electric field, the emerging light would remain unchanged and linearly polarized. This example shows the general principle of modifying the orientation of the LC optical axis (the director) by electric fields in order to manipulate the polarization of light. Practical LCDs utilize variations on this basic concept.

1.4 The Twisted Nematic Cell

LCDs are nonemissive (i.e., they need some external lighting source to generate an image). This can be ambient lighting in the case of the reflective display in a calculator, or a backlight in the case of a transmissive display in a notebook computer. The electro-optical behavior of the liquid crystal layer modulates the light from the external light source to form an image or pattern corresponding to the electronic data signal information supplied to the display pixels.

The twisted nematic (TN) mode of operation, which forms the basis of many practical LCDs, was first described by Schadt and Helfrich [2] and Fergason [3] in 1971.

The TN cell basically consists of two glass plates with transparent conductive electrodes patterned on their inner surfaces. A thin LC layer with thickness d = 4–10 µm is sandwiched between the conductive electrodes, as shown in Fig. 1.10. Light enters the LC cell after first passing through a linear polarizer attached to the outside of the display glass. The cell shown in the figure operates in the e-mode, since the polarization direction and the director orientation coincide.

At the surface of the conductive electrodes, alignment layers ensure the proper orientation of the LC molecules so as to obtain a 90-degree twist. In the relaxed state, without applied field, the 90-degree twist of the LC director results in a 90-degree rotation of the polarization direction in the LC cell, in a waveguiding fashion. It can be shown [10] that the light emerges from the cell almost perfectly linearly polarized if the condition $\Delta n.d >> 0.5\ \lambda$ is satisfied, where λ is the wavelength of the light.

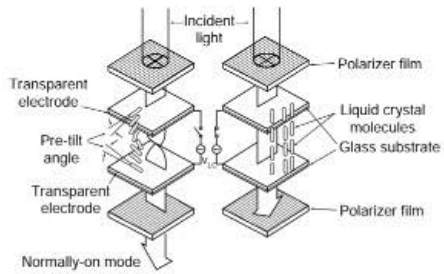

Figure 1.10: Operation of twisted nematic (TN) LC cell.

The second linear polarizer outside the second glass substrate is oriented perpendicular to the first one and will therefore transmit the light. This is called the normally white or normally on mode, since light is transmitted when no voltage is applied to the cell.

The TN effect uses LC fluids with a positive dielectric anisotropy. As a result, the lowest energy state in an electric field occurs when the director is parallel to the electric field direction. When a voltage larger than V_T is applied across the LC, the LC molecules will start deviating from their quiescent state in response to the electric field and the director will tend to line up along the field direction perpendicular to the glass surfaces. This happens initially in the center of the cell farthest away from the transparent electrodes. At the glass surfaces the LC molecules remain parallel to the electrodes. The angle of the director along the z direction is called the director profile. With increasing voltage, more molecules will align parallel to the field. At sufficiently high voltage, the twist is removed and the LC will no longer rotate the polarization direction, so that the exit polarizer now blocks the light. The threshold voltage V_T is defined as the voltage at which the LC molecules start tilting and is different from $V_{th,10}$ in Table 1.1. V_T can be approximated by

$$V_T = \pi \sqrt{\frac{K_{11}}{\varepsilon_0 \Delta\varepsilon}}. \tag{1.6}$$

It is important to note that in the TN cell, V_T and the entire transmission-voltage curve is, in this first approximation, independent of the cell gap d. In manufacturing, this allows some variation in the cell gap, controlled by spacers, without affecting the gray scale behavior. Such tolerances aid in achieving a high manufacturing yield. The physical reason behind the independence of cell gap can be intuitively grasped: with an

increase in cell gap, the electric field causing the LC molecules to line up perpendicular to the glass surfaces is reduced. On the other hand, the influence of the anchoring force to keep the LC director parallel to the glass surfaces is reduced as well. These two forces cancel each other out, as can be mathematically proven, so that the LC director profile is independent of cell gap at a fixed voltage, even though the electric field varies.

When the second polarizer is parallel to the first one, light is blocked in the relaxed (zero voltage) state and transmitted with 4 V applied (the normally black mode). At intermediate voltage levels, a continuous gray scale can be achieved. In Fig. 1.11 the transmission-voltage curves of the TN cell are shown for the normally white and normally black mode.

The LC cell is operated with an AC square wave voltage without a DC component in order to prevent electrochemical degradation of the LC cell structure. DC components in excess of about 50 mV can cause charging of the alignment layer by residual ions in the LC fluid, leading to image retention and other problems in displays. When a periodic waveform $V(t)$ with sufficient frequency is applied to the cell, the transmission curve depends on the root-mean-square voltage V_{rms} of the waveform

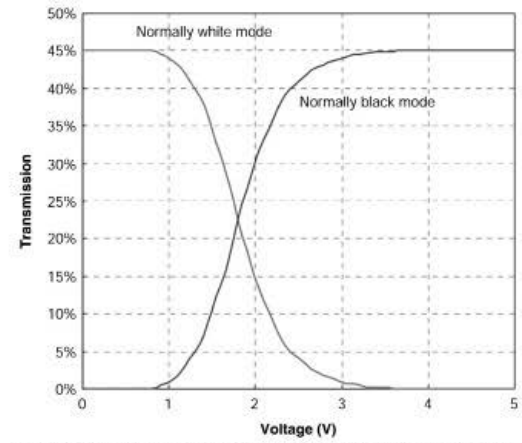

Figure 1.11: Transmittance-voltage curve for TN cell in normally white and normally black mode.

$$V_{rms} = \sqrt{\frac{1}{T_{wf}} \int_0^{Twf} V^2(t)\,dt}, \tag{1.7}$$

where T_{wf} is the period of the waveform, in displays twice the frame period. In the case of a pure AC square wave voltage with amplitude +/– V_{amp},

$$V_{rms} = V_{amp}. \tag{1.8}$$

Since the LC molecules are not polar, their orientation does not change when the polarity of the voltage is reversed. In other words, changing rapidly from positive applied voltage to negative applied voltage of the same magnitude at a normal display refresh rate of, for example, 60 Hz has no effect on the director profile. When there are short transient voltages of less than 1 msec applied to the LC layer, the LC response time is usually too slow to react. They normally do not affect the transmission, as long as the RMS voltage does not change significantly.

The TN mode of operation was offered as an example to show how an electric field can change the orientation of the LC molecules and, therefore, the polarization direction and transmission in the cell. There are numerous other LC modes of operation, some of which lead to displays with better viewing angle characteristics. They include the in-plane-switching and vertical-alignment modes, to be described in Chapter 6.

1.5 Limitations of Passive Matrix Addressing

In small LCDs with limited alphanumerical information, such as calculator and electronic watch displays, the transparent ITO electrodes are patterned into segments, as shown in Fig. 1.12. Each segment is individually addressed by the electronics. This approach is practical only for low information content displays.

To obtain LCDs with more picture elements (or pixels), a matrix approach is used. In passive matrix LCDs, the conductive transparent electrodes are patterned as stripes perpendicular to each other on the two opposing substrates (Fig. 1.13). This allows a dot matrix with M rows and N columns (i.e., M×N pixels), to be addressed by M+N external connections. The price to pay for this approach is that the voltage across each pixel is no longer independently controlled. At any time, only one row of pixels is selected and receives data from the column drivers. The data information supplied to the other rows of pixels can, however, modify the average voltage on the pixel.

Dot matrix displays with a one-line-at-a-time driving method, called multiplexing, were developed in the early 1980s. As the number of lines increased, the contrast ratio suffered as a result of the gradual transmission-voltage curve of the 90-degree TN cell. Alt and

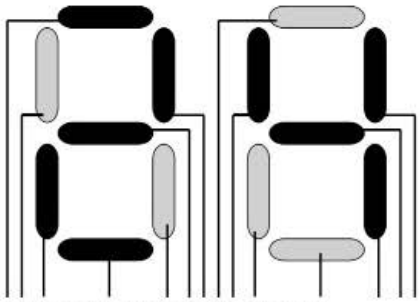

Figure 1.12: Segmented addressing in an alphanumeric display with two digits and seven segments per digit.

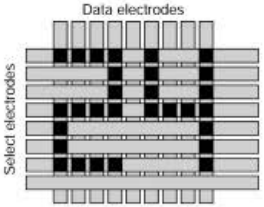

Figure 1.13: Passive matrix addressing.

Pleshko [11] formulated the limits of multiplexing in RMS responding displays. They calculated the optimum voltage ratio between the ON and OFF state as a function of the number of multiplexed lines *N*:

$$\frac{V_{on}}{V_{off}} = \left(\frac{\sqrt{N}+1}{\sqrt{N}-1}\right)^{1/2}. \tag{1.9}$$

In Fig. 1.14 the Alt–Pleshko equation is graphically represented. In a one-line-at-a-time multiplexing scheme, the voltage margin between the ON and OFF state decreases as the number of rows increases. It results in a reduced contrast ratio unless an LC mode with a

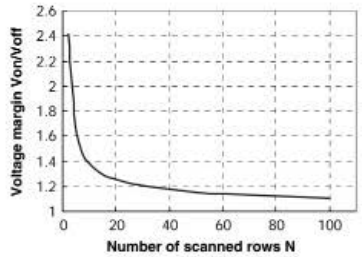

Figure 1.14: Graphical presentation of the Alt-Pleshko equation showing the reduction in contrast ratio with an increase in number of select lines.

very steep transmission-voltage curve is employed. This prompted the development of the super-twisted nematic (STN) cell, which has approximately 270 degrees of twist of the LC layer. It has a much steeper curve, so that a larger contrast ratio T_{on}/T_{off} can be obtained, even when V_{on}/V_{off} is reduced (see Fig. 1.15).

In the late 1980s, STN LCDs were developed. Contrast ratios exceeding 50 have been achieved in 200- to 600-line STN displays. In the higher-resolution displays, such as SVGA types with 600×800 pixels, STN displays are used in a dual scan mode. By dividing the screen in two halves with each half having its own set of data drivers, only 300 lines need to be multiplexed in dual scan STN displays. Multi-line addressing schemes, in which more than one line is selected at a time in STN LCDs, have also been developed; they further improve the contrast ratio and maximum number of addressable rows in passive matrix displays.

Although dual scan STN displays have been applied in early notebook computers, their response time and contrast ratio are relatively poor in comparison with CRTs and active matrix LCDs, precluding high image quality. They are no longer used in laptop displays. The best solution to obtain a high quality, high information content LCD is to add a switch at each pixel and control voltage independently at each pixel to obtain the intended gray level. This emulates a direct-driven pixel and is called active matrix addressing, the subject of the remainder of this book.

The three methods to address LCDs (direct, passive matrix, and active matrix) are listed in Table 1.2 with examples of applications. For all displays with higher information content, a matrix addressing scheme is required to limit the number of interconnects.

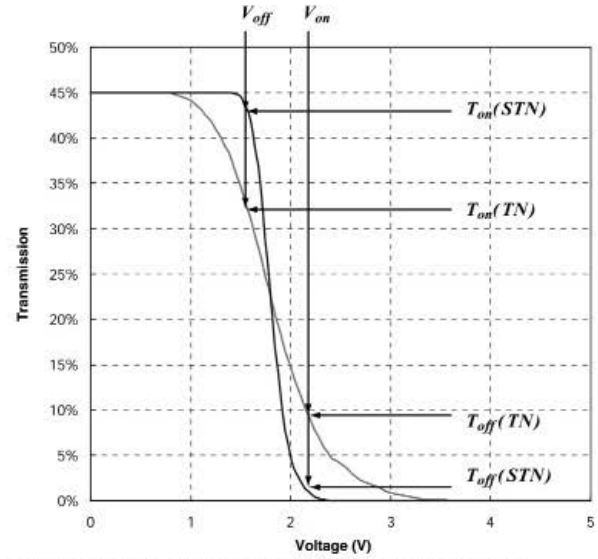

Figure 1.15: Transmittance voltage curve of a TN cell showing the reduction in contrast ratio T_{on}/T_{off} for reduced voltage margin V_{on}/V_{off}. For the STN curve, contrast is much better.

Table 1.2: Addressing methods for LCDs

LCD Type	Addressing Method	Number of Interconnects	Examples
Segmented	Direct drive	One per segment	Watch, calculator
Passive matrix	Multiplexing one row at a time	M + N for M × N matrix	PDAs, cell phones, early notebooks
Active matrix	Switch at each pixel—one row at a time	M + N for M × N matrix	Notebooks, flat panel monitors, LCD TV

References

1. G.H. Heilmeier, L.A. Zanoni, and L.A. Barton, "Dynamic Scattering: A New Electro-Optic Effect in Certain Classes of Nematic Liquid Crystals," *Proc. IEEE*, 56, pp. 1162–1170 (1968).
2. M. Schadt and W. Helfrich, "Voltage-Dependent Optical Activity of a Twisted Nematic Liquid Crystal," *Appl. Phys. Lett.*, 18, pp. 127–128 (1971).
3. J. Fergason, "Display Devices Utilizing Liquid Crystal Light Modulation," U.S. Patent No. 3,731,986.
4. B.J. Lechner, F.J Marlowe, E.O. Nester, and J. Yults, "Liquid Crystal Matrix Displays," *Proc. IEEE*, 59, pp. 1566–1579 (1971).
5. F.J. Marlowe and E.O. Nester, "Alternating Voltage Excitation of Liquid Crystal Display Matrix," U.S. Patent No. 3,654,606.
6. T.P. Brody, J.A. Asars, and G.D. Dixon, "A 6x6 Inch 20 Lines-per-Inch Liquid-Crystal Display Panel," *IEEE Trans. Electron. Devices*, ED-20, pp. 995–1001 (1973).
7. S. Morozumi, "4.25 in. and 1.51 in. B/W and Full-Color LC Video Displays Addressed by Poly-Si TFTs," *SID 1984 Digest*, pp. 316–317 (1984).
8. P.G. LeComber, W.E. Spear, and A. Ghaith, "Amorphous Silicon Field-Effect Device and Possible Application," *Elect. Lett.*, 15, pp. 179–181 (1979).
9. Matsushita a-Si pocket television marketed in 1984.
10. See, for example, L.M. Blinov, *Electro-Optical and Magneto-Optical Properties of Liquid Crystals*. New York: Wiley (1983).
11. P.M. Alt and P. Pleshko, "Scanning Limitations of Liquid Crystal Displays," *IEEE Trans. Electron Devices*, ED-21, pp. 146–155 (1974).

CHAPTER

2

Operating Principles of Active Matrix LCDs

2.1 The Case for Active Matrix

Passive matrix LCDs are relatively easy to manufacture and do not require very large investments. An active matrix LCD, on the other hand, consists of thin film semiconductor circuitry on a glass substrate and shares some of the manufacturing complexity of integrated circuits on semiconductor wafers.

The efficient production of active matrix LCDs requires large capital investments at the same level of wafer fabs for IC manufacturing. The incentive for an LCD producer to make this investment rather than sticking with passive matrix LCDs is simple: image quality, including resolution, maximum size, contrast ratio, viewing angle, gray scale, and video performance is much better in AMLCDs than in passive matrix LCDs. The resolution limitation of the passive matrix was addressed in the previous chapter. Another drawback of passive matrix addressing is that the capacitance of the select and data buslines increases with the square of the diagonal size of the LCD. Since the buslines in passive matrix LCDs consist of transparent conductors with relatively high resistance, the RC delays and power consumption in large passive LCDs become unmanageable.

By adding a semiconductor switch at each pixel, the drawbacks of multiplexing in a passive matrix are eliminated. In the active matrix configuration, the voltage at each pixel and therefore its transmission and gray level can be accurately controlled.

A conventional semiconductor process on crystalline Si wafers could, in principle, be used for AMLCDs. In fact, this has been successful in reflective microdisplays for projection and personal viewers and is commonly referred to as liquid crystal on silicon (LCOS).

For larger displays, however, several factors preclude the use of crystalline silicon. First, it is opaque for visible light and is therefore not compatible with transmissive, backlit displays such as used in notebooks or desktop monitors. Secondly, processed silicon wafers

have a limited size (not exceeding 12 in.) and are too expensive. In the semiconductor industry there is a constant push for smaller and more compact circuitry by reducing design rules, which is not needed for AMLCD fabrication.

In an AMLCD most of the viewing area consists of the transparent pixel electrodes. The semiconductor switch and address lines cover only a small fraction of the pixel area. There is no strong incentive to move to advanced submicron design rules since, for large displays with larger pixels, most features actually become larger. In other words, apart from the need for transparent substrates, the use of crystalline wafers would be overkill for the simple circuitry required in most AMLCDs.

Thin film processing has come to the rescue; it allows simple circuitry to be manufactured on large glass substrates with relatively modest design rules and an acceptable, reduced number of process steps.

In terms of operation, the AMLCD is comparable to dynamic random access memory (DRAM). Like the DRAM, the AMLCD consists of arrays of cells in which a voltage is stored. In the case of most LCDs this is not a digital voltage, but an analog voltage to represent different gray levels.

The business model for AMLCD manufacturers also shows some resemblance to that of memory manufacturers. To a large degree, both products have become commodities with constant price pressure and their markets are cyclical in the sense that there are periods of excess supply and excess demand.

2.2 Requirements for Active Matrix Switching Devices

The LC pixel in an LCD can, for all practical purposes, be treated as a low-leakage capacitor. This capacitance needs to be charged from the data voltage at one polarity to the data voltage of opposite polarity during each refresh cycle to obtain an AC voltage without a DC component across the LC pixel. In static images the amplitude of the data voltage across the LC pixels remains constant; only their polarity will change in every frame to prevent degradation of the LC cell. When the displayed information changes (as in video displays with moving images), the amplitude may change as well, so that the gray level can be varied according to the image data.

In Fig. 2.1 the geometry of the LC capacitance C_{LC} for the pixel is shown. It is given by the equation

$$C_{LC} = \frac{\varepsilon_0 \varepsilon_{LC} wl}{d}, \tag{2.1}$$

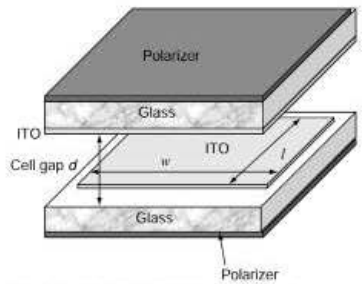

Figure 2.1: Geometry of the LC pixel capacitance.

where ε_0 is the permittivity constant in vacuum, ε_{LC} is the dielectric constant of the LC material, w and l are the side dimensions of the pixel electrode, and d is the LC layer thickness (also called the LC cell gap). Since the LC dielectric constant depends on the orientation of the molecules, the LC pixel capacitance varies significantly with applied voltage.

For example, in a TN cell that uses LC fluid with a positive dielectric anisotropy, the LC director will be perpendicular to the electric field between the pixel electrodes for applied voltages below the threshold. Then, $\varepsilon_\perp$ should be substituted for ε_{LC} in Eq. 2.1.

When 5–10 V AC is applied so that the LC molecules will line up along the electric field direction, $\varepsilon_{||}$ should be substituted in Eq. 2.1. As a result, the capacitance can increase by a factor of two to three. For intermediate applied voltages there is a continuous variation of the effective dielectric constant of the LC layer from $\varepsilon_\perp$ to $\varepsilon_{||}$. LC pixel capacitances in practical LCDs are typically 1 pF or less.

Figure 2.2 shows the circuit of four pixels in a passive matrix LCD. The solid lines represent the circuitry on one substrate, while the dotted lines represent the circuitry on the opposite substrate. In the passive matrix LCD, the LC pixel capacitors are simply formed where the striped transparent electrodes intersect (see also Fig. 1.13 in Chapter 1). The select and data lines are on opposite substrates.

In a TFT-based AMLCD (Fig. 2.3), both select and data lines are on the active matrix substrate, along with the pixel electrode and storage capacitor. The counter-electrode of each LC pixel capacitor, indicated by the dotted line, is a single common transparent

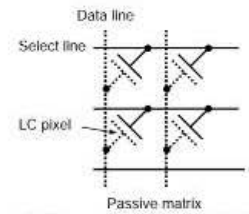

Figure 2.2: Circuit diagram for four pixels in a passive matrix LCD.

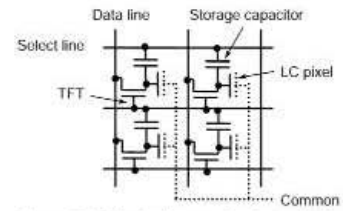

Figure 2.3: Circuit diagram for four pixels in an active matrix LCD.

electrode on the opposite substrate (which usually also has color filters). This common electrode is shared by all pixels in the array.

After the LC pixel capacitance is charged up to the data voltage, the TFT is switched OFF and the pixel electrode on the active array is floating. The pixel capacitor should retain its data voltage for the remainder of the frame time until the next address time. As discussed in Sec. 1.2 in Chapter 1, the LC fluid needs to have a high resistivity to prevent leakage currents. The capacity to retain charge is often expressed in the voltage holding ratio (VHR), which is defined as

$$VHR = \frac{V_{rms}}{V_{peak}}, \tag{2.2}$$

$$V_{rms} = \sqrt{\frac{1}{2T_f}\int_0^{2T_f} V^2(t)\,dt}, \tag{2.3}$$

where V_{rms} is the RMS voltage, V_{peak} is the peak voltage of the LC pixel waveform, and T_f is the frame time, as shown in Fig. 2.4.

In addition to the LC pixel capacitance, most AMLCDs also have an auxiliary storage capacitance connected in parallel to the LC capacitance (as shown in Fig. 2.3). The storage capacitor uses a thin film dielectric with negligible leakage current and its capacitance value is voltage-independent. Therefore, the storage capacitor acts as a buffer to suppress the undesirable voltage dependence and potential leakage current in the LC capacitance. With a storage capacitor at each pixel it is easier to control the RMS voltage on the pixel and therefore its gray level.

In Fig. 2.5 the generic, basic circuit for the switch at each pixel is shown. When one row is selected, all the switches on that row are turned ON and the data voltages are transferred to the pixel electrodes. Ideally, the ON resistance of the switch is zero and the OFF resistance is infinite. In practice, the requirements can be much relaxed. In a display with N rows and a refresh rate of 60 Hz, the frame time T_{frame} to refresh the entire display will be 16.6 msec and the line time T_{line} to address one row will be T_{frame}/N or less. In the case of an XGA display with 768 rows, this translates into a maximum line time of 21 μsec to select one row.

The ON current I_{on} of the switch should be sufficient to fully discharge the LC pixel capacitance and charge it to the opposite polarity voltage V_{on} during the line time. This leads to

$$I_{on} > \frac{2\,(C_{st}+C_{LC})\,V_{on}}{T_{line}}. \tag{2.4}$$

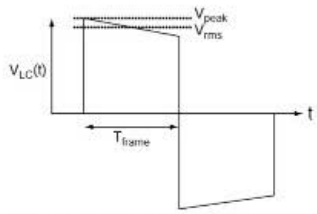

Figure 2.4: Voltage across LC versus time.

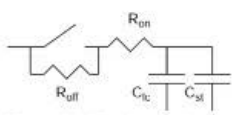

Figure 2.5: Basic switch configuration in an AMLCD pixel.

The OFF current I_{off} should be low enough to retain the charge on the pixel during the frame time

$$I_{off} < \frac{(C_{st}+C_{LC})\,\Delta V}{T_{frame}}, \tag{2.5}$$

where ΔV is the maximum tolerable voltage loss from the pixel capacitance during the frame time.

When realistic values for a 15-in. XGA display are substituted in Eqs. 2.4 and 2.5, C_{st} = 0.3 pF, C_{LC} = 0.3 pF, and ΔV = 20 mV, we get

$$Ion > 1\,\mu A \text{ and } I_{off} < 0.5\,pA. \tag{2.6}$$

In other words, the ON/OFF current ratio has to exceed six orders of magnitude. The current levels are quite low and can be achieved by transistors using thin film semiconductors such as amorphous silicon (a-Si).

Since the pixels do not draw a current after being charged up during each refresh cycle, the power consumption in the LCD itself is low. Most of the power consumption in transmissive LCDs is usually in the backlight.

Active matrix LCDs can be classified into direct-view displays and light valves (Fig. 2.6). Light valves or microdisplays are used for projection applications and as personal viewers and viewfinders. Microdisplays can be transmissive or reflective. Transmissive types use high-temperature poly-Si TFTs, while reflective types employ crystalline Si circuitry.

Direct-view displays can be further categorized according to the type of switch used at each pixel. The vast majority of AMLCDs on the market use a-Si or poly-Si thin film Transistors (TFTs). Table 2.1 lists some of the pertinent properties of the various

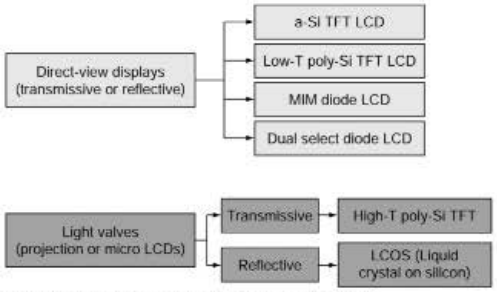

Figure 2.6: Classification of active matrix LCDs.

Table 2.1: Different types of switches for AMLCDs and their main applications

Switching device	Mobility (cm^2/Vsec)*	Highest processing temperature†	Major applications
a-Si TFT	0.3–1	~ 300°C (glass)	Notebooks, flat panel monitors, LCD TVs
High-T poly-Si TFT	100–300	~ 1000°C (quartz)	Projection light valves, viewfinders
Low-T poly-Si TFT	10–200	~ 500°C (glass)	PDAs, notebooks, projection light valves, viewfinders
Crystalline Si MOSFET	400	~ 1100°C (C-Si)	Projection light valves, viewfinders
Thin film diode		< 300°C (glass)	Handheld devices

* Mobility determines the potential to integrate peripheral electronics.
† Highest processing temperature determines substrate choice.

switches, along with display applications in which they are common. The field effect mobility of the TFT (mostly a semiconductor material property) determines the feasibility of designing row and column drivers directly on the glass for a more integrated solution. The highest process temperature determines the type of substrate. For processing below 600°C, low-cost glass substrates can be used. If there is any process step exceeding 1000°C, as in high-temperature poly-Si LCDs, the substrate will be expensive quartz. High-temperature poly-Si TFTs are therefore used only in small displays for projection systems.

Amorphous silicon TFTs have become dominant in large-area displays such as those used in notebook computers, flat panel desktop monitors, and LCD televisions. Low-temperature poly-Si-based LCDs are somewhat less common and are mostly applied in smaller devices, including mobile phones, PDAs, and projection light valves, where their higher processing cost is offset by integration of some of the peripheral electronics on the display glass.

Thin film diodes with ON and OFF currents satisfying Eqs. 2.2 and 2.3 are suitable for LCDs as well. Thus far they have mostly been applied in displays with a limited number of gray levels, such as cell phones.

2.3 The Thin Film Transistor

Thin film transistors (TFTs) are cousins of the transistors used in semiconductor chips. In terms of switching speed and operating voltage, they are inferior to state-of-the-art MOS transistors in crystalline Si. However, they are quite adequate as a simple ON/OFF pixel

switch in AMLCDs with a 60-Hz refresh rate. In Fig. 2.7 the top view and cross section of a basic TFT are depicted. The TFT has three terminals: the gate, source, and drain. The gate is separated from the semiconductor film by a gate insulator layer, and the source and drain make contact to the semiconductor. One type of TFT, the N-channel TFT, operates similarly to a field-effect N-channel metal oxide semiconductor (NMOS) transistor in crystalline silicon. It is switched ON by applying a positive voltage on the gate. The insulator acts like a capacitor dielectric, so that in the semiconductor channel an opposing negative charge is induced (see Fig. 2.8). This negative charge creates a conductive channel for electrons flowing from the source to the drain. The magnitude of the current depends on the dimensions of the conductive channel (the channel length L and the channel width W), on the capacitance of the gate insulator per unit area C_g, on the properties of the semiconductor film, and on the applied gate voltage. When a negative voltage is applied to the gate, the channel is depleted of electrons and negligible current flows.

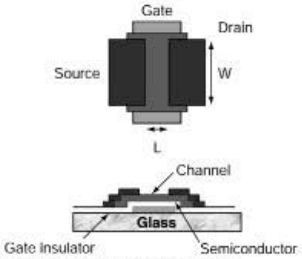

Figure 2.7: Top view and cross section of basic TFT.

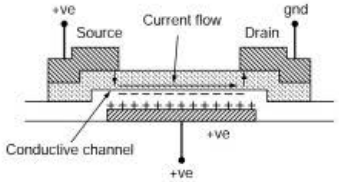

Figure 2.8: Conductive channel formation and current flow in TFT.

The ON current I_{ds} of the TFT can be described, in a first approximation, by the same equations used for traditional NMOS transistors in crystalline Si [1]:

$$I_{ds} = \mu C_{\varepsilon} \frac{W}{L} V_{ds}(V_g - V_{th} - 0.5V_{ds}) \text{ for } V_{ds} V_g - V_{th} \quad (2.7)$$

$$I_{ds} = \mu C_{\varepsilon} \frac{W}{2L} V_{ds}(V_g - V_{th})^2 \text{ for } V_{ds} > V_g - V_{th}. \quad (2.8)$$

Here μ is the field effect mobility of the thin film semiconductor, a material property, and V_{th} is the TFT threshold voltage, which depends on both the semiconductor and the gate insulator, and on their interface.

Equations (2.7) and (2.8) describe, respectively, the linear and saturation regimes of operation for the TFT, as illustrated in Fig. 2.9.

In the ON state of the TFT, when a data voltage is applied to the source, the drain with the LC load capacitance will charge up to the same voltage, thereby transferring the data

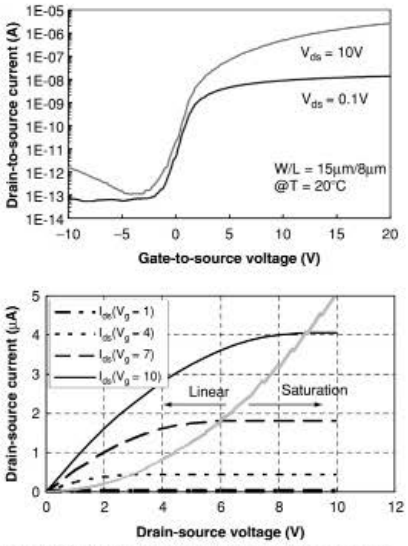

Figure 2.9: Current-voltage characteristics of a-Si TFT.

signal from the data line to the pixel electrode. The TFT is turned OFF when applying a negative voltage to the gate. Since in the N-channel TFT the source and drain contacts block the injection of positive charge carriers (holes), there will be negligible current flow in the OFF state.

Similar equations and considerations apply to P-channel TFTs, in which charge transport is by holes. They are switched ON by a negative gate voltage and switched off by a positive gate voltage.

Many TFTs are of the staggered type, in which the source and the drain have an overlap region with the gate (as shown in Fig. 2.7). The overlap causes a parasitic capacitance that can have an impact on display performance unless the pixel is addressed by an appropriate drive scheme.

The earliest TFTs for LCDs used CdSe semiconductor thin films. Since CdSe is not a standard material in the semiconductor industry, special deposition and etching processes needed to be developed to build CdSe-based TFT LCDs. Although CdSe TFTs showed good performance in AMLCDS, they have never been able to overcome the drawbacks of not being mainstream. They are now relegated to small research efforts.

2.4 Thin Film Silicon Properties

Silicon is a very familiar material in the semiconductor industry and is therefore the preferred choice for use in AMLCDs. Thin films of silicon on glass are, however, inferior in quality to crystalline silicon. This is illustrated in Fig. 2.10, where the atomic structure of c-Si, p-Si and a-Si are schematically compared. In c-Si, the Si atoms are all four-fold coordinated and constitute a perfect crystal lattice with long-range order of the Si atom

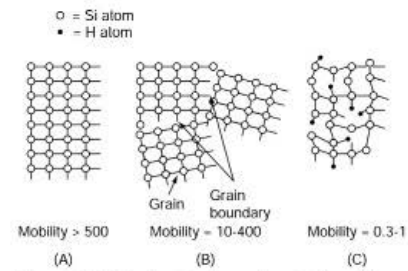

Figure 2.10: Atomic structure of crystalline silicon (A), poly-crystalline silicon (B) and amorphous silicon (C).

positions. As a result, electrons and holes can flow with high velocities v_e and v_p when an electric field E is applied:

$$v_e = \mu_e E \text{ and } v_p = \mu_p E. \tag{2.9}$$

The values of the mobilities μ_e for electrons and μ_p exceed 500 cm^2/Vsec in crystalline silicon.

Low-temperature poly-Si thin films are first deposited as amorphous films, and then crystallized by laser annealing or thermal annealing. The annealing temperature cannot exceed 600°C when low-cost glass substrates are used. Sometimes seed materials such as Ni or preferential crystal growth from certain locations are used. The quality of poly-Si varies greatly depending on deposition and crystallization methods, but invariably it has grain boundaries that reduce the mobility by creating barriers for the flow of electrons and holes (see Fig. 2.10B). Some improvement can be obtained by passivating the grain boundaries with hydrogen in a post-hydrogenation step. The grain size is important in determining TFT characteristics. Preferably, to maximize the mobility, there are no grain boundaries in the channel area of the TFT. A number of techniques have been developed to crystallize the silicon films, including excimer laser annealing (ELA), solid phase crystallization (SPC), sequential lateral solidification (SLS), and metal-induced lateral crystallization (MILC). They result in TFTs with mobilities ranging from 10–400 cm^2/Vsec, the electron mobility often being higher than the hole mobility.

The concept of hydrogenation is important in amorphous silicon as well. The structure of amorphous silicon is more irregular, so that there is no long-range order and no crystal lattice. Nonetheless, since amorphous silicon films are deposited from the decomposition of SiH_4 gas, 5–10% hydrogen is automatically built in during film growth. The hydrogen acts to terminate dangling bonds in the loose a-Si network (Fig. 2.10C) and is essential to improve its electronic properties. The type of a-Si used in TFT LCDs is therefore often referred to as hydrogenated amorphous silicon or a-Si:H. The electron field effect mobility is only 0.3–1 cm^2/Vsec in a-Si, but is adequate for pixel switches in TFT LCDs. The hole mobility is much lower, so that practical p-type TFTs are impossible in a-Si.

Hydrogenated amorphous silicon, as used in LCDs, is a reddish-colored thin film with a thickness between 30 and 200 nm. It can be readily deposited on large glass surfaces by plasma-enhanced chemical vapor deposition. Some of its properties are listed in Table 2.2. It has a band gap of 1.7 eV, (considerably larger than crystalline and poly-crystalline Si [1.1 eV]), a very low dark conductivity, and high photoconductivity. The low dark conductivity makes it relatively easy to obtain a low OFF current in the TFT. The high photoconductivity is an undesirable property of a-Si, since it can cause unwanted photo-leakage currents in the TFT. To prevent photo-leakage, the a-Si channel in TFTs

Table 2.2: Some properties of a-Si films

a-Si film property	Typical value	Unit
Hydrogen content	5–10	%
Dark conductivity intrinsic film	10^{-10}–10^{-9}	$(\Omega cm)^{-1}$
Dark conductivity n^+ doped film	10^{-2}–10^{-1}	$(\Omega cm)^{-1}$
Photoconductivity in sunlight	10^{-4}	$(\Omega cm)^{-1}$
Energy gap	1.75	eV
Field effect mobility	0.3–1.0	cm^2/Vsec

is sandwiched between opaque layers to shield it as completely as possible from both ambient light and backlight in the LCD.

Amorphous silicon can be easily doped in the gas phase during deposition, to obtain n-type or p-type films with many orders of magnitude higher conductivity than undoped films. N-type films are used as contact layers to the source and drain of the TFT. The field effect mobility, which is important for the ON current of the TFT (see Eqs. 2.5 and 2.6), is only 0.3–1 cm^2/Vsec and much lower than that of c-Si (500–1000 cm^2/Vsec). Amorphous silicon is therefore used primarily in circuits with relatively low switching speeds (i.e., as the pixel switches in AMLCDs).

2.5 Amorphous Silicon TFTs

Amorphous silicon TFTs have been dominant in notebook and desktop monitor LCDs and in LCD televisions, as a result of their relatively easy processing on very large glass substrates and a limited number of process steps. Amorphous silicon TFTs are N-channel enhancement-type field-effect transistors. As mentioned in the previous section, the electronic properties of a-Si do not allow the fabrication of high-quality p-type TFTs. P-channel a-Si TFTs cannot be made sufficiently conductive to get acceptable ON current for application in displays.

Three different types of a-Si TFTs are shown in Fig. 2.11. The back-channel-etched (BCE) inverted staggered TFT is the most commonly used; it has good performance and a relatively straightforward manufacturing process. Another type is the trilayer (or etch-stopper) TFT. Both the BCE and the trilayer TFT have a bottom gate. The intrinsic a-Si layer on top of the silicon-nitride gate insulator forms the channel.

The source and drain electrodes have an overlap region with the gate and make contact to the a-Si layer via a heavily doped thin n-type a-Si interface layer. The purpose of this a-Si n^+ layer is twofold: it acts as a low-resistance ohmic contact for electrons to

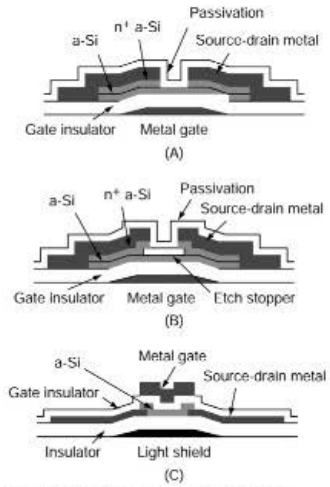

Figure 2.11: Three types of a-Si TFTs: (A) back-channel-etched TFT, (B) etch-stopper or trilayer TFT, and (C) top-gate TFT.

maximize the ON current, and in the OFF state it blocks the injection of holes into the intrinsic i-layer to minimize the leakage current. Since the n^+ layer is conductive, it needs to be removed from the channel area to obtain a low OFF current. This is done by a back-etch after the source and drain electrodes are patterned—hence, the name back-channel-etched TFT. The back-etch process is quite critical and needs to be uniform across the entire manufacturing substrate. Since it is difficult to obtain significantly different etch rates for the a-Si n^+ layer and the undoped intrinsic layer (i-layer), good process control is required to completely remove the n^+ layer from the channel without etching through the i-layer.

In the trilayer or etch-stopper TFT (Fig. 2.11B), the n^+ back-etch is less critical, since there is an extra silicon-nitride etch stopper layer on top of the channel. The etch stopper is deposited and patterned before the n^+ contact layer. Amorphous silicon and silicon-nitride can be selectively etched in dry and wet etch systems. During the back-etch of the n^+ layer there is much better etch selectivity possible against the silicon-nitride etch stopper layer, enhancing the process latitude. The trilayer TFT also has a

thinner i-layer, which can suppress photo-leakage currents in the TFT. The major drawback of the trilayer TFT is that it requires an extra deposition and patterning step.

The top-gate a-Si TFT (Fig. 2.11C) is less common. In this configuration the source and drain electrodes are deposited and patterned first, followed by the a-Si layer. The gate insulator (usually silicon-nitride) needs to be deposited on top of the a-Si layer, which usually leads to somewhat lower-performance TFTs in terms of ON current. To suppress photo-leakage currents, a light shield needs to be deposited and patterned prior to the actual TFT process. It is separated from the TFT by an extra insulator layer. The extra processing required for the light shield and the insulator make the top-gate TFT less attractive.

Amorphous silicon is not a very stable material and its structure can be modified by strong illumination or by injection of charge carriers. In addition, the interface between amorphous silicon and the gate insulator (e.g., silicon-nitride) can accumulate charge during operation of the TFT. As a result of this charge trapping, the threshold of the a-Si TFT can shift over time. This effect has been studied in detail, since it can have a bearing on the lifetime of a TFT LCD. The threshold shift versus time can be expressed by the following equation:

$$\Delta V_{th} = \left(V_g - V_{th}\right) * \left(\frac{t}{\tau}\right)^{\beta}, \qquad (2.10)$$

where β and τ are constants that can depend on temperature and the quality of the a-Si and a-Si/SiN interface.

The measurement results of threshold shift in non-optimized a-Si TFTs are shown in Fig. 2.12.

Fortunately, the threshold shifts are of opposite polarity during the ON time and the OFF time of the a-Si TFT, so that partial cancellation of the threshold shift occurs. The TFT in an AMLCD functions as an ON/OFF switch to load the pixel data on the pixel capacitor. Therefore, some variation of the TFT threshold across the area is acceptable, as long as the drive scheme can accommodate the variation. It also helps that for a few microseconds after switching ON an a-Si TFT, a transient current occurs that is about 2× higher than the steady-state current. The bottom line is that a-Si TFT threshold shifts have been proven to be small enough to not affect the lifetime of well-designed AMLCDs for up to 50,000 hours.

2.6 Poly-Silicon TFTs

Poly-silicon TFTs (Fig. 2.13) can be subdivided into the high-temperature variety (built on quartz) and the low-temperature type (built on low-cost glass). High-temperature poly-Si TFTs are manufactured with a process that is very similar to semiconductor

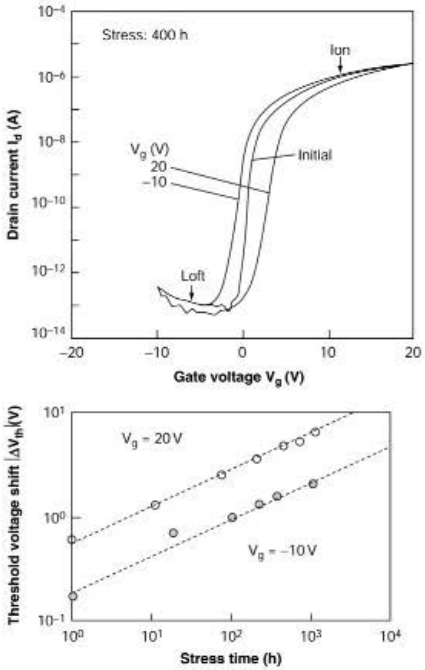

Figure 2.12: Threshold voltage shift in a-Si TFTs after bias stress.

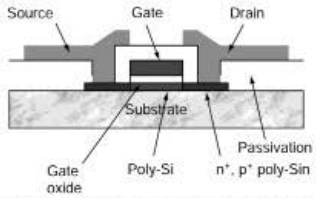

Figure 2.13: Cross section of poly-Si TFT.

processing, with thermally grown oxides, ion implantation, and other steps familiar in semiconductor fabrication. Low-temperature poly-Si TFTs can be produced on large glass substrates with specially developed laser crystallization, ion doping, and gate oxide deposition steps.

With both high- and low-temperature poly-Si, N-channel or P-channel devices can be built so that low-power CMOS circuitry may be integrated along the periphery of the display. The current-voltage characteristics of a-Si and poly-Si TFTs (Fig. 2.14) underscore the difference in mobility of a factor of about 100 and the corresponding difference in ON current. Amorphous silicon TFTs have a low OFF current, sufficiently low to retain charge on the pixel capacitor. Poly-Si TFTs, however, have orders of magnitude higher OFF current, too high for a pixel switch unless special precautions are taken. The high OFF current is caused by high electric fields at the highly doped drain and the imperfect crystalline structure of the poly-Si material. In Fig. 2.15 two methods are shown to reduce the OFF current in poly-Si TFTs. A dual gate structure can be utilized to split the source-drain voltage between two channels and thereby reduce the electric field at the drain. Using an extra process step to create a lightly doped drain (LDD) area has a similar effect. The resulting current-voltage characteristic is shown in Fig. 2.16.

The development and manufacturing of low-temperature poly-Si LCDs has received significant investments because row and column drivers can be integrated on the glass, thereby eliminating the external row and column driver chips. It has been demonstrated that additional circuitry such as D/A converters, DC/DC converters, graphics processors, and even microprocessors can be integrated on the glass as well.

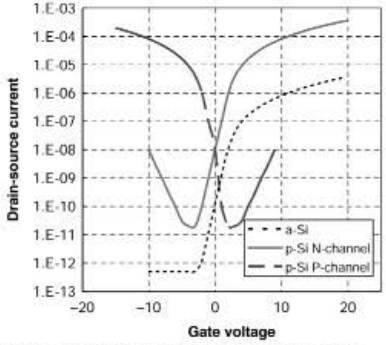

Figure 2.14: Comparison of amorphous silicon and poly-crystalline silicon TFT characteristics.

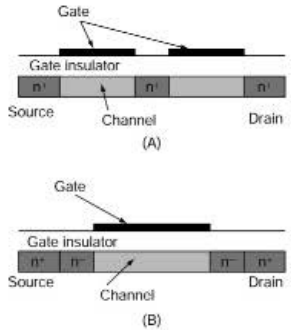

Figure 2.15: Methods to reduce OFF current in poly-Si TFTs: (A) dual gate structure and (B) lightly doped drain structure.

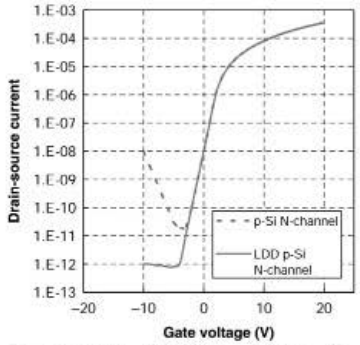

Figure 2.16: Poly-Si TFT characteristics with and without lightly doped drain (LDD) structure.

2.7 Basic Pixel Circuit and Addressing Methods

A TFT pixel array circuit (Fig. 2.17) consists of select buslines, data buslines, a TFT at each pixel, and a storage capacitor in parallel with the LC pixel capacitance. The function of the storage capacitor, as mentioned before, is to act as a buffer and reduce the effects of the

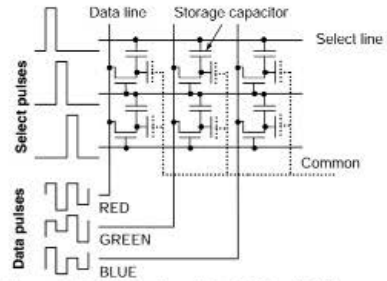

Figure 2.17: Operation of TFT LCD with drive waveforms.

voltage dependence and leakage of the LC capacitance. With a storage capacitor at each pixel, it is easier to obtain uniform gray level performance across the display.

The storage capacitor can be connected to the adjacent select line to maximize aperture ratio in the display. The counter electrode of the LC pixel capacitor is the common ITO electrode on the opposite substrate (the color plate). The display operates by switching on the TFTs one row at a time by a gate pulse with a pulse width of 10–50 μsec, depending on display resolution. The gate pulses are supplied from gate driver circuits, which can either be external or integrated on the glass. While one row is selected, the data signals for that row are applied to the data buslines from peripheral electronic data circuits and transferred by the TFT to the pixel electrodes. When the row is deselected, the TFTs switch OFF and the data voltage is stored for the remainder of the frame time of 16.7 msec (at a 60-Hz refresh rate), while the other rows are scanned. All rows in the display are sequentially selected during the frame time, so that the voltage on each pixel is refreshed once during each frame time. During the next frame time, the polarity of the data signals is reversed, so that all pixels are charged with opposite polarity voltage to obtain the required AC drive without a DC component. For static images, the pixel voltage is simply opposite for odd and even frames, so that the orientation of the LC molecules and the gray levels of the pixel do not change. For moving video images, the amplitude of the pixel voltage can change as well, in addition to its polarity. This causes the LC orientation and therefore the transmittance of the pixel to change over time.

Most AMLCDs are color displays. Color is obtained by using three subpixels per pixel, each having a color filter of one of the three primary colors (red, green, and blue). The color filters are patterned on the top plate opposing the active matrix substrate and

separated from the TFT array by the LC layer. The top plate is therefore often referred to as the color plate. A color pixel is obtained by the additive color principle: at close-up, the individual color subpixels may be observed, but from a distance the eye will average the luminance from the three subpixels. When all three colors (R, G, and B) are transmitting, the viewer will perceive the pixel as white; when only R and G are transmitting, yellow will be observed; and combinations of B and G and R and B result in cyan and magenta being displayed.

On the TFT array the three subpixels per pixel are identical, but on the color plate they have different color filters.

A close-up look at the pixel circuit (Fig. 2.18) reveals a number of parasitic circuit elements that can degrade display performance. The parasitics are denoted by the dotted elements. Resistive leakage through the LC or the TFT will both discharge the LC pixel capacitor and affect gray scale uniformity. The parasitic capacitance C_{gd} between the gate and the drain of the TFT causes a voltage division effect with the LC pixel capacitance. This leads to a negative pixel voltage shift ΔV_{pix} of around 1 V on the LC voltage when the gate of an a-Si TFT is switched OFF, as shown in Fig. 2.19.

$$\Delta V_{pix} = \frac{C_{gd}}{C_{gd} + C_{st} + C_{lc}} \Delta V_g, \qquad (2.11)$$

where C_{gd} is the gate-drain capacitance, C_{st} is the storage capacitance, C_{lc} is the LC capacitance, and ΔV_g is the gate voltage change when the row is deselected.

The pixel voltage shift is always negative and could therefore lead to a DC component on the pixel voltage, if the common counter-electrode would be held at the center voltage of the video data signal.

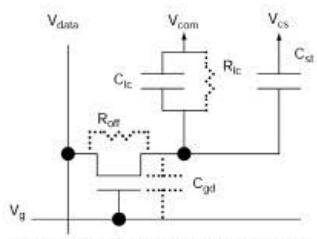

Figure 2.18: TFT LCD pixel circuit with parasitic circuit elements.

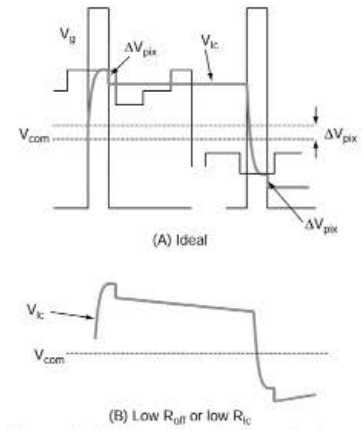

Figure 2.19: Voltage waveforms applied to the select (gate) line and source (data) line with resulting voltage across the LC pixel in ideal case (A) and with leakage through LC or TFT (B).

To eliminate the DC component across the LC, the voltage on the common ITO counter electrode V_{com} is offset by the same voltage to compensate for this pixel voltage shift. As a result of the voltage dependence of the LC capacitance, it turns out to be difficult to completely eliminate the DC component for all gray levels across the entire display area, especially in large displays. Failure to minimize the DC components leads to many undesirable display artifacts, such as image retention, flicker, and non-uniform gray levels. Optimized drive methods are used to reduce the DC component and to prevent it from causing flicker and image retention, particularly in gray scale. Some of these methods will be addressed in Chapter 4.

The storage capacitor in a TFT pixel circuit can be connected to an adjacent gate line or to a specially added common bus (Fig. 2.20). Connection to the gate line maximizes the pixel aperture ratio but tends to increase the load capacitance on the row select lines. This makes it difficult to use this configuration for displays with a diagonal size larger than about 20 in.

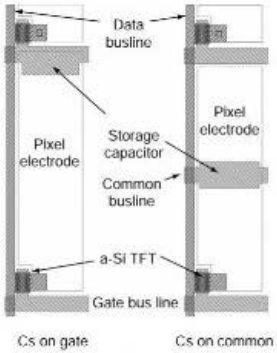

Figure 2.20: Pixel layouts with storage capacitor connected to the gate line (Cs on gate) and with storage capacitor connected to a common bus (Cs on common).

A common storage bus takes up some space in the pixel area and therefore reduces the pixel aperture ratio and the transmittance of the display The RC delay on the gate lines is, however, smaller so that larger displays exceeding 20 in. in diagonal size use this configuration.

2.8 Diode-Based Displays

Instead of a three-terminal TFT, a two-terminal switch or thin film diode (TFD) may be used at each pixel in an AMLCD. There are several ways to implement TFD LCDs. A TFD in this context can be either a rectifying diode or a bi-directional diode, also called a metal-insulator-metal (MIM) diode or a nonlinear resistor. The bi-directional diode has very low current at voltages below about 5 V and starts conducting when a voltage above 10–15 V of either positive or negative polarity is applied.

During the 1980s and early 1990s, several companies worked on rectifying amorphous silicon PIN diodes for AMLCDs. They can be produced with very high rectification (ON/OFF) ratios of eight or more orders of magnitude. At least two rectifying diodes per pixel are needed, one to charge the pixel to positive polarity, the other to negative

polarity. In terms of manufacturing, PIN diode LCDs do not have a significant advantage over TFT LCDs and have therefore not been commercially successful.

MIM diode displays have had some commercial success. Their major attraction is a simple, low-cost manufacturing process for the active matrix array with only two or three photo-masks.

In the case of bi-directional MIM diodes, a single diode per pixel can, in principle, be used since it can charge up the pixel to either polarity and is therefore compatible with the AC voltage on the LC capacitor.

In Figs. 2.21 and 2.22, typical current-voltage curves of several bi-directional diodes are shown on linear and semi-logarithmic scales, respectively. The basic circuit and drive scheme of a single TFD LCD are shown in Fig. 2.23. In diode displays, the data lines are ITO stripes on the color plate, as in passive matrix STN LCDs.

Several semi-insulator materials have been used, including Ta_2O_5, Si-rich SiN_x and diamond-like carbon (DLC). The dominant conduction mechanism in bi-directional TFDs is Frenkel–Poole conduction. The Frenkel–Poole effect is the dramatic increase of charge carriers in certain insulators under a high electric field. It is caused by the thermal excitation

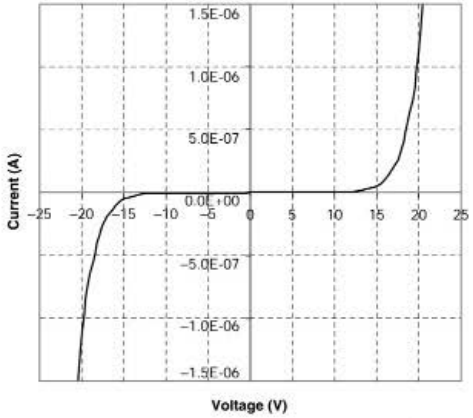

Figure 2.21: Linear current-voltage characteristic of SiN_x diode.

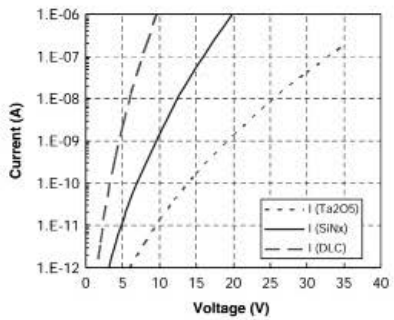

Figure 2.22: Typical semi-logarithmic current-voltage characteristics of Ta2O5, Si-rich SiNx and diamond-like carbon (DLC) diodes (reprinted with permission from the Society for Information Display).

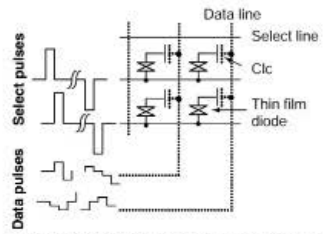

Figure 2.23: Circuit and drive waveforms of a thin film diode LCD.

of charge carriers from traps when the Coulombic barrier for their escape is lowered by the high electric field. This leads to a field-dependent conductivity in the material:

$$\sigma(E) = \sigma_0 \exp(\alpha \sqrt{E}), \tag{2.12}$$

where σ_0 is the zero field conductivity and α the nonlinearity coefficient:

$$\sigma_0 = q\mu n \exp\left(-\frac{\Phi_0}{kT}\right), \tag{2.13}$$

$$\alpha = \frac{1}{kT}\sqrt{\frac{q^3}{\pi \varepsilon_0 \varepsilon_r}}. \tag{2.14}$$

Here T is the absolute temperature, k is Boltzmann's constant, q is the electronic charge, ε_0 is the permittivity in vacuum, ε_r is the dielectric constant, Φ is the trap depth for the charge carrier, μ is the mobility of the charge carriers, and n is the carrier density. The dielectric constants for Ta_2O_5, Si-rich SiN_x and diamond-like carbon (DLC) are, respectively, 24, 9, and 4.

The best diodes are obtained with a semi-insulator with a low dielectric constant ε_r, as follows from Eq. 2.14. A low dielectric constant also minimizes the diode capacitance, so that cross-talk is reduced. From this perspective, DLC appears to be a good candidate for further development. Ta_2O_5 diodes have been widely used in small mobile displays and are obtained by anodizing Ta. Unfortunately, Ta_2O_5 has a high dielectric constant and relatively poor current-voltage characteristics, which precludes large, high-resolution displays. Si-rich SiN_x has the advantage that it can be processed in standard PECVD equipment familiar in every a-Si TFT LCD line.

The diode current in the nonlinear resistor can be derived from Eq. 2.12:

$$I = S\kappa V \exp\left(\beta\sqrt{|V|}\right) \tag{2.15}$$

$$\beta = \frac{\alpha}{\sqrt{d}}, \tag{2.16}$$

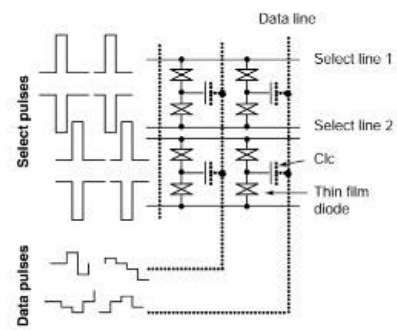

Figure 2.24: Circuit and drive waveforms of a dual select diode AMLCD.

where S is the diode area, V is the applied voltage, d is the thickness of the insulator in the TFD and κ and β are material parameters which depend on temperature and on the dielectric constant of the insulator film.

The TFD and the LC capacitor are in series in Fig. 2.23 and this makes the LC voltage extremely susceptible to small variations in the diode characteristics over time and across the display. Unfortunately, it is difficult to make TFDs very uniform over large areas. In addition, the insulator typically used in MIM diodes (anodized Ta_2O_5) leads to diodes with marginal ratios between ON and OFF current.

The series connection of the diode and LC capacitor also causes a strong dependence of the LC voltage on signal propagation delays on the buslines, another factor limiting gray-scale performance, especially for large-diode LCDs.

Single-MIM-diode displays have therefore been only successful in small applications such as cell phones with a limited number of gray levels.

An approach that eliminates the drawbacks of the single-MIM-diode pixel circuit is the dual select diode (DSD) AMLCD, which has a pixel circuit as shown in Fig. 2.24. By applying opposite polarity pulses to the two select lines, the pixel electrode voltage is accurately reset during each select time.

Unlike in the single-TFD circuit, variations in the TFD across the display area and over time are basically cancelled out in the differential DSD pixel circuit. The propagation delays on select and data addressing pulses are also cancelled out to a large degree in DSD LCDs. This leads to much more uniform gray levels and the potential to scale up to large-area displays with diagonal size exceeding 30 in. This technology is under development.

2.9 Plasma-Addressed LCDs

During the 1990s a totally different technology for AMLCDs was developed, based on a plasma-addressing technique rather than on transistor or diode switches.

Plasma-addressed liquid crystal displays (PALC displays) were the first type of AMLCDs with a diagonal size over 40 in. They employ a hybrid technology with plasma channels used to address one row at a time. The plasma channels are separated from the LC layer by a microsheet of glass with a thickness of only 50 μm. The pixel electrodes are reset to a predetermined voltage during each select time. PALC displays have ITO data lines patterned on the color substrate. The color plate process for PALC displays is similar to that in STN passive matrix LCDs and diode LCDs, which also have ITO data lines on the color plate.

In PALC displays the reset operation of each pixel is performed by a plasma channel between a cathode and an anode busline. The plasma channels are used only for addressing. Display luminance is controlled independently by a backlight. PALC displays require high voltage select drivers.

The combination of plasma technology with LCD technology for PALC displays considerably increases process complexity. Issues with PALC displays include varying decay times of the plasma, bending of the microsheet between the plasma and the LC layer, and process integration problems. This technology has therefore not matured to mass production.

References

1. S.M. Sze, *Physics of Semiconductor Devices*. New York: Wiley (1969).

CHAPTER

4

AMLCD Electronics

The design of the display glass assembly plays an important role in the image quality of an AMLCD. Equally important are the display electronics, which must supply accurate data signals to each pixel. The incoming video signals are either computer-generated or processed from an image acquisition by, for example, a digital camera, television camera, or camcorder. The task of the display electronics is to obtain optimum image quality based on the incoming video signal information.

4.1 Drive Methods

As mentioned earlier, each pixel in the AMLCD is driven with a square wave AC voltage. Ideally, the residual DC component on the pixel voltage is negligible. In practical displays it is unfortunately almost impossible to eliminate the DC component entirely for all gray levels and across the entire display area. The result is that the transmittance of the pixel varies slightly between odd and even frames, as shown in Fig. 4.1.

When the refresh rate is 60 Hz, the frequency of this luminance variation will be 30 Hz since the complete cycle of positive and negative charging of the pixel occurs at 30 Hz. The human eye perceives luminance variations of a few percent at less than 40–50 Hz as flicker. The luminance variations can be smoothed out by using an LC fluid and cell structure with a slow response time, so that the luminance amplitude variations in Fig. 4.1 are below the flicker limit. However, this would cause severe smearing of fast-moving video images and defeats one of the purposes of active matrix drive methods.

Another problem with the DC component on the pixels is that it can cause image sticking or image retention. This leads to burn-in effects on the LCD when a still image is displayed for a prolonged period of time.

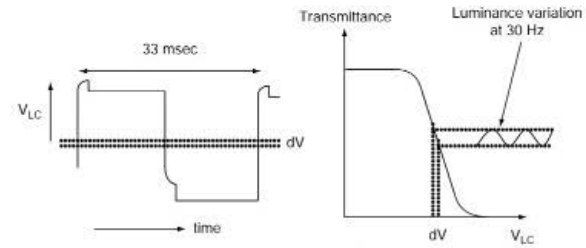

Figure 4.1: Effect of DC voltage component dV of LC voltage on luminance variation.

One way to eliminate flicker is to operate the display at 90 Hz or higher frame rates. Then, the luminance variation will occur at 45 Hz or higher frequencies and will not cause flicker. Since most video and graphics information is supplied to LCD panels at lower refresh rates, this is often not a practical solution.

The most common method to eliminate flicker is the use of inversion drive methods. In this approach, data voltages are applied which alternate the polarity of the voltage on adjacent pixels, so that the human eye perceives an area of multiple pixels as flickerless as a result of spatial averaging. With these polarity inversion methods, individual pixels can still have flicker when viewed close up. At normal viewing distances the flicker becomes imperceptible.

The flicker is minimized or eliminated with this method but image sticking is not reduced; thus, minimizing the DC component on the pixel voltage to less than about 50–100 mV remains crucial.

The polarity can be alternated per row (row or line inversion), per column (column inversion), or by a combination of both (pixel or dot inversion) (Fig. 4.2). Dot inversion gives the best image quality in terms of flicker and also minimizes both vertical and horizontal cross-talk on the display.

In color displays it is important that subpixels of one color have alternating polarity for adjacent pixels, so that flat fields of one color will not exhibit flicker. In a vertical stripe configuration with red (R), green (G), and blue (B) subpixels, this condition is automatically satisfied with dot inversion and also with full pixel inversion, also called color group

IPR2025-01330 Page 00031

inversion (Fig. 4.3). As can be seen, in each frame each of the primary color subpixels has opposite polarity compared to the nearest neighbor subpixel with the same color.

The timing and polarity of the data signal on odd and even data buslines is shown in Fig. 4.4 for the different inversion methods, in the case that all pixels are driven at the same gray level. In frame inversion, all pixels receive the same polarity data signal for odd frames and the opposite polarity for even frames, resulting in flicker. In column inversion, adjacent columns have opposite data polarity and change polarity for each frame. In line or row inversion, the data polarity on each pixel changes every line in addition to every frame. Dot inversion combines row and column inversion. In all cases, the driving wave forms on the select lines (the rows) are the same.

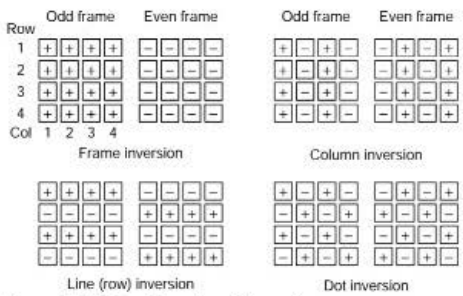

Figure 4.2: Various inversion drive schemes.

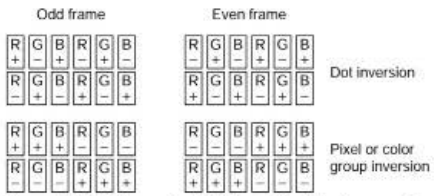

Figure 4.3: Dot inversion (left) and pixel (color group) inversion (right) in color LCDs with an RGB vertical stripe color filter arrangement.

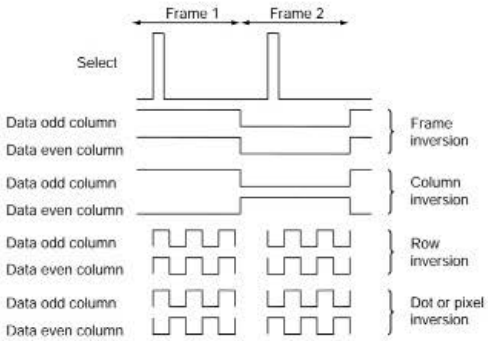

Figure 4.4: Timing of signals in various inversion drive schemes when all pixels are switched on.

In panels for desktop monitors, LCD televisions, and most notebook displays, the voltage on the common ITO electrode on the color plate is held at a constant DC bias voltage V_{com} (Fig. 4.5). The entire voltage range of more than 10 V between the extremes of the positive cycle and the negative cycle must be supplied by the data driver. In actual display operation, the V_{com} voltage is offset by about 1 V in a-Si TFT LCDs to compensate for the pixel voltage shift described in Chapter 2, Sec. 2.6.

In order to reduce driver cost and keep data driver output voltages low, some notebook panels and most small mobile applications employ V_{com} modulation (also called common plane switching), in which the voltage on the color plate switches each line time by about 5 V. Part of the voltage V_{LC} across the LC is then derived from the V_{com} modulation:

$$V_{LC}(+) = V_{data}(+) - V_{com}(+), \tag{4.1}$$

$$V_{LC}(-) = V_{data}(-) - V_{com}(-). \tag{4.2}$$

Since the voltage across the LC pixel is the difference between V_{com} and the data driver signal voltage, this allows the use of low-cost, low-voltage data drivers with a full range of 5 V or even 3.3 V when the LC cell has a low operating voltage. A driver IC that can be made in a standard 3.3-V process can be easily procured from many IC fabs at low cost. When the voltage on the color plate is changed every line time, the polarity of the data

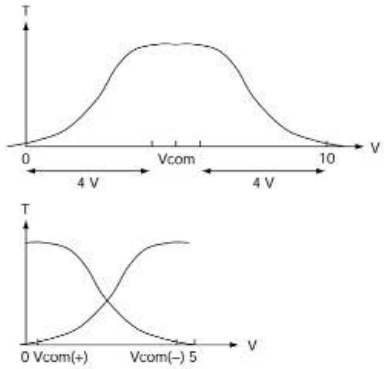

Figure 4.5: Transmittance versus data voltage for full range drive (top) and V_{com} modulation drive (bottom).

voltages supplied to the pixels needs to change every line time as well. V_{com} modulation at the line frequency is therefore used in conjunction with line inversion (row inversion) data drivers. The timing for V_{com} modulation is shown in Fig. 4.6. For activated (ON) pixels, the data voltage is out of phase with the V_{com} modulation, while for non-activated (OFF) pixels it is in phase.

A drawback of V_{com} modulation is that it is incompatible with dot inversion and requires extra electronics to switch the large capacitance load of the V_{com} electrode with the correct timing. This would become a problem for large displays. Most notebooks and all desktop monitors and large LCD televisions therefore use a constant V_{com} and dot inversion (also because dot inversion generally gives the best image quality).

The V_{com} bias voltage is set to compensate for the pixel voltage shift when the select pulses are turned off so as to minimize the residual DC component on the LC pixel voltage. The pixel voltage shift depends on the data voltage, as outlined in Chapter 2, Sec. 2.6 and is different for negative and positive voltage across the LC pixel. To minimize DC components for all gray levels at both pixel polarities, the gamma reference voltages that control gray scale are often set independently for each data polarity. The gamma reference voltages match the incoming video data to the

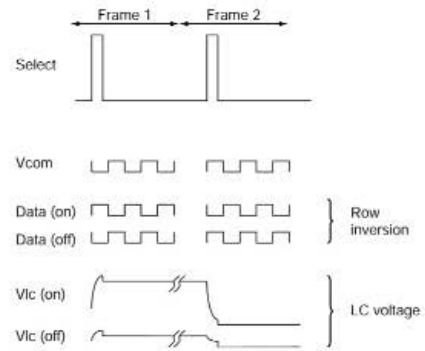

Figure 4.6: Timing of signals and LC voltage in Vcom modulation schemes for all pixels on and all pixels off.

desired gray scale. There are usually about 10 gamma reference voltages. For an 8-bit, 256-level gray scale, the intermediate gray scales are obtained from interpolation between the gamma correction voltages.

This is illustrated in Fig. 4.7, where $V_1, V_2,...,V_{10}$ are the gamma reference voltages, V_{ref} is the video center reference voltage, *AVdd* is the supply voltage, and *AVss* is ground. Best performance is achieved when $V_1, V_2,...,V_{10}$ are independently optimized, which means that, in general, $|V_{ref} - V_6| \neq |V_{ref} - V_5|$, $|V_{ref} - V_7| \neq |V_{ref} - V_4|$, etc.

In order to get more than eight bits of gray scale, a technique called frame rate control (FRC) has been developed. With FRC, the gray level voltage can be different between odd and even frames or between four subsequent frames, so that intermediate gray levels can be generated. For example, if during the odd frame the voltage for gray level i and during the even frame the voltage for gray level i+1 is applied, an extra gray level between levels i and i+1 is effectively displayed. This makes it possible to have a 9-bit gray scale with an 8-bit data driver.

The difference in voltages between levels i and i+1 is generally too small to cause a significant DC component on the LC voltage or to cause flicker. The eye will perceive the intermediate gray level.

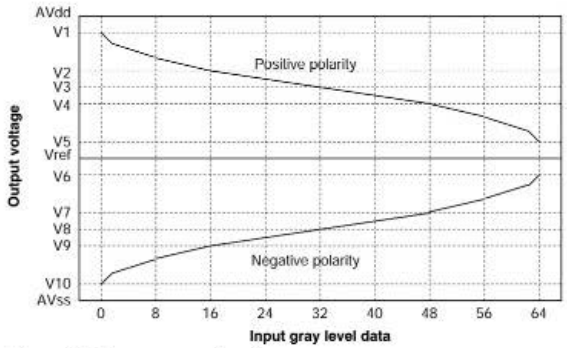

Figure 4.7: Gamma correction diagram.

Similarly, this technique can be used during four subsequent frames to generate a 10-bit gray scale with an 8-bit data driver.

4.2 Row Select and Column Data Drivers

In Fig. 4.8 a block diagram of a TFT LCD module is shown. Directly attached to the display glass are the driver ICs for the rows and the columns. The row driver IC generates the select pulses sequentially addressing each row in the display. It is often referred to as the gate driver, since it switches the TFTs ON and OFF by applying a select voltage to the gate; in the case of a-Si TFTs, this is a positive pulse of about 20 V.

The column drivers supply the video data signals to the data lines connected to the source of the TFTs at each pixel. They are commonly referred to as the source drivers. Gate and source drivers are mixed-signal ICs designed typically with 0.25–1 μm design rules. For most driver ICs there is no need to use advanced design rules below 0.25 μm. The die area is pad limited (i.e., the large number of outputs and their spacing govern how much silicon real estate is required, not the relatively simple electronic circuitry on the chip).

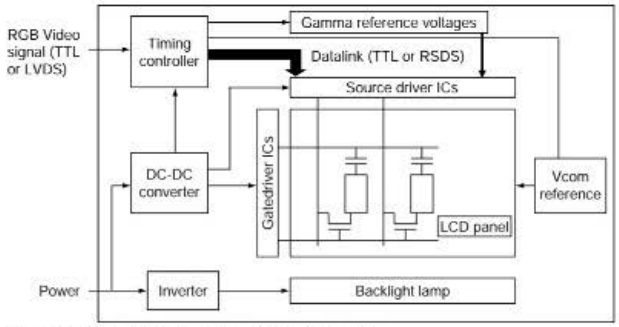

Figure 4.8: Block diagram for a TFT LCD module.

An XGA TFT LCD with 768 rows and 1024 × 3 columns typically requires three gate driver ICs with 256 output channels each, and eight source driver ICs with 384 channels each. They can be packaged in a tape carrier package (TCP) for attachment to the glass with tape automated bonding (TAB). Alternatively, they are directly bonded upside-down to the glass with chip-on-glass (COG) technology. Since both row and column drivers require a large number of output channels on one side of the chip, the aspect ratio of the die is usually high (e.g., 20 mm × 1 mm).

In Fig. 4.9 a block diagram of a gate driver is shown. It has a relatively simple architecture with a bi-directional shift register, level shifters, and output buffers. The shift register transfers a start bit at STVD (which can be considered a vertical sync pulse) through the chip, selecting one row line at a time. When the select bit emerges at the end of the chip it is transferred through STVU to the second row driver IC, where it functions as the start bit. Multiple chips can be cascaded in this fashion.

In this cascade type of operation, all 768 rows in the XGA display are sequentially addressed. The direction of the start bit can be reversed by the DIR input, so that the vertical mirror image can be displayed on the LCD. The DIR function also ensures that the row driver ICs can be mounted either at the left or the right side of the display area.

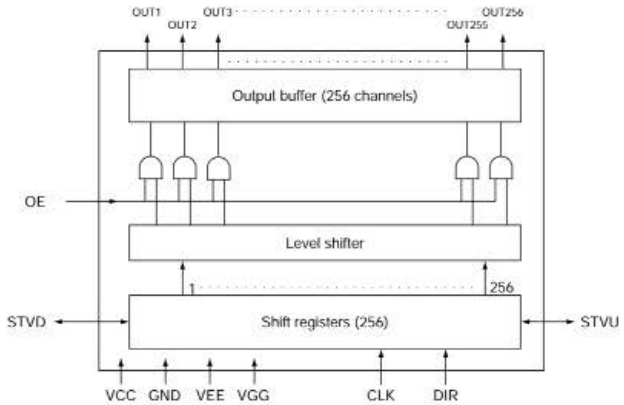

Figure 4.9: Basic architecture of a gate driver IC with 256 channel outputs for use in XGA and SXGA panels (three or four chips per panel, respectively).

The OE input to the row driver allows the select pulse for the rows to be turned OFF before the end of the line time. This is especially important for large displays where the RC delays on the rows require the rows to be turned OFF for a few microseconds before the data voltage on the columns is changed in order to avoid cross-talk. The level shifters raise the logical voltage levels of 0 and 3.3 V to output levels of –5 V and about 20–25 V, respectively. The final levels are compatible with the required ON and OFF voltage levels on the gates of the a-Si TFTs. Output buffers reduce the output impedance to a sufficiently low level in order to drive the gate lines on the AMLCD.

The clock frequency of the row select driver is quite low (around 50 kHz), not much higher than the product of refresh rate (e.g., 60 Hz) and the number of rows (768 for an XGA display). In Table 4.1 the input and output pins of a typical gate driver are listed. A timing diagram is shown in Fig. 4.10.

The digital data driver for the columns, connected to the sources of the TFTs, is somewhat more complex. Its basic block diagram is shown in Fig. 4.11. It basically converts serial digital video input signals into parallel analog data signals for one row. These analog signals representing the intended gray levels are then all simultaneously

Table 4.1: I/O pins of a basic row (gate) driver IC for a-Si TFT LCDs

Pin	Input/ Output	Description	Typical value
CLK	I	Clock signal controlling shift register—equal to line frequency	50 kHz
DIR		Direction of operation of bi-directional shift register	0 or VCC
STVD	I/O	Input start bit when operating when DIR=1, output bit for starting next cascaded row driver IC when DIR=0	0 or VCC
STVU	I/O	Input start bit when operating when DIR=0, output bit for starting next cascaded row driver IC when DIR=1	0 or VCC
OE	I	Output Enable to enable output voltage to the TFT LCD rows	0 or VCC
OUT1,..., ...,256	O	Output channels driving the rows (gates) of the TFT LCD	VGG or VEE
VCC	I	Logical voltage supply	3.3 V
GND	I	Ground voltage for logical supply	0 V
VEE	I	Low analog supply voltage for rows	–5 V
VGG	I	High analog supply voltage for rows	20 V

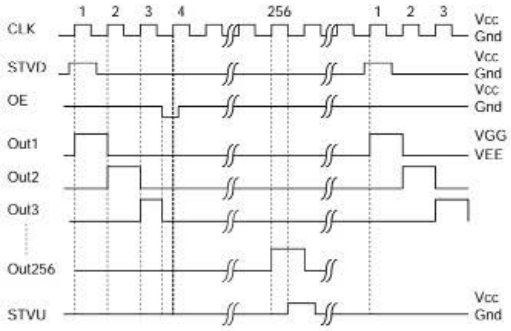

Figure 4.10: Timing diagram of a row driver.

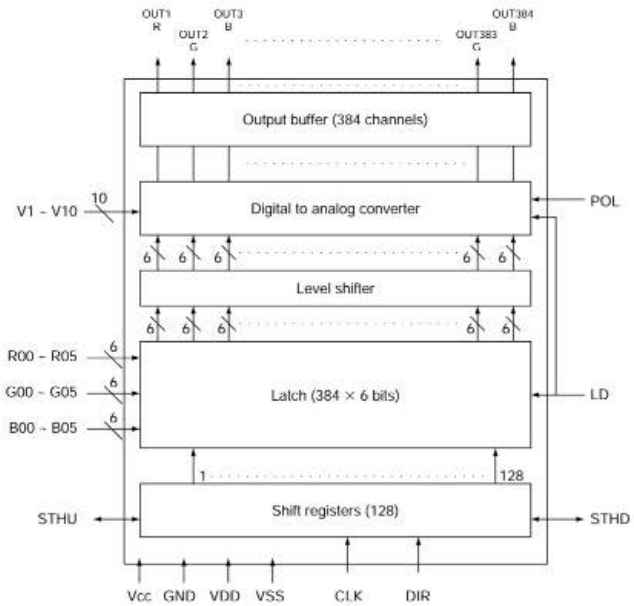

Figure 4.11: Basic architecture of a source driver IC with 384 channel outputs for use in XGA and SXGA panels (eight or ten chips per panel, respectively).

applied to one row of pixels when the row is selected. Like the gate driver, the source driver has a bi-directional shift register with cascading functionality to connect multiple chips together and allow mounting at either the top or the bottom of the viewing area. The 6-bit digital data signals for red, green, and blue channels are latched into a 128×3-line latch and then level shifted from the logical levels to the VDD level. The D/A converter has input reference voltages to convert the digital levels to the appropriate gray scale levels.

The reference voltage inputs to the D/A converter (DAC) ensure the desired gamma correction. The POL input to the DAC controls the polarity of the output signals so that dot, line inversion, or column inversion may be selected. Output buffers reduce the

output impedance of the output channels in order to rapidly charge the column line capacitance of the LCD to within a fraction of one line select time.

The operating frequency of the source driver is much higher than for the row driver (around 65 MHz), larger than the product of refresh rate (e.g., 60 Hz) and the number of pixels (768×1024 for an XGA display).

In Table 4.2 the input and output pins of a typical source driver are listed. A timing diagram is shown in Fig. 4.12.

For notebook displays, 6-bit data drivers with 6-bit gray scale (18-bit colors) are common, while for desktop monitors and LCD televisions, 8-bit data drivers (24-bit colors) are used.

Table 4.2: I/O pins of a basic 6-bit column (source) driver IC for a-Si TFT LCDs

Pin	Input/ Output	Description	Typical value
CLK	I	Clock signal controlling shift register—equal to pixel dot frequency	65 MHz
DIR	I	Direction of operation of bi-directional shift register	0 or VCC
STHD	I/O	Input Start bit when operating when DIR=1, output bit for starting next cascaded row driver IC when DIR=0	0 or VCC
STHU	I/O	Input Start bit when operating when DIR=0, output bit for starting next cascaded row driver IC when DIR=1	0 or VCC
POL	I	Selects polarity of the output channel voltages to the columns	0 or VCC
LD	I	Switches new data signals to the outputs and latches their polarity	0 or VCC
V1, ... V10	I	Voltage bias levels to set gamma correction	
R00–R05, G00–G05, B00–B05	I	Digital video input signals for red, green, and blue color pixels	
OUT1,..., ...,384	O	Output channels driving the columns (sources) of the TFT LCD. OUT1,4,7,... for red pixels, OUT2,5,7,... for green pixels, OUT3,6,9,... for blue pixels	VDD<OUTx< VSS
VCC	I	Logical voltage supply	3.3 V
GND	I	Ground voltage for logical supply	0 V
VSS	I	Low analog supply voltage	0 V
VDD	I	High analog supply voltage	10 V

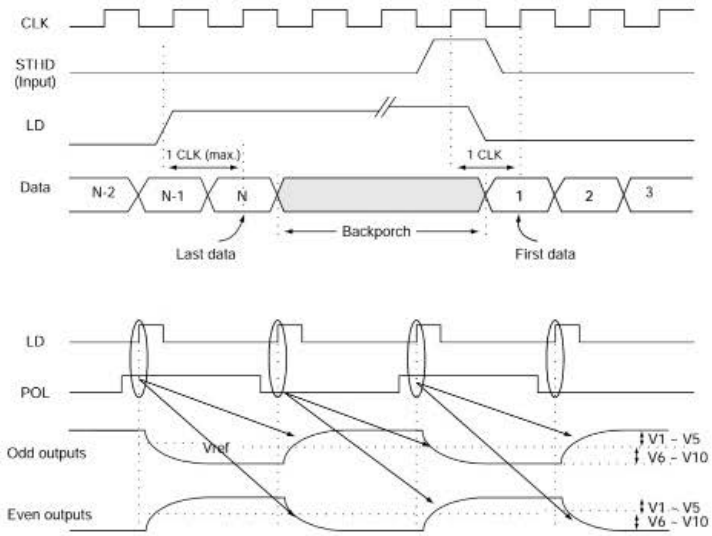

Figure 4.12: Example of a timing diagram for a column driver. Top four wave forms show clocking in of data. Bottom four wave forms show latching of analog output voltage to the output using the POL signal to obtain dot inversion.

Analog data drivers, which receive an analog video signal, are used in some consumer electronic LCDs, but are gradually being phased out.

4.3 Timing Controllers, Display Controllers, and Interfaces

In the block diagram of Fig. 4.8, the timing controller (TCON) is the chip that supplies the control and video signals to the row and column drivers. For the row driver, they are the vertical clock, the vertical start bit, the output enable signal, and the logical bit that controls the direction of the shift register (see Table 4.1). For the column driver, they include the horizontal clock, the input start bit, the polarity signal to control the polarity of the data voltage applied to the LCD, the gamma reference control voltages, and the digital video data signals (see Table 4.2).

For low-resolution displays, the data link between TCON and the column driver is in transistor-transistor-logic (TTL) format, which switches the digital signal typically between 0 and 3.3 or 5 V. For higher-resolution displays beyond SVGA (600×800 pixels), the frequency of the data signals becomes so high for TTL as to cause electromagnetic interference (EMI) and signal fidelity problems. Therefore, XGA and higher-resolution displays use a method of differential signaling to cancel out most of the EMI. These interface architectures are based on low voltage differential signaling (LVDS) [1] or reduced swing differential signaling (RSDS) standards [2]. RSDS has become the de facto standard in most cases for the video interface between the timing controller and the data drivers.

The timing controller receives a video signal which is already compatible with the resolution of the LCD panel. Since notebook displays are permanently attached to the laptop computer, these digital signals are directly generated by the graphics controller circuitry in the computer.

Figure 4.13 shows a photograph of an XGA TFT LCD module or panel, as supplied by the AMLCD manufacturer to notebook manufacturers. It includes the backlight unit but not the inverter for the backlight. The backlight consists of a cold cathode fluorescence (CCFL) stick lamp at the edge of a light guide, which evenly distributes the light across the viewing area of the panel. This particular module has only one PCB and uses chip-on-glass row and column drivers. Flexible interconnect tape connects the PCB to the inputs of the data drivers and scan drivers on the glass. The control signals for the

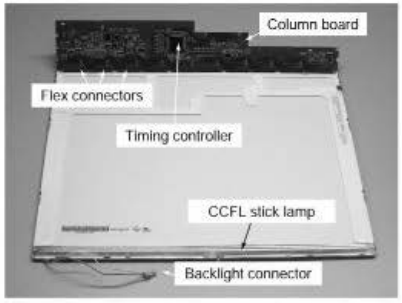

Figure 4.13: View of back of a TFT LCD module for notebook displays.

three scan drivers are routed on the glass along the right side of the panel. The PCB is folded back in the photograph to expose the timing controller. Normally, the PCB is folded flat against the panel to obtain a very thin module with a thickness of only a few millimeters.

For standalone LCD desktop monitors, the design is somewhat different. They need to be compatible with hookup to a variety of computers with analog and digital video output formats and resolutions. Usually the module, without the inverter, is supplied to display integrators who build the complete monitors. They add the inverter to operate the backlight, a monitor controller board, and a front panel control board. The unit is then mounted in the final enclosure with a stand. The front panel control has the ON/OFF switch, brightness, contrast, and hue controls.

Figure 4.14 shows the back of a display panel for desktop monitors, including the backlight inverter, front panel control board, and the monitor controller board. The backlight inverter drives stick lamps on both sides of the panel to obtain sufficient brightness. The monitor controller board supplies processed video signals to the timing controller on the column board.

The monitor controller board accepts different video signal formats and converts them to the proper format for the timing controller. For hookup to computers, these formats include at least analog RGB video (also called analog VGA) and, for dual mode

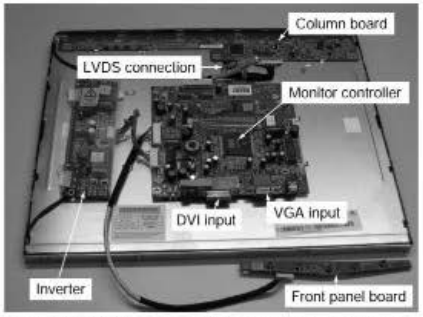

Figure 4.14: View of back of a TFT LCD panel for a desktop monitor including monitor controller board, inverter, and front panel control board.

monitors, they also include digital video interface (DVI) [3]. The analog VGA and DVI connectors are indicated in the photograph. In some cases there also inputs for S-video, component video, and composite video for operation as a television and for connection to external DVD players and other consumer electronics.

The main chip on the monitor controller board usually can perform scaling functions, convert the different formats, provide on-screen display (OSD), picture-in-picture (PIP), and other functionality. It has a built-in microcontroller and can perform some image processing, color management, and gamma control functions. In some cases, LVDS transmitters are built in. The interface format for the data-link between the monitor controller board and the timing controller is LVDS to minimize EMI.

Detailed descriptions of video and interface formats are outside the scope of this book; for more information, the reader is referred to the literature and several excellent books [4,5]. It should be noted that new, improved standards in video data transfer techniques and interfaces are still periodically introduced. For example, for notebook panels and LCD television, the point-to-point differential signaling (PPDS) interface architecture has been proposed by National Semiconductor [6] to reduce the number of inputs to each data driver by more than 60%. This is achieved by a point-to-point distribution of the digital video signals. It reduces the number of video inputs to each chip from 18 to 2 for 6-bit video. In addition, the gamma reference voltages are digitally generated in the timing controller rather than hardwiring them as 10 analog voltages to each data driver. D/A converters inside the data driver generate the analog gamma reference voltages from one digital serial input. For the PPDS interface, new timing controllers and data driver ICs have been developed.

In the LCD monitor market there is an alternative business model in which more of the monitor integration is performed at the AMLCD panel manufacturer. In this so-called smart panel approach, a single display controller chip is used that combines the functions of the monitor controller chip and the timing controller chip. This leads to a higher level of integration at the expense of design flexibility.

4.4 Integration of Electronics on Glass

As mentioned in previous chapters, some of the peripheral electronics of the TFT LCD can be integrated on the glass. The low mobility of a-Si TFTs precludes the design of high-speed circuitry with a-Si TFTs.

Despite this hurdle, there have been successful efforts to integrate a-Si TFT row drivers, and this technology has now been commercialized in small displays and notebook panels

[7]. The row driver circuits require only 10–30 kHz clock frequency, which can be easily achieved with a-Si TFTs. The major challenge with a-Si TFTs is to avoid large threshold voltage shifts in TFTs with high duty ratios in shift registers, buffers, and level shifters. They reduce the lifetime of the display. A careful consideration of the a-Si TFT threshold shift and an optimized row driver circuit is needed to get a lifetime exceeding 10,000 hours [8]. There have also been reports on displays in which both row and column drivers are integrated with a-Si TFTs [9]. By integrating peripheral electronics on the glass, the reliability of the display system is enhanced since there are fewer interconnects and interconnect failures are less likely.

The vast majority of integration efforts have focused on poly-Si TFTs, mostly of the low-temperature variety—low-temperature poly silicon (LTPS). In Fig. 4.15 the operating frequency of a shift register is plotted as a function of the poly-Si TFT mobility and for different design rules of the TFT channel length L.

As explained in Sec. 4.2, the operating frequency of the row driver circuits does not exceed more than about 50 kHz, which is easy to achieve with LTPS TFTs and even with a-Si TFTs. The data drivers are more difficult to implement, but have been successfully integrated on the glass in small mobile commercial products, such as PDAs, with a relatively low pixel count. In Sec. 4.2 it was shown that the data driver for an XGA display requires a clock frequency of 65 MHz. According to Fig. 4.15, it would take a

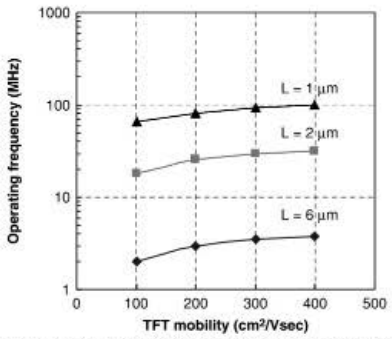

Figure 4.15: Dependence of shift register operating frequency on TFT mobility for different design rules of the gate length L

process with 1-μm design rules to integrate the data drivers in an XGA display and a TFT mobility more than 100 cm^2/Vsec.

Increasingly, other functionality such as D/A converters, timing controllers, graphics controllers, and DC/DC converters are also considered for integration. Displays with a higher level of integration are often referred to as "system-on-panel" or "system-on-glass." Figure 4.16 shows an example of a configuration for a system-on-panel. By adding the DC/DC converter on the glass, a single power supply voltage of, for example, 3.3 V for the entire system is possible. One joint program by Sharp and Semiconductor Energy Labs succeeded in integrating a microprocessor and audio circuitry on the glass [10] as well. Since the design rules for LTPS (1–2 μm) are much less advanced than for state-of-the-art integrated circuits (~0.1 μm), the peripheral circuitry occupied an area larger than the display area and the microprocessor had the speed and performance of a 1980s-era processor. Such a high level of integration is therefore more a capability demonstration than a practical solution.

The decision to include more circuitry on the glass depends on a trade-off between cost and performance. A reduction in manufacturing yield is also possible with more integrated circuitry on the glass and is taken into account.

It should be noted that the functionality achieved with a system-on-panel LTPS display can often be obtained at lower cost using an a-Si TFT LCD with discrete external ICs attached with chip-on-glass bonding. The latter approach is a trend for mobile phone displays where a single chip, with a single power supply and bonded by COG, is used to address the rows and columns in 176(×3)×220 pixel color a-Si TFT LCDs. Single-chip driving is expected to be extended to displays with even more pixels. The single chip

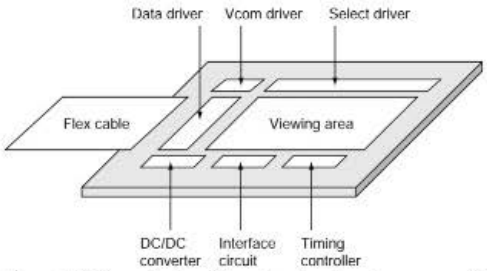

Figure 4.16: Example of configuration for a "system-on-panel."

includes built-in timing controllers, graphics controllers, and other functionality. This trend is supported by IC foundries, which now offer 40-V processes with 0.18-μm design rules so that the power management can also be integrated.

To counter the move toward small, portable applications using a-Si TFT LCDs with single-chip driving, LTPS manufacturers are proposing to include functionality in the viewing area of the display, such as memory built into the pixel, saving power and eliminating the need for continuous refresh of static images. Other approaches include the addition of photosensor arrays in the display viewing area to function as ambient light sensors, scanners, optical touch panels, or fingerprint sensors.

4.5 Backlights

Most AMLCDs operate in the transmissive mode. They can be considered electronically controlled transparencies on a light box—the backlight. It is obvious that many display parameters, including brightness, depend strongly on the backlight. For color displays, the combination of backlight spectrum and color filter spectra determines the color coordinates in the display, as will be outlined in Chapter 5.

In this section we are concerned about the electrical, electronic, and mechanical issues regarding backlights. There are basically two mechanical implementations of a backlight: edge lighting and surface lighting.

An essential requirement for portable, battery-powered applications is to keep power consumption in check and minimize overall panel thickness. This is achieved by edge lighting with light guides. Edge lighting uses one or more lamps, typically cold cathode fluorescent lamps (CCFL) tubes, at the edge of the display, in combination with a thin light guide that distributes the light evenly across the display surface. They allow a thin and lightweight design. Edge lighting with one stick lamp is the backlight of choice for notebook LCDs. They give a display luminance as high as 250 cd/m^2 when used in combination with brightness enhancement films (see also Chapter 6). Stick lamps with a diameter less than 2 mm are available for notebook LCDs.

Figure 4.17 shows the configuration of the edge light with a CCFL stick lamp. The light guide has a diffuse reflector on its back side and a diffuser on the LCD side. For larger displays (exceeding 15 in.) used in monitors, one to three stick lamps on both long edges of the display are often employed in combination with a thicker and heavier light guide.

The other type of CCFL backlight has a cavity configuration with multiple stick lamps or U-shaped lamps (Fig. 4.18) behind the LCD panel. This configuration is used in LCD televisions and in some monitors requiring higher brightness.

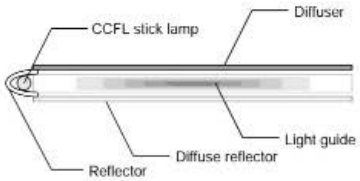

Figure 4.17: CCFL backlight configuration for notebook LCDs.

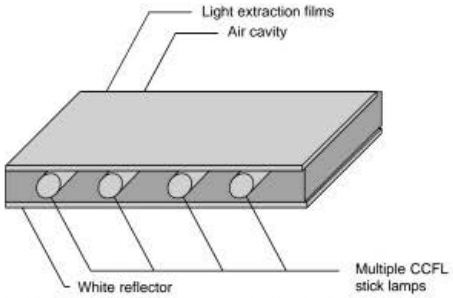

Figure 4.18: Cavity backlight construction.

To obtain uniform luminance across the display area, the light from the lamps needs to be redistributed with a diffuser, leading to some loss in efficiency. In this configuration it is also important that the lamps age approximately the same over time to avoid bands with varying brightness on the LCD after prolonged operation. Large modules with surface backlighting tend to be much lower in weight than large edge-lit panels because the thick, heavy light guide is replaced with an air cavity with stick lamps.

Cold cathode fluorescent lamps (CCFLs) are sealed glass tubes with an electrode at each end. They are filled with an inert gas mixed with a small amount of mercury. To operate the lamp, a high voltage is applied between the electrodes, causing the gas to ionize and emit ultraviolet light. The inner surface of the tube is coated with phosphor layers. The UV rays excite these phosphor layers so that they emit light in their characteristic wavelengths. For color LCDs the CCFL phosphors have three dominant wavelengths

corresponding to the primary colors, red, green, and blue. By adjusting the type and mixing ratio of the three phosphors, there is control over the color performance of the backlight. The lamps are made with different diameters and can be linear or have various shapes such as a U-shape or a serpentine shape.

A high-frequency, high-voltage driving wave form to sustain the discharge in the lamp is supplied from a DC/AC inverter, a transformer that converts the DC input voltage of 3.3 or 5 V into a sine wave of more than 1000-V peak-to-peak amplitude. The optimum frequency is around 50 kHz.

Display brightness can be controlled by dimming the backlight. Dimming is achieved by pulse width modulation, which affects the average current through the lamp. Dimming ratios with CCFLs are typically less than 100:1.

CCFLs have an efficiency of around 25%, which corresponds with about 120 lm/W. (See Chapter 5 for a definition of lumens.) The rest of the input power is lost in the discharge and in heating. The operating temperature range is 20 to 60°C. Between the lamps and the display glass, several plastic films are inserted to redirect the light. Some of them diffuse the light to improve uniformity and others enhance brightness in the direction normal to the display at the expense of oblique directions. These films are discussed in more detail in Chapter 6.

Although CCFLs are inexpensive and bright, they have some drawbacks in terms of lifetime, temperature operating range, and the presence of small amounts of mercury, which pose a hazard at disposal.

Several other types of light sources for LCDs have therefore been developed and have entered the marketplace. They include hot cathode fluorescent lamps (HCFLs), mercury-free Xenon-based flat lamps, and LED-based backlights.

HCFL backlights are receiving renewed interest after initial use in high-end applications such as avionic cockpit displays. The main reasons for their use in avionics are that they can have dimming ratios of 10,000:1 and a wider operating range, required for this application.

HCFLs are common in household applications. They include a tungsten filament, which creates thermionic emission of electrons when heated. As a result, they are easier to strike and dim than CCFLs, which rely on secondary emission of electrons. The renewed interest in HCFLs is caused by the move to scanning backlights for LCD televisions to improve motion portrayal (see also Chapter 6, Sec. 6.6.1.). They have typically wider diameters of about 16 mm and the maximum lamp current for an HCFL is in the range of 50 mA to 1 A, significantly higher than the 10–20 mA typical for CCFLs. They can

therefore be operated intermittently at higher brightness than CCFLs. The initial drawback of lower lifetimes in HCFLs has been addressed and overcome as well.

The Xenon-based flat lamp [11] has external electrodes and phosphors coated on the inside of flat glass substrates to convert the UV radiation from the Xe plasma into visible light. It has several advantages over CCFLs. While the individual CCF stick lamps in a cavity backlight require diffusers and other measures to improve uniformity, the Xe flat lamp is much more uniform by itself. By using external electrodes, which are not exposed to the plasma, it also has a longer lifetime, approximately 100,000 hours to half brightness, as compared to 50,000 hours or less for CCFLs. The elimination of mercury reduces environmental concerns about disposal. Mercury-free backlights are becoming mandated in a number of countries.

The Xe flat lamp also can provide more saturated colors for a wider color gamut of 75% of NTSC, as compared to 65% for conventional CCFL-based displays (see Chapter 5 for definitions of color performance). The operating temperature range is −20 to 80°C so that they can meet outdoor performance requirements. CCFLs, on the other hand, show a drop-off in efficiency below about 20°C and above 60°C and are therefore less suitable for outdoor applications.

The major drawback of Xe flat lamps is their higher cost, which has prevented their penetration into mass markets. With volume production of LCD televisions, this may change.

A third major backlight technology is based on light-emitting diodes (LEDs). With the dramatic improvement in efficiency of red, green, and especially blue LEDs over the past decade, they have become attractive for many lighting applications, including LCD backlights. LEDs can be operated with low-voltage DC power supplies, and brightness is proportional to the current through the LED. The increasing popularity of LED lighting in general is related to significant improvements in their optical efficiency and packaging, including optimally designed heat sinks which allow much higher currents and brightness. A basic LED emits light in a narrow wavelength region, controlled by the energy gap of the semiconductor material (such GaAlAs or GaInP). White-emitting LEDs can be obtained by a UV-emitting LED in combination with visible light-emitting phosphors.

The challenge for R, G, and B LED backlights is the mixing of the three colors from multiple individual point sources to obtain a uniform backlight. This has been achieved [12], although the power conversion efficiency is still only about 50% of that of a CCFL backlight. Some of the advantages of LED backlights are a wide color gamut (100% of NTSC is possible) and a long lifetime. A drawback so far has been a much

higher cost, although the manufacturing cost of the LEDs themselves continues to be lowered. Figure 4.19 shows a spider diagram comparing the characteristics of CCFL, Xe, and LED backlights in terms of lifetime, uniformity, maximum size, color gamut, power consumption, and manufacturing cost (with the caveat that especially the latter two keep improving). Larger values on the diagram indicate more favorable characteristics.

The light from LEDs can easily be pulsed with faster-than-microsecond response times by changing the driving supply from DC to pulsed. LED backlights are therefore also of interest in field-sequential LCDs without color filters, in which the red, green, and blue LEDs are turned on at different times to obtain temporal color mixing. This will be discussed in more detail in Chapter 6.

4.6 Power Consumption

The power consumption in a transmissive TFT LCD module can be subdivided into backlight power, power for the scan driver, the data driver, and the control circuit (Fig. 4.20). Typical power consumption in a 10.4-in. display is about 3 W at 150 cd/m^2 brightness and is dominated by backlight power. This underscores the importance of high-aperture designs and other brightness enhancements to limit battery power use in portable applications.

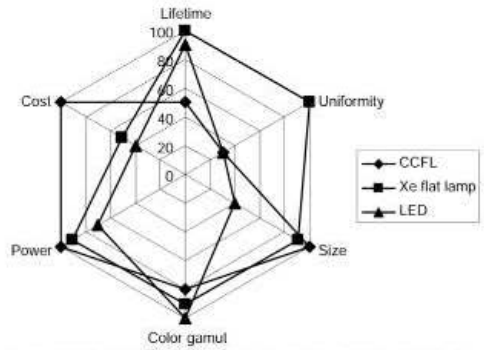

Figure 4.19: Comparison of different backlight technologies.

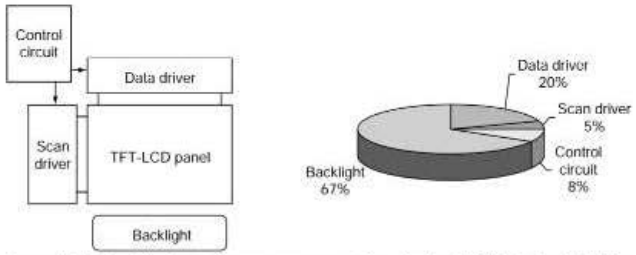

Figure 4.20: Contributions to power consumption of about 3 W in typical 10.4-in. backlit TFT LCD with 150 nits brightness.

A 20-in. LCD television has a power consumption of about 50 W, including all the electronics. This compares favorably with a 20-in. CRT television, which uses about 100 W. It has been calculated that in Japan alone the transition from CRT to LCD televisions will save 5 billion kWh annually.

To further reduce power consumption in portable LCDs, there have been many efforts to eliminate the backlight by developing reflective LCDs with acceptable image quality. They are applied in some handheld products, but the need to view most displays under any ambient lighting conditions has prevented reflective displays from becoming a mainstream technology. A more successful approach is the transflective LCD, in which each pixel is partially transmissive and partially reflective. The reflective area ensures display legibility at high ambient lighting such as outdoor conditions. The transmissive area is used in dark and low ambient lighting conditions. The differences between transmissive, reflective, and transflective displays are discussed in more detail in Chapter 6.

References

1. http://www.siimage.com/documents/SiI-WP-007-A.pdf
2. http://www.national.com/appinfo/displays/
3. http://www.siimage.com/documents/SiI-WP-007-A.pdf
4. K. Jack, *Video Demystified, A Handbook for the Digital Engineer*. Newnes: Elsevier Science (2001).
5. R. Myers, *Display Interfaces: Fundamentals and Standards*. New York: SID-Wiley Digital Video Interfaces (2002).
6. http://www.national.com/appinfo/fpd/ppds.html

7. J. Jeon, K.S. Choo, W.K. Lee, J.H. Song, and H.G. Kim, "Integrated a-Si Gate Driver Circuit for TFT-LCD Panel," *SID 2004 Digest*, pp. 10–13 (2004).
8. H. Lebrun, T. Kretz, J. Magarino, and N. Szydlo, "Design of Integrated Drivers with Amorphous Silicon TFTs for Small Displays," *SID 2005 Digest*, pp. 950–953 (2005).
9. R.G. Stewart, J. Dresner, S. Weisbrod, R.I. Huq, D. Plus, B. Mourey, B. Hepp, and A. Dupont, "Circuit Design for a-Si AMLCDs with Integrated Drivers," *SID 1995 Digest*, pp. 89–92 (1995).
10. T. Ikeda, Y. Shionoiri, T. Atsumi, A. Ishikawa, H. Miyake, Y. Kurokawa, K. Kato, J. Koyama, S. Yamazaki, K. Miyata, T. Matsuo, T. Nagai, Y. Hirayama, Y. Kubota, T. Muramatsu, and M. Katayama, "Full-Functional System Liquid Crystal Display Using CG-Silicon Technology," *SID 2004 Digest*, pp. 860–863 (2004).
11. http://www.osram.de/download/osram_planon_en.ppt
12. http://www.lumileds.com

CHAPTER

6

Improvement of Image Quality in AMLCDs

Over the past 15 years, the performance of AMLCDs has dramatically improved. Depending on the requirements for a particular application, the characteristics described in the previous chapter have been optimized. They include power consumption for portable devices, viewing angle for desktop monitors and televisions, contrast ratio, brightness, color gamut, and video response times for LCD televisions. In Table 6.1 the importance of different performance characteristics is listed for various applications. For mobile applications such as notebooks, PDAs, cell phones, camcorders, and digital cameras, low power consumption is essential to prolong battery life.

For non-portable, large AMLCDs the viewing angle and response time tend to be more of a concern. Many efforts have gone into the development and commercialization of AMLCDs with application-specific optimization of the viewing characteristics. These improvements are described in this chapter.

6.1 Brightness Improvements

The brightness of transmissive LCDs depends to a large extent on the backlight intensity. The most straightforward way to increase display luminance is therefore to turn up the backlight or to design brighter backlights. The display luminance is then proportional to the backlight intensity and can reach more than 1000 cd/m^2. However, there are drawbacks to raising backlight luminance. First, it increases power consumption, which is undesirable (particularly for portable applications). Second, it may require a different construction of the backlight (for example, multiple lamps rather than single lamp edge lighting) and can also have a negative impact on backlight lifetime. Third, high backlight intensity can cause heating of the display beyond 40–50°C, where display image quality may start deteriorating. Alternatives to raising the backlight intensity are addressed in the following subsections.

Table 6.1: Importance of AMLCD characteristics for various applications

Parameter	Small mobile	Laptop	Desktop	Television
High brightness	x	x	Δ	o
Wide viewing angle	x	x	o	o
Wide color gamut	x	Δ	Δ	o
Fast video response time	Δ	Δ	Δ	o
Sunlight readability	o	Δ	x	Δ
Low power consumption	o	o	x	x
Low weight	o	o	x	x
Thin profile	o	o	Δ	Δ

o, very important; Δ, important; x, less important.

6.1.1 Increased Color Filter Transmission

Besides the backlight, the components of the assembly determine the final display luminance, as shown in the previous chapter in Fig. 5.5. The first polarizer transmits about 42% of the light. The black matrix opening on each pixel (the aperture ratio) is typically 40–70% and the color filters transmit about 25% of white light (averaged over the red, green, and blue filter). Other layers and the exit polarizer further reduce luminance so that total transmittance is only 5–10%. It is difficult to increase the transmittance of the polarizers or color filters without affecting contrast ratio or color saturation, respectively. There is a trade-off between color gamut and brightness. By reducing the density of color pigments in the color filter materials, their transmittance at fixed thickness can be increased. This has an effect similar to reducing the thickness of the color filters: it increases the spectral width of the color filter and reduces color gamut and color saturation.

The trade-off is illustrated in Fig. 6.1, where the filter curves and chromaticity coordinates labeled 2 have twice the filter thickness or twice the pigment density as compared to those labeled 1. Thinner color filters are common in mobile phone displays where power consumption is more important than a wide color gamut. Since the color filter spectra become wider for thinner filters, display luminance improves at the expense of color purity. In Fig. 6.1B, the resulting color gamuts are schematically compared.

6.1.2 High-Aperture Ratio Designs

Efforts to improve AMLCD transmittance have focused on pixel aperture ratio. In conventional designs (Fig. 6.2A), the aperture is limited to less than about 55% because the

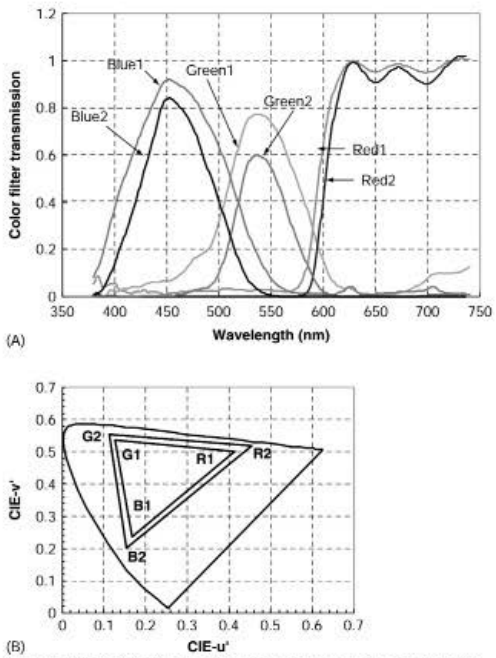

Figure 6.1: Effect of color filter thickness or pigment density on color filter spectra and color gamut.

black matrix on the color plate needs to overlap the ITO pixel electrodes on the TFT array by at least 4 or 5 μm. This is to allow for tolerance in the color-plate-to-active-plate alignment during manufacturing and to prevent light leakage at pixel edges.

In the black-matrix-on-array design of Fig. 6.2B, stripes of gate metal are added at the edge of the ITO pixel and determine the pixel opening. They block light entering the edge of the pixel under an angle. Since the registration of the layers on the TFT array to each other is very accurate (better than 1 μm), this makes a larger aperture of around 65% possible.

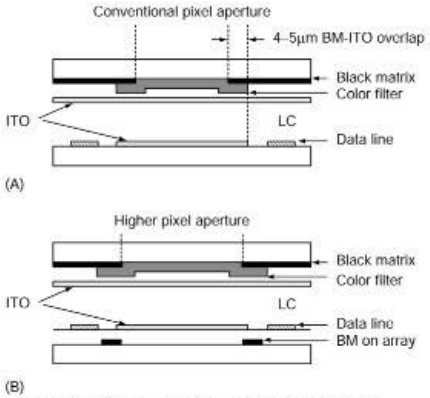

Figure 6.2: Pixel opening in conventional and in black-matrix-on-array designs.

In super-high-aperture designs (Fig. 6.3), the ITO pixel electrode overlaps the data and select buslines so that the buslines effectively function as the black matrix [1]. This leads to an even higher aperture of up to 80%. A thick polymer interlevel dielectric is used in super-high-aperture designs to passivate the TFT array. The ITO pixel electrode is patterned on top of the transparent polymer and makes contact to the TFT and the storage capacitor through vias in the polymer. The polymer is quite thick (2–3 μm) and has a relatively low dielectric constant of 2.7–3.5 to minimize the capacitance between the overlapping pixel electrode and buslines, required to keep vertical cross-talk in check.

The polymer has the added benefit of planarizing the TFT array surface and minimizing the LC disclinations at pixel edges, discussed in Chapter 5, Sec. 5.7. In principle, the black matrix becomes redundant and can be left out. However, this would expose the light-sensitive channel of the a-Si TFT to ambient light and would also cause the ambient light to reflect off the metal buslines, increasing display reflectance. An opaque, low-reflectance black matrix layer on the color plate is therefore still needed above the TFT channel as a light shield to prevent photo-leakage currents in the TFT and to minimize display reflectance. In a super-high-aperture design, however, the pixel opening in the black matrix can be much larger, as shown in Fig. 6.4. Obviously, the aperture ratio also depends strongly on the design rules and the pixel size. For larger pixels and more aggressive design rules, it tends to increase.

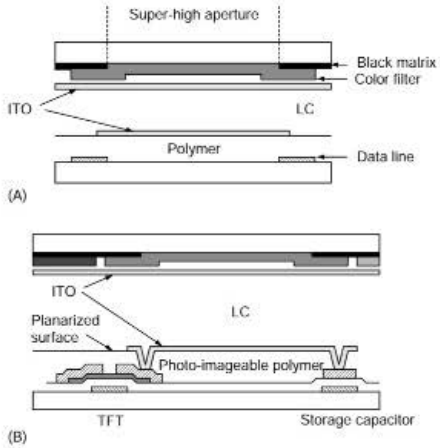

Figure 6.3: Cross section of super-high-aperture pixel through the data buslines (A) and through TFT and storage capacitor (B).

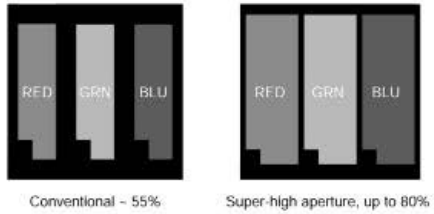

Figure 6.4: Comparison of aperture ratios in conventional and super-high-aperture ratio pixel designs as observed on a close-up view of an AMLC.

High aperture is important for portable applications, allowing the backlight intensity to be lowered while maintaining display luminance. The reduced power consumption in the backlight extends battery life. Alternatively, a higher brightness can be achieved without an increase in power consumption when the backlight intensity remains constant.

The material for the polymer in super-high-aperture designs may be the same as that used for the color filters except that the color pigments are not present. For example, it can be a photodefinable clear acrylic. Like the color filters, it is photo-imageable (i.e., it does not need photoresist coating, developing, and stripping, but is in itself a resist material).

Expanding on this concept, it is logical to go one step farther by simply replacing the polymer dielectric with color filter materials on the TFT substrate. This is called the color-filter-on-array (COA) method; see Fig. 6.5.

By patterning the color filters on the TFT array, the highest possible aperture is achieved (Fig. 6.5). The transparent polymer is replaced by separately patterned red, green, and blue color filters in each subpixel [2]. In the COA method the top plate has only a blanket transparent ITO layer. If the color filters cover the TFT channel they can also block most of the ambient light, eliminating the need for a black matrix. Since the common ITO layer is not patterned, there is no longer any critical alignment between the two glass plates and aperture is maximized. For very large substrates in Generation 6 and 7 facilities, it is very difficult to maintain accurate overlay accuracy between the top plate and the TFT array plate for all displays on the substrate. The COA design eliminates this problem and has therefore been considered in these advanced facilities. The drawback of the COA method is that the manufacturing complexity of the active substrate is significantly increased with at least two extra deposition and patterning steps, which can have an impact on yield.

6.1.3 Alternative Color Filter Arrangements

There are other methods to increase brightness without turning up the backlight. One that has received a lot of attention is alternative color filter arrangements. For example,

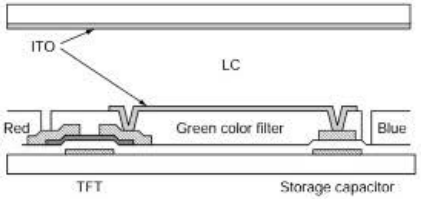

Figure 6.5: Cross section of a pixel in a COA (color-filter-on-array) TFT.

the use of four subpixels with red, green, blue, and white color filters was proposed and implemented in avionic TFT LCDs more than ten years ago and has now also been proposed for commercial products [3]. The white subpixel serves to increase the maximum luminance by almost 50%. It can be separately patterned as a transparent polymer without color pigment. Since color filter factories are normally set up to pattern only three color filters, the white subpixel can be left open without any material. This would make the LC cell gap larger in the white subpixel by about 2 µm, which can lead to contrast ratio problems. A blanket transparent polymer overcoat, not requiring pixelized patterning, is therefore used to planarize the color filter plate and make the cell gap more uniform.

The four subpixels can be arranged in a vertical stripe or in a quad structure, as shown in Fig. 6.6. To maximize aperture ratio, an RGBW quad arrangement is preferred, which also has the advantage of reducing the number of data driver ICs [3]. A drawback of an RGBW quad is the doubling of the number of rows and reduction of the line select time by 50%, making the quad arrangement more susceptible to propagation delays on the gate lines. This is only an issue for large and high-resolution displays. Special image processing algorithms are needed to convert RGB video signals to RGBW signals while maintaining the gray scale gamma. The overall color gamut can be slightly reduced with this approach. When the RGBW subpixel configuration is combined with a high-aperture design, the transmittance of the AMLCD can approach 15%.

6.1.4 Brightness Enhancement Films

Display screens in notebook computers and many other portable devices are generally viewed by a single person at an angle close to normal to the screen. The image quality and brightness at oblique angles is therefore less important in these applications. The

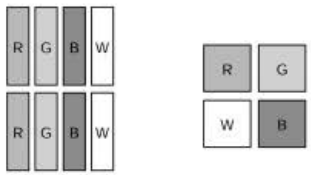

Figure 6.6: RGBW color filter arrangements to improve brightness.

brightness at normal angles can be enhanced without increasing power consumption in the backlight by adding brightness enhancement films (BEF™) between the backlight and the display [4]. In the simplest configuration, the enhancement comes at the expense of a luminance loss at some oblique angles. The BEF™ film, produced by 3M, is basically a transparent prismatic film made from plastic, as shown in Fig. 6.7. It redirects the diffuse light from the backlight by refraction. The prisms have, for example, an angle of 90 degrees and a pitch of 20–50 µm. Some of the light is refracted toward the viewer and some is reflected back to be recycled in the backlight and reused. By using two BEF™ films (in notebooks, cell phones, and PDAs), even higher luminance can be achieved. The result is an increased brightness at normal angles of up to a factor of two.

More expensive brightness-enhancement films include polarization recovery. They transmit light of one polarization direction and reflect the other polarization component back into the direction of the backlight. The reflected component loses its polarization in the diffuse reflector of the backlight, so that it is recovered and can contribute to display luminance after a single or multiple reflections. This DBEF™ film [4] can increase luminance by up to a factor of four. Its manufacturing cost is quite high, however, so that it is used mostly for high-end applications.

In Fig. 6.8 an example is shown of the brightness enhancement obtained with various stacks of 3M's Vikuity™ films. The best performance in the figure is for a configuration which includes an enhanced specular reflector (ESR) behind the backlight.

6.2 Readability Under High Ambient Lighting Conditions

A unique feature of LCDs is their potential for very low reflectance as compared to emissive displays such as CRTs, plasma displays, and electroluminescent displays. This makes the LCD the display of choice when sunlight readability is required in high-end or out-

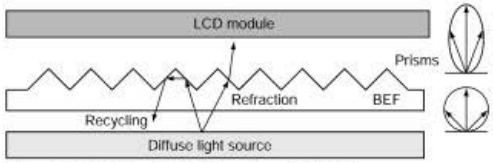

Figure 6.7: Light path in 3M's prismatic brightness enhancement film (BEF™).

door applications. However, this feature is not automatic; it needs some special steps in the manufacturing process. Without these special steps, specular reflectance is not particularly low (Fig. 6.9A). A Cr black matrix reflects about 6% and the polarizer about 7%, for a total reflection of more than 13%.

The effective contrast ratio CR_{eff} under ambient lighting is significantly reduced when there are reflections from the display:

$$CR_{eff}(A_0) = \frac{I_0 + RA_0}{(I_0/CR_0) + RA_0}, \tag{6.1}$$

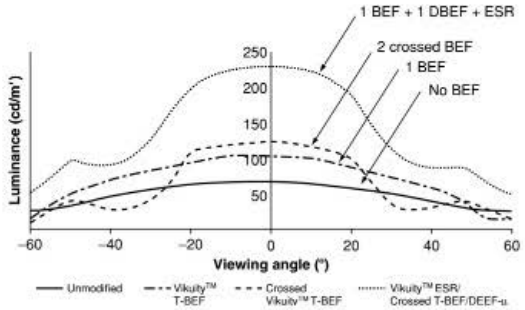

Figure 6.8: Example of brightness enhancement for different film stacks of 3M Vikuity™ films.

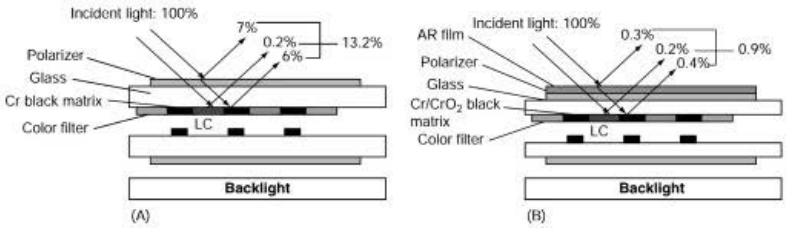

Figure 6.9: Conventional AMLCD (A) and AMLCD with minimized reflectance by adding AR film on a polarizer and by use of low reflectance Cr/CrO2 black matrix (B).

where A_0 is the ambient light intensity, I_0 is the transmitted light intensity for a fully white driven area on the display, R is the reflectance of the display (which is independent of the display image content in a first approximation), CR_0 is the contrast ratio in the dark, and I_0/CR_0 is therefore the luminance transmitted for a fully OFF dark pixel in the absence of ambient light.

R can be the specular reflectance causing glare, in which case CR_{eff} is the specular contrast ratio under an angle complementary with the incident angle. R can also be the diffuse reflectance, in which case CR_{eff} is the diffuse contrast ratio.

The reflected ambient light RA_0 is approximately the same in the ON state and OFF state. It has no information, it competes with the light transmitted through the display containing information, and therefore it reduces contrast ratio and causes glare.
In Fig. 6.10 the effective contrast ratio CR_{eff} is plotted as a function of the ambient light/display luminance ratio A_0/I_0 for different values of the reflectance R. As shown in the figure, the contrast ratio decreases asymptotically to 1 for high ratios of ambient lighting to display luminance.

In AMLCDs without special precautions, as well as in emissive displays, the display reflectance is typically more than 5%, so that contrast ratio drops off rapidly in bright outdoors conditions. For example, for a display with a dark room contrast ratio CR_{eff} = 300, the effective contrast ratio CR_{eff} = 20, when I_0 = 1000 cd/m², R = 5% and RA_0 = 50

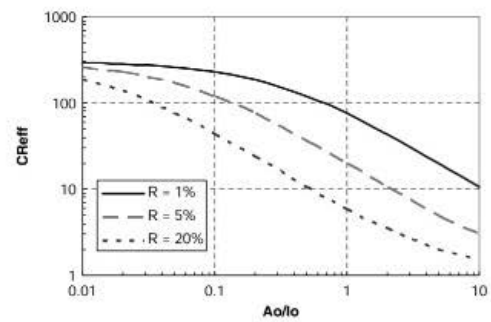

Figure 6.10: Effective contrast ratio versus relative ambient light level for different values of display surface reflections.

cd/m^2 (see Eq. 6.1 and Fig. 6.10). A high display reflectance also explains the annoying glare on emissive displays (such as plasma displays) when they are viewed in a bright environment.

In backlit AMLCDs a high contrast ratio can be maintained even at high ambient lighting by increasing I_0 and minimizing R. The unique opportunity exists to reduce the reflectance R to less than 1%. This is possible because the refractive index of the color filters is almost the same as that of glass (n = 1.5), so that reflections at the glass-color filter interface are negligible.

By using a CrO_2/Cr black matrix with 0.4% reflectance or a black polymer black matrix with even lower reflectance and an AR coating on the polarizer, total reflectance in TFT LCDs can be dramatically reduced to less than 1% (Fig. 6.9B). The glare can be further reduced by an anti-glare treatment on the front polarizer, as shown in Fig. 6.11. The surface is roughened so that incident light is scattered. This is a standard process on notebook LCDs and LCD monitors. In LCD televisions an additional AR coating on the glare-treated surface optimizes ambient light performance. The reflectance of less than 1% in LCD televisions compares favorably to around 12% in CRT television and 8% in plasma displays.

Taking these precautions makes the AMLCD legible even under bright sunlight conditions, provided that the backlight intensity is sufficient to overcome the reflected light. For outdoor applications it is recommended to avoid anti-glare coatings, and use only an AR coating on a smooth surface. The diffused ambient light outdoors can be as high as 10,000 fC, which will add a large RA_o factor and significantly reduce CR_{eff}.

6.3 Color Gamut Improvements

The color gamut shown in Fig. 5.2 in Chapter 5 limits the number of reproducible colors to the triangle derived from the three primary colors. As explained in Sec. 6.1.1. in this

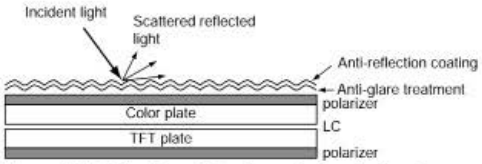

Figure 6.11: Reduction of glare by anti-glare treatment.

chapter, more saturated colors can be obtained with denser color filters, at the expense of luminance. A more attractive approach is to use a backlight with narrower peaks matching color filters with equally narrow width. For example, a well-designed LCD with an RGB LED backlight can have a better color gamut (close to 100% NTSC).

Another method to increase color gamut is the use of more than three primaries. LCDs with four and six primary colors have been demonstrated, by employing additional subpixels with different color filters. This approach requires extra processing and conversion of RGB data signals to multiple color signals in image processing. An example of the resulting improvement possible in the color gamut is schematically shown in Fig. 6.12 for a display with six primary colors. The addition of more color subpixels, which each transmit a smaller fraction of the backlight intensity, is likely to reduce luminance. Whether this color improvement is practical in terms of cost therefore depends on the application.

6.4 Wide Viewing Angle Technologies

An often-quoted drawback of conventional TN LCDs has been their poor viewing angle behavior. When observed straight on, contrast ratio and color gamut can be excellent. When the viewer turns his or her head and looks at a notebook display under an oblique angle, the contrast ratio drops fast, colors become less saturated and, under some angles, image inversion can even occur. This viewing angle behavior is usually acceptable for devices smaller than 15 in. with a single user, such as notebooks, PDAs, and cell phones.

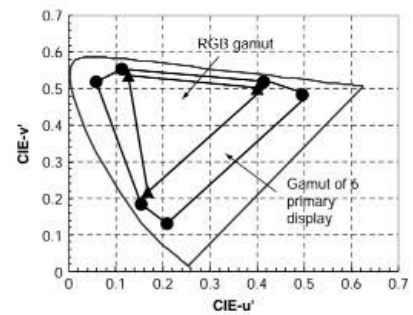

Figure 6.12: Increase in the color gamut by using more than three primary colors.

The origin of the problem was explained in Chapter 5, Sec. 5.3. and illustrated in Fig. 5.9. It can be traced back to the variation of the viewing angle relative to the LC director.

For larger, conventional TN LCDs, such as 17-in. and larger desktop monitors or LCD televisions, a single viewer at a distance of 10 or 20 in. will look at different corners of the screen under different viewing angles and the variation of contrast with viewing angle becomes objectionable. When there are multiple viewers looking at the display from different angles, similar image quality deterioration occurs.

A number of dramatic improvements in viewing angle have been developed over the past 10 years. The most important ones are:

- The addition of retardation compensation films,
- The in-plane-switching (IPS) LC mode, and
- The multidomain-vertical-alignment (MVA) LC mode.

6.4.1 Compensation Films

Retardation or compensation films are added outside the display glass assembly. They are attractive because they do not require a change in LCD manufacturing up to the final lamination of the polarizers, and they maintain the pixel aperture ratio of the original panel. Retardation films compensate for the variation over angles in the phase difference between the two orthogonally polarized components of the light wave in the LC layer.

They improve horizontal and, to a lesser degree, vertical viewing angle in TN mode LCDs. They are also used in some LCDs operating in different modes. Basically, the contrast ratio (the ratio of white to black luminance) is improved over viewing angle. Since white luminance is mostly limited by the backlight, the key to improvements is to reduce luminance in the dark state over angles.

An example is shown in Fig. 6.13 for the normally white TN cell which uses an LC fluid with positive optical anisotropy. Two so-called discotic retardation films are added outside each of the glass substrates. The films have a negative optical anisotropy and a gradually tilted optical axis. In the dark state of the normally white TN cell (with voltage applied), the LC director is similarly gradually tilted from the surface to the center of the cell. As shown in the figure, a pair-wise cancellation of the retardation in the LC fluid with positive Δn and the retardation in the film with negative Δn occurs. The total retardation of a light ray traversing the TN cell and compensation films becomes independent or less dependent on viewing angle, as shown in Fig. 6.13. The result is a significant reduction of dark luminance over wide viewing angles and a better contrast ratio over viewing

angle. The discotic negative birefringence film was developed and commercialized by Fuji Photo Film[30] [5] and has been widely used on smaller LCD monitors.

This basic concept has been implemented with a variety of compensation films on both sides or on one side of the cell.

6.4.2 In-Plane-Switching Mode

Arguably, the best viewing angle is achieved in a different LC mode, the in-plane-switching (IPS) mode (Fig. 6.14). In the IPS mode the data voltage is applied between electrodes on

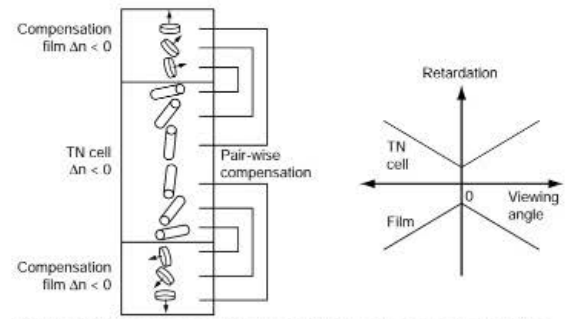

Figure 6.13: Example of a TN cell combined with compensation films and resulting retardation versus viewing angle.

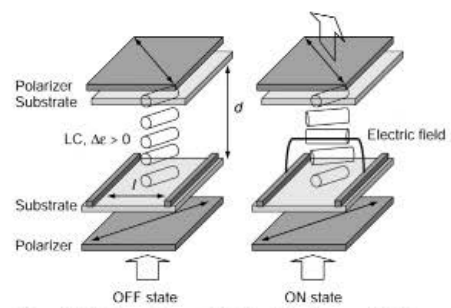

Figure 6.14: Operating principle of in-plane switching.

the TFT array, so that the electric field is parallel to the glass plates. The lateral electric field causes the LC molecules to rotate parallel to the plates. Since the LC director always remains parallel to the glass plates, this leads to a fairly symmetric, very wide viewing cone. The dielectric anisotropy $\Delta\varepsilon$ of the LC fluid is usually positive. For $\Delta\varepsilon > 0$, the LC molecules line up parallel to the lateral electric field.

In Fig. 6.14 the basic operation of the IPS mode is shown. The alignment layers on both surfaces are rubbed under an angle of 45 degrees with the electrodes on the active matrix substrate. Linearly polarized light enters the cell parallel to the LC director. In the absence of an electric field, the orientation of the LC director is uniform throughout the cell and light emerges without a change in polarization. The exit polarizer is oriented perpendicular to the first polarizer and therefore blocks the light. When a voltage is applied between the electrodes in the ON state, the LC molecules line up to the field and the angle between the LC director and the polarization direction becomes gradually 45 degrees with increasing voltage.

The transmission T of this normally black IPS cell with crossed polarizers can then be described by the following equation:

$$T = T_0 \sin^2(2\theta(V)) . \sin^2\left(\frac{\pi \Delta n . d}{\lambda}\right), \tag{6.2}$$

where T_0 is a constant depending on the polarizer transmittance and aperture ratio of the cell and $\Theta(V)$ is the angle between the LC optical axis and polarization angle of the incident light, which can be varied with the applied voltage V. Δn is the LC optical anisotropy, d is the cell gap, and λ is the wavelength. The cell gap is chosen so that $\Delta n.d = 0.3$ µm. This means that the last term in Eq. 6.2 is close to unity in the visible spectrum.

At $V = 0$, the LC optical axis is parallel to the incident polarization angle, so that $\Theta = 0°$ and $T = 0$. At high voltage (~7 V) most of the LC molecules are lined up parallel to the electric field (when $\Delta\varepsilon > 0$) so that $\Theta = 45°$ and $T = T_0$. Like the TN cell, the IPS cell is operated with an AC square wave voltage without the DC component.

The threshold voltage V_{th} for the IPS mode is

$$V_{th} = \pi\left(\frac{l}{d}\right)\sqrt{\frac{K_{22}}{\varepsilon_0 \Delta\varepsilon}}, \tag{6.3}$$

where l is the spacing between the lateral electrodes across which the electric field is applied, K_{22} is the LC elastic constant for twist deformation, ε_0 is the permittivity in vacuum, and $\Delta\varepsilon$ is the dielectric anisotropy. V_{th} is the voltage at which the LC molecules in the center of the cell commence to rotate. It depends on l/d and is about 2–3 V. To

reduce the threshold voltage and operating voltage of the IPS mode, special LC fluids have been developed with a large $\Delta\varepsilon$.

An example of the electro-optical response of an IPS cell for different wavelengths, corresponding to Eq. 6.2 is shown in Fig. 6.15.

Figure 6.16 shows some examples of pixel layouts for an IPS TFT LCD. The lateral electric field is applied between the drain electrodes, on which the data voltage is stored, and the counter electrodes, which are held at a constant bias. The pixel storage capacitor is formed by the overlap area of the counter electrode and the drain electrode. An ITO pixel electrode is not needed in this design. With both pixel electrodes on the TFT array, there is also no longer a need for a common ITO electrode on the color filters. However, to prevent sensitivity to external fields, a grounded ITO layer is often added as a shield between the front polarizer and the color plate. Since the pixel electrodes are opaque metal layers, they obscure the pixel opening significantly as compared to a TN TFT pixel. The pixel opening in IPS TFT LCDs is typically less than 50%.

Equation (6.3) shows that the threshold voltage of the IPS mode depends on both electrode spacing and the LC cell gap. In the TN cell, on the other hand, the electrode spacing is the same as the cell gap so that the threshold is independent, to a first approximation, of the cell geometry (see also Chapter 1, Sec. 1.4.). More accurate control of the cell gap in manufacturing is therefore needed for the IPS mode than for the TN mode.

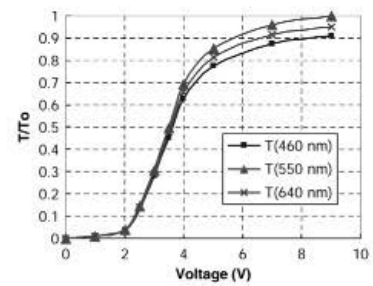

Figure 6.15: Transmittance-voltage curve for a typical IPS cell at different wavelengths.

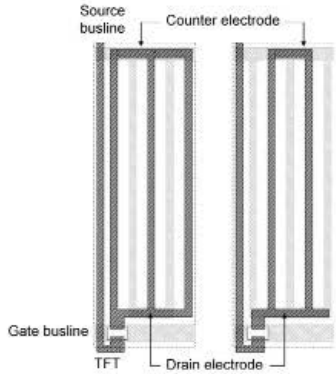

Figure 6.16: Examples of pixel layouts for an IPS cell.

Small electrode spacings give a lower operating voltage in the IPS mode. There is, however, a trade-off between operating voltage and aperture ratio. For a smaller electrode spacing, a larger fraction of the pixel area is occupied by the opaque metal electrodes. Aperture ratio is generally much lower than in the regular TN mode with or without compensation films. This is the price to pay for the viewing angle improvement. To maximize the aperture ratio, the electrode spacing has been increased from $l/d \approx 3$ to $l/d \approx 7$ in conjunction with the development of 15-V data driver ICs, which can apply +7 and −7 V on the pixel in the dot inversion mode.

The IPS mode was originally commercialized by Hitachi [6] and has been implemented by a number of companies in monitors and LCD televisions. Of all LC modes, it arguably maintains the best image quality over viewing angles. Not only is the contrast ratio larger than 10× up to 170-degree viewing cones, but the color shift and gamma shift over viewing angle are also minimal.

Drawbacks of the IPS mode are a somewhat lower peak contrast ratio at normal angles and a lower aperture ratio to accommodate the multiple electrodes on the pixel. The early IPS LCDs also had slow response times, exceeding 50 msec. With the development of better LC fluids specifically for IPS and with optimized cell structures, the response times have been reduced to be acceptable for television and contrast ratio has been improved to more than 600:1.

A number of variations and improvements on IPS, such as Super-IPS® introduced by Hitachi and True Wide IPS® introduced by LG Philips LCD, have pushed the state of the art even farther. With the original IPS pixel designs with the rectangular electrode configuration of Fig. 6.16, some asymmetry in the viewing cone occurred. In Super-IPS® LCDs the lateral pixel electrodes are in a chevron pattern, as shown schematically in Fig. 6.17.

Both the entrance polarizer axis and the initial LC molecule orientation at V = 0 are vertical. There is a difference in the electric field direction in different sections of the pixel, so that the LC molecules rotate in opposite directions. As a result, there is more than one domain in each subpixel. This tends to further widen the viewing angle and improve symmetry of the viewing cone. It also reduces the color shift over viewing angle [7]. In Fig. 6.17 the angle between the polarizer and the lateral electric field is about 60 to 70 degrees. In this case, the angle Θ between the entrance polarizer and the LC director can exceed 45 degrees so that the transmittance-voltage characteristics show a peak at $\Theta(V) = \pi/4$ and then decline (Fig. 6.18), in accordance with Eq. 6.2.

The rise and fall response times in the IPS mode are given by

$$\tau_r = \frac{\gamma_1}{\varepsilon_0 \Delta\varepsilon E^2 - \frac{\pi^2 K_{22}}{d^2}}, \tag{6.4}$$

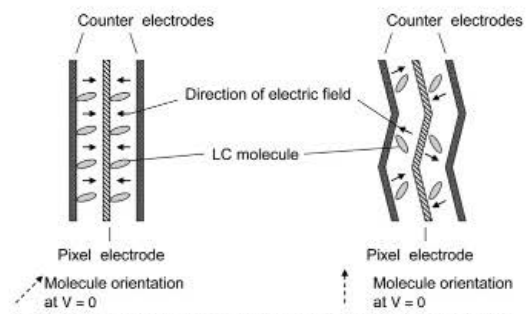

Figure 6.17: Electrode configuration of a conventional IPS (left) and a Super IPS (right) pixels.

$$\tau_f = \frac{\gamma_1 d^2}{\pi^2 K_{22}}, \tag{6.5}$$

where E is the electric field applied between the lateral electrodes. As in the TN mode, the response times depend strongly on cell gap d. Reducing d improves video performance but increases the threshold voltage of the IPS mode (Eq. 6.3). Since maintaining uniformity in manufacturing becomes increasingly more difficult for thinner cell gaps, a practical value is around 4 μm. With the development of LC fluids with high $\Delta\varepsilon$ specifically for the IPS mode, good video performance has been achieved.

A variation on the IPS mode is the fringe-field-switching (FFS) mode introduced by BOE Hydis. It has excellent viewing angle, comparable to IPS, and minimizes one of the drawbacks of IPS: the limited transmittance. In the FFS mode a higher aperture ratio is obtained by the use of a continuous common ITO electrode separated from ITO grid electrodes by a dielectric. Both electrodes are on the active matrix array and are transparent, so that the pixel opening can be significantly larger than in most IPS TFT LCDs, where both electrodes are opaque.

6.4.3 Vertical Alignment

Another successful approach to improve viewing angle is the vertical alignment (VA) mode (Fig. 6.19). In the VA mode the nematic LC molecules are aligned perpendicular to the glass plates in the absence of an electric field. This requires a different type of alignment layer. The rubbing process is eliminated in the VA mode, which translates into a yield advantage.

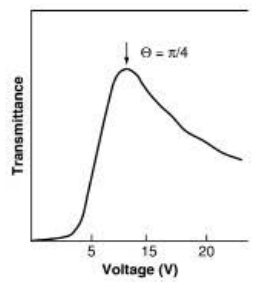

Figure 6.18: IPS T-V curve when Θ can exceed π/4.

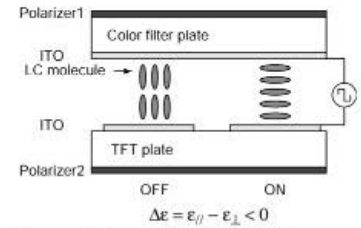

Figure 6.19: Operating principle of the vertical alignment (VA) mode.

LC fluids for the VA mode are specially formulated to have a negative dielectric anisotropy $\Delta\varepsilon$ of −3 to −4. These LC fluids have lateral polar substituents that induce a dipole moment perpendicular to the long axis (the director) of the molecule, hence the negative dielectric anisotropy.

This means that when a voltage is applied between the transparent electrodes on the two plates, the long axis (the director) of the LC molecules rotates to become oriented parallel to the plates. The operating principle of the VA mode is illustrated in Fig. 6.19.

In the basic VA mode the molecules can start tilting with their director in any plane perpendicular to the glass substrates. For situations with partial tilt, this would lead to domains with varying retardation under oblique angles and therefore varying, uncontrolled contrast.

In order to obtain a more symmetrical viewing angle, the pixel is subdivided into domains, in each of which rotation starts with well-defined different initial tilt. This is called the multi-domain vertical alignment (MVA) mode (see Fig. 6.20). The multiple domains are obtained by adding protrusions on both substrates. They cause the pixel to have areas of different preferential tilt direction in the cell when an electric field is applied between the two substrates.

The cell operates with crossed polarizers in the normally black mode. Without applied field, most LC molecules line up perpendicular to the substrate surfaces so that the polarization is not changed. The exit polarizer blocks the light. When a moderate field is applied, the LC molecules tilt preferentially in a direction controlled by the protrusions so that the polarization is partially altered to obtain a mid-gray level. At high field, the center molecules line up parallel to the surfaces as a result of the negative dielectric anisotropy. The LC fluid now rotates the polarization direction depending on the angle

of the entrance polarizer and the LC director. The two or four domains have the effect of making the viewing angle symmetric in two or four directions.

Figure 6.21 shows a pixel layout of a protrusion design to obtain four domains per pixel for the MVA mode. A zigzag grid of protrusions at 90 degrees on the active and color

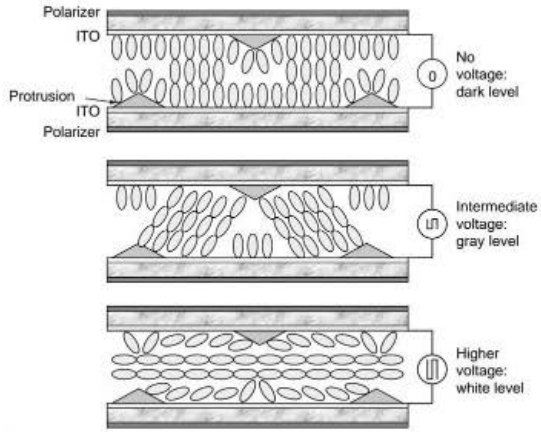

Figure 6.20: Multi-domain vertical alignment (MVA) using protrusions on the two substrates.

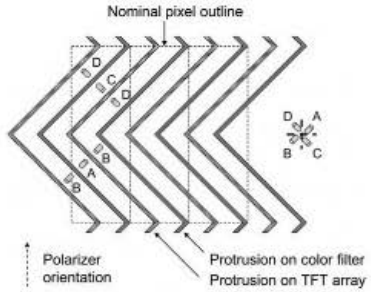

Figure 6.21: Protrusion design for a four-domain MVA LCD [8].

plates is used. The entrance polarizer is vertical along the column lines so that the LC director in each of the four domains will be oriented at +/–45 degrees with the polarizer orientation in the presence of an electric field. The protrusions block the light and therefore need to be kept small to minimize impact on the aperture ratio. The aperture ratio, however, will be smaller than in a regular TN mode with or without compensation films. In Fig. 6.22 a transmittance-voltage curve for the MVA mode is shown.

The MVA mode is popular in desktop monitors and LCD televisions, and combines a wide viewing angle with a fast response time. It was originally introduced by Fujitsu [8] and has been adopted by a number of manufacturers.

Variations and improvements, called patterned vertical alignment (PVA® and super-PVA®), and premium-MVA® mode, have been introduced by Samsung and AU Optronics, respectively. Some improvements have protrusions on only one substrate and aperture ratios as high as 67% have been achieved. Of particular interest is Samsung's PVA mode, which eliminates the protrusions altogether and instead uses patterned ITO areas on both the TFT and color substrate to obtain multiple domains, as shown in Fig. 6.23. An extra ITO patterning and etching step on the color plate is needed for the PVA process. As in the MVA mode, a four-domain design is common with zigzag-shaped slits in the ITO layers. To maximize aperture ratio, the data buslines can also be designed in a zigzag pattern [9].

In the dark state of the PVA mode (V = 0), the LC molecules are perfectly lined up perpendicular to the glass plates. As a result, there is no residual retardation and the contrast ratio can be virtually equal to the extinction ratio of the polarizers. With the optimized

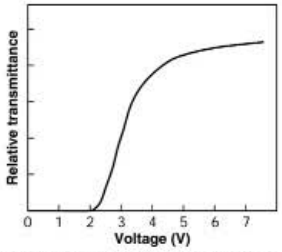

Figure 6.22: Typical transmittance curve for an MVA LCD.

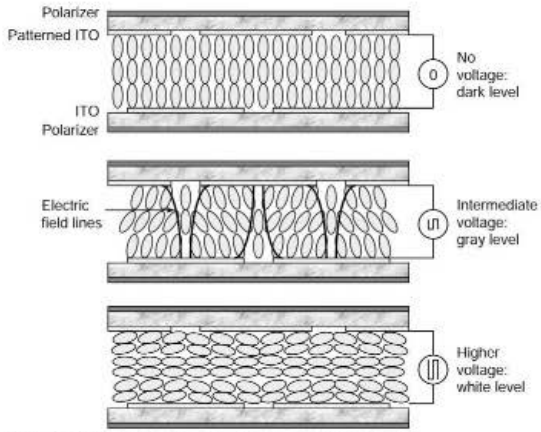

Figure 6.23: Patterned vertical alignment (PVA) mode.

super-PVA mode [9], a contrast ratio larger than 1000 at normal viewing angles has been achieved (Fig. 6.24). A contrast ratio exceeding 1000:1 is particularly important for LCD television where any light leakage in low ambient lighting conditions is objectionable.

In the protrusion-based MVA mode it is more difficult to achieve a contrast ratio of 1000:1 because the small tilt near the protrusions causes some residual retardation and light leakage in the dark state (V = 0). IPS-mode LCDs have a lower peak contrast ratio as well, but usually have an even better contrast ratio off-axis than is shown in Fig. 6.24. As compared to the original contrast versus viewing angle curve of a standard TN cell shown in the previous chapter (Fig. 5.6), the MVA, PVA, and IPS modes have all demonstrated tremendous progress in image quality.

MVA-mode LCDs use a special alignment layer to cause the vertical orientation of the LC molecules at the substrate surfaces. Unlike the TN and IPS modes, this orientation layer does not need a rubbing process, which is considered a yield advantage in manufacturing for the MVA and PVA modes.

To compensate for the off-axis retardation in the zero field dark state, MVA-mode AMLCDs do, however, usually require retardation films added outside the glass assembly.

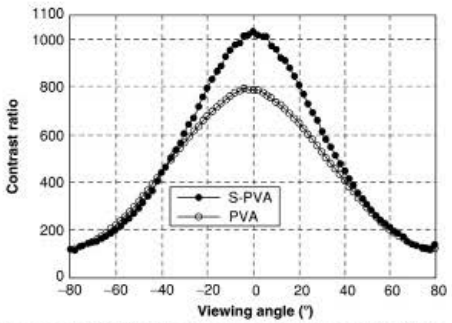

Figure 6.24: Contrast ratio versus viewing angle for PVA and S-PVA mode (reprinted with permission from the Society for Information Display).

A variation on the VA mode is the advanced super view or axially symmetric vertical alignment (ASV®) mode used by Sharp in their LCD televisions. In the ASV method (Fig. 6.25), the domains have random directions leading to a completely symmetric viewing cone.

6.4.4 A Comparison and Other Viewing Angle Improvement Methods

The viewing angle behavior of LC cells can be quantitatively expressed as contrast ratio versus left/right and upper/lower viewing angles, as shown in Figs. 5.6 and 5.8 in Chapter 5. These plots show the performance only at azimuth angles of 0, 90, 180, and 270 degrees. To include all azimuth angles, it is customary to plot the viewing angle behavior in contrast contour plots with azimuth angle ϕ and polar angle θ as parameters, as defined in Fig. 6.26.

These two angles are used to generate the contrast contour plots shown in Fig. 6.27 for unmodified TN-, compensated TN-, IPS-, and MVA-mode cells. The iso-contrast curves enclose areas with higher contrast. The plots are representative for measured results with the caveat that improvements are still regularly reported and that there is some variation from one manufacturer to the next. For both the MVA mode and the IPS mode, a contrast ratio exceeding 10:1 has been achieved for polar angles up to 80 degrees at all azimuth angles.

There are a few other, less popular methods to improve viewing angle, notably the multi-gap normally black TN mode and the TN mode with collimator-diffuser combination.

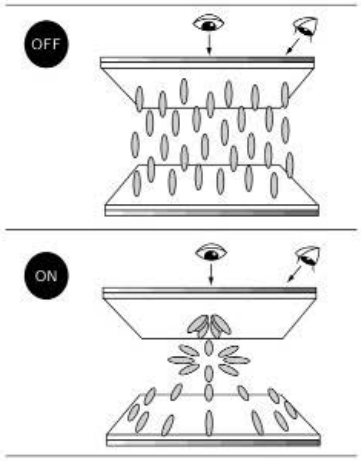

Figure 6.25: Operating principle of the ASV mode.

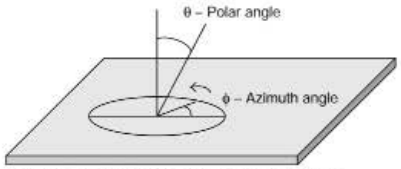

Figure 6.26: Definition of polar and azimuth angles for measuring and plotting contrast contours.

The normally black (NB) TN mode has better contrast ratio at off-angle viewing than the normally white mode, but a lower peak contrast ratio with a white backlight. The contrast ratio varies with wavelength and LC cell gap according to the Gooch–Tarry theory (Fig. 6.28), as was described in Chapter 5, Sec. 5.2.

The NB TN LCD can be designed with different cell gaps for each color so that the cell operates in the first minimum for red, green, and blue light. This is done by tailoring the cell gaps according to the following equations:

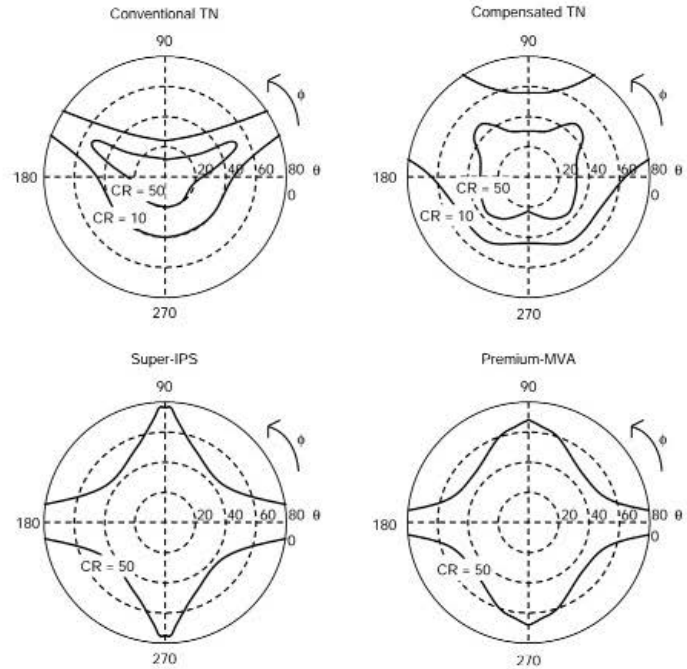

Figure 6.27: Contrast contour plots for four different LC modes.

$$d_R = \frac{\sqrt{3}}{2}\frac{\lambda_R}{\Delta n}, \tag{6.7}$$

$$d_G = \frac{\sqrt{3}}{2}\frac{\lambda_G}{\Delta n}, \text{and} \tag{6.8}$$

$$d_B = \frac{\sqrt{3}}{2}\frac{\lambda_B}{\Delta n}; \tag{6.9}$$

where d_R, d_G and d_B are the LC cell gaps for the red, green, and blue subpixels and λ_R, λ_G and λ_B are the peak wavelengths for the three primary colors. The color filter thicknesses are adjusted to obtain the different cell gaps, as shown in the inset of Fig. 6.28. A high peak contrast ratio and relatively wide viewing angle can be simultaneously achieved this way. However, the multiple cell gaps are very difficult to control accurately and consistently in manufacturing, and this mode has therefore been used only in high-end avionic cockpit displays but not in mainstream displays.

The collimator-diffuser approach (Fig. 6.29) avoids altogether the problem with off-angle viewing in the TN mode by collimating the light so that it passes through the LC cell

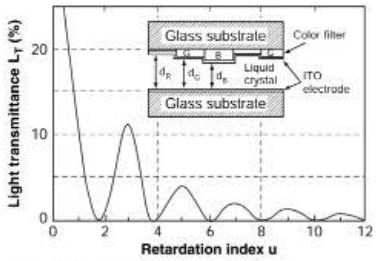

Figure 6.28: OFF state transmission in normally black TN mode with multi-gap configuration in inset.

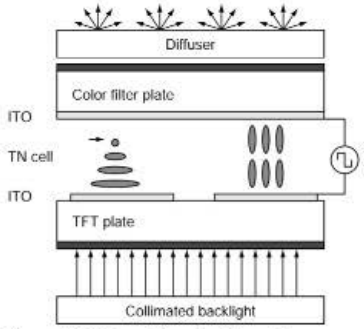

Figure 6.29: Operating principle of the collimator-diffuser mode.

mostly perpendicular to the glass plates with good contrast. A diffuser after the exit polarizer scatters the light. Its drawback is increased power consumption in the backlight and light loss in the front diffuser.

In Table 6.2 the major three viewing angle enhancement methods are compared with each other and with the conventional TN mode in terms of image quality, power consumption, and manufacturability. All three methods give much better image quality over angles than the conventional, uncompensated TN mode. Response times are not listed in the table because all three basic modes. TN, IPS, and MVA, have made similar progress toward video performance.

There is still active ongoing research to improve the different modes for televisions and monitors in terms of response times, color shift over angles and gray scale, and aperture ratio. The improvements and refinements are labeled with superlatives, some mentioned before, such as Super-IPS®, Advanced Super-IPS®, True Wide IPS®, super PVA® and premium MVA®.

6.5 Enhancement of Video Performance

When conventional LCD desktop monitors and notebook panels are used to display video from a DVD, for example, the image quality is inferior to that on a CRT. Although the contrast ratio for static images on such displays can exceed 500:1, for moving images degradation in the dynamic contrast ratio is seen and the edges of moving objects blur. This makes the viewing experience less than acceptable. Faster LC fluids have been developed with a lower rotational viscosity and the cell gap can be reduced to about 4 μm to improve response time (see Eqs. 5.11 and 5.12 in Chapter 5). These measures can lower the transition time from full ON to full OFF and vice versa to 8 msec for TN and MVA modes.

Table 6.2: Comparison of different viewing angle improvement modes

	Conventional TN	Compensated TN	IPS	VA
Viewing angle	-	x	0	Δ
Peak CR	Δ	Δ	Δ	0
Gamma shift over angle	-	x	0	Δ
Color shift over angle	-	x	0	Δ
Power consumption	0	0	x	Δ
Manufacturability	0	0	Δ	Δ

0, very good; Δ, good; x, less; -, poor.

However, this by itself does not reduce smearing of moving video images sufficiently for application of LCDs in televisions. In video imagery the majority of transitions are between intermediate gray levels, which have longer response times, according to Eq. 5.11. The response time between different gray levels can exceed 50–80 msec in a conventional TN cell.

Another factor influencing motion portrayal is the hold-type character of an LCD (i.e., the luminance is continuous during each frame time). A data voltage is applied to each pixel once per frame time and maintained during the entire frame until the next refresh. This sample-and-hold mode of operation cannot eliminate an afterimage on the retina and causes blurring of fast-moving objects on the LCD. The problem is exacerbated when the display is large and/or viewed from close-up. This is contrary to the impulse-type character of CRTs, in which each pixel emits light for only a fraction of the frame time.

In the following two sections, two solutions for these basic problems in LCDs are described:

1. Response time compensation by overdrive techniques, and
2. Emulation of impulse-type operation in an LCD.

6.5.1 Response Time Compensation

In Sec. 5.5 in the last chapter, the response times for the TN mode were given in Eqs. 5.11 and 5.12. These are the times for transitions from full ON to full OFF and vice versa. The rise time is voltage-dependent, so for transitions between intermediate gray levels the response times can exceed several frame times and are not short enough for high-quality video. The resulting image lag and motion blur is unacceptable for LCD televisions. In addition to rise and fall times of the LC cell in excess of a frame time, a contributing factor is the slow variation of the LC capacitance with voltage. When the data voltage on the pixel changes significantly, it can take more than a frame time for the LC capacitance to stabilize at its new value. Since a constant charge is loaded onto each pixel during active matrix addressing, the voltage may change during the frame time from V_{start} to V_{end} according to the equation

$$V_{end} = \frac{C_{start}}{C_{end}} V_{start}, \tag{6.10}$$

where C_{start} and C_{end} are the LC capacitance at the beginning and end of the frame time, respectively.

The adverse effects of both slow response times and dynamic LC capacitance can be countered by response time compensation [10]. To improve video performance, overshoot data voltages are used so that the target luminance is reached after one frame time. The principle of this response time compensation is illustrated in Fig. 6.30. The final gray level *i* cannot be obtained within one frame time by applying data level *i*. Instead, an overshoot data signal or boost level *k* is applied to the pixel and is stored on the pixel for one frame time. The overshoot level causes the display luminance to settle at the new gray level *i* within one frame time. The overdrive method requires signal processing and empirically optimized lookup tables for level-to-level transitions.

An example of the electronics required to implement response time compensation is shown in Fig. 6.31. One frame of incoming video signals is stored in a first in, first out (FIFO) frame buffer. The video data for each pixel in this frame is then compared with the video data for the next frame. Depending on the starting and ending gray level, an overshoot or undershoot voltage is added to the steady-state data signal for a particular gray level. The signal boost for each gray level transition is derived from a lookup table,

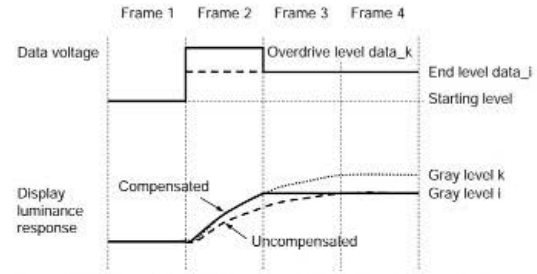

Figure 6.30: Overdrive data levels applied to speed up optical response time of display luminance between gray levels.

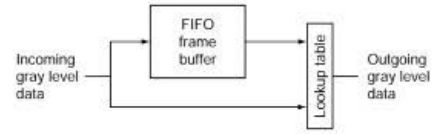

Figure 6.31: Basic block diagram for response time compensation.

which is optimized for the particular LC mode and cell structure used (TN, IPS, or MVA). The boost signal is usually inserted during one frame only, after which the steady-state gray level is applied (assuming no change in gray level in the subsequent frame).

The overdrive functionality with the lookup table and the comparison circuit can be integrated into the timing controller of the display or in separate added circuitry. The frame buffer memory is typically external in an SDRAM chip.

The plots in Fig. 6.32 demonstrate typical improvements in response times achieved by the overdrive method. When combined with faster LC fluids, response times of 8 msec have been obtained for all gray level transitions.

6.5.2 Emulation of an Impulse-Type Display

Even when the response times could be reduced to zero, the video performance of LCDs would still be inferior to that of CRTs. CRTs are impulse-type displays in which brief excitations of the phosphor result in brief repeating light pulses, which are integrated by the human eye and perceived as continuous while they are actually intermittent (Fig. 6.33). On the CRT, the edge of a moving object therefore remains sharp.

In an LCD (a hold-type display), the luminance is continuous. The eye traces a fast-moving object on the LCD screen as indicated by the arrow in Fig. 6.33. When integrating over the frame time, the average luminance leads to a blurry edge on the object.

One method to improve video performance is increasing the frame rate to, for example, 120 Hz. When all the gray-to-gray level transition times are also reduced to 8 msec, a faster frame rate of 120 Hz gives a clearly visible improvement. However, this does not solve the problem entirely and it also complicates the electronics and requires larger TFTs to charge up the pixels in half the time.

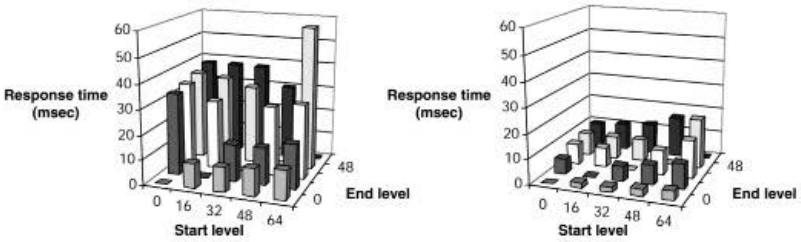

Figure 6.32: Example of uncompensated (left) and compensated (right) gray level response times.

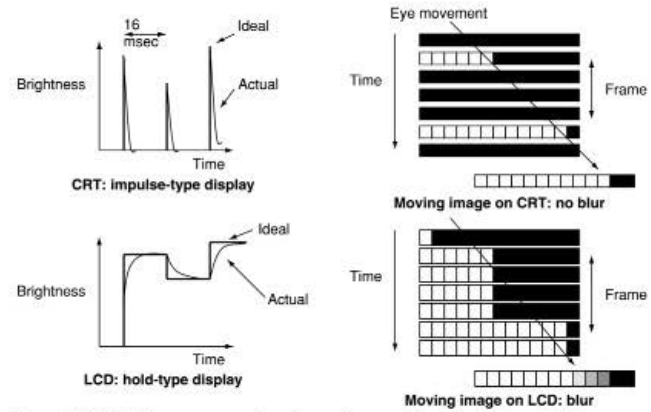

Figure 6.33: Brightness versus time for and perception of moving objects on a CRT and an LCD.

Another way to address the problem is to switch the backlight ON and OFF to get the impulse-type operation. This can be done be flashing the entire backlight at once after writing the data information on the displays, as shown in Fig. 6.34A. The LC transmittance has to be stabilized before the backlight turns ON. Part of the frame time is used for writing data and the second part for illumination. This causes a problem because the allowable LC response time for pixels at the bottom of the display will be shorter than for the top, causing moving objects with blurred edges at the bottom of the display for practical finite response times.

A better solution is a scanning backlight with, for example, six stick lamps and the timing shown in Fig. 6.34B. The physical configuration is depicted in Fig. 6.35. In this case the entire frame time can be used for writing data and the allowable LC pixel response time is the same at the top and the bottom of the display. An LC response time for all gray-to-gray levels of about two-thirds or one-half the frame time is sufficient to prevent moving objects with blurred edges.

The use of this scanning backlight emulates an impulse-type display and virtually eliminates blur of moving objects, as illustrated in Fig. 6.36. Motion on LCDs with scanning backlight appears more like a movie. Film projectors also darken the screen for about 50% of the time, during the mechanical advance to the next film frame. In the projector this is done by a shutter behind the lens.

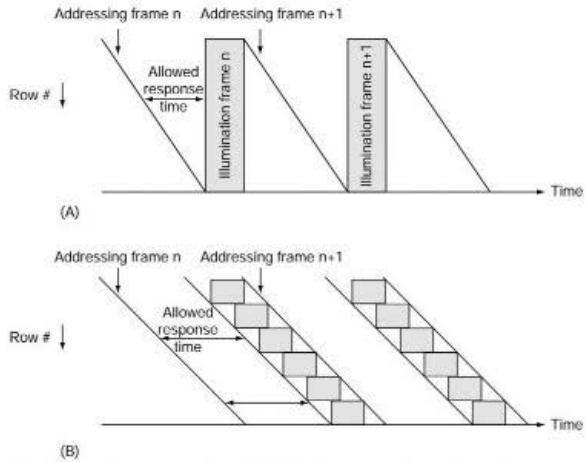

Figure 6.34: Synchronization of blinking backlight (A) and scanning backlight (with six lamps) (B) to vertical scanning of the LCD.

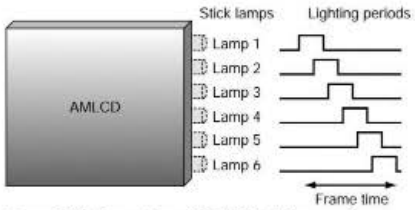

Figure 6.35: Operation of AMLCD with scanning backlight to improve video performance.

When one lamp in the scanning backlight is ON at a time and its brightness is not increased, an obvious drawback is that the average brightness is decreased by a factor of six. Since this is unacceptable, the lighting periods of the individual lamps will overlap in practical scanning backlights. There will be a trade-off between brightness and motion blur.

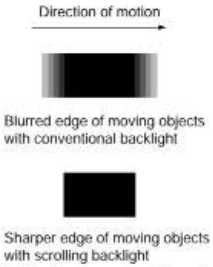

Figure 6.36: Qualitative improvement in motion portrayal with impulse-type (scanning or scrolling) backlight.

The scanning or scrolling backlight improves not only sharpness, but also the contrast and color purity of moving images. As explained in Chapter 4, Sec. 4.5, hot cathode fluorescent lamps (HCFLs) are a good match with scanning backlights. They can operate at higher currents to obtain very high luminance and can also be easily dimmed for intermittent operation. In the most advanced scanning backlights, both duty cycle and dimming level are dynamically controlled based on the video content and the ambient lighting conditions. With the gamma curve of the LCD also being dynamically adjustable depending on image content and ambient lighting, superior display performance is achieved with a sophisticated, correlated control of backlight and LCD electronics.

LEDs are compatible with scanning backlights as well. The peak current in the LEDs can be increased for shorter duty ratios so that the average luminance can be maintained quite well. LED backlights are also relatively easy to operate intermittently with current pulses at low voltage and will be attractive for scanning backlights, when their cost can be further reduced.

Another method to emulate an impulse-type display is to insert black data during part of the frame. To avoid flicker this needs to be done during part of the 16-msec frame and therefore requires very fast LC response times.

6.6 Large Size

With the advent of Generation 5, 6, and 7 production lines for a-Si TFT LCDs, it has become possible to build very large displays with a size approaching that of the largest

plasma displays. Before LCDs larger than 40 in. or with resolution higher than SXGA became possible, several technical hurdles had to be overcome. One is, of course, manufacturing yield, discussed in Chapter 3, Sec. 3.9. Another is the line resistance of the select and data buslines. When the signal propagation delays on the buslines becomes a significant fraction of the line select time, LCD performance can deteriorate.

This is the case also for 20- to 25-in. displays with very high resolution in the UXGA to QUXGA range, developed for graphics and medical imaging applications. They have a very short line select time, as shown earlier in Table 5.3.

Table 6.3: Resistivities of metal films used as buslines in LCDs

Metal	Resistivity (μΩcm)
Ta	80–200
Cr	20
Mo	13
AlNd	7
Al	4
Cu	2.5

Long buslines or short select line times both require the use of low-resistance gate lines to minimize the RC propagation delays. Figure 6.37 shows how the select pulse is distorted along the select line of a large or high-resolution display. The load on each pixel can be represented by a resistance R/N and capacitance C/N, where N is the number of pixels on a row. A distributed network of these capacitors and resistors represents the entire row. Both the rise time and the decay time of the gate pulse are increased at the end of the row line.

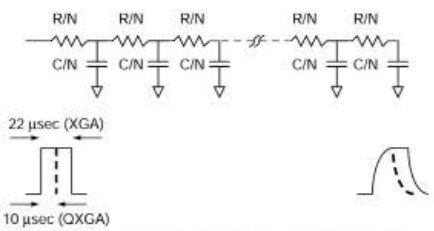

Figure 6.37: Equivalent circuit for gate busline with resistance R, capacitance C, and N pixels with example of gate pulse distortion along rows in XGA and QXGA cases.

With the aid of circuit simulations the effect of propagation delays on the LC pixel voltage can be predicted. The pixel charging is faster for the negative charging cycle than for the positive cycle, as a result of the higher gate voltage relative to the negative data voltage than to the positive data voltage. The pixel may not charge up completely to the positive data voltage (Fig. 6.38).

After the negative charging cycle, the pixel voltage shift from the parasitic gate-drain capacitance further reduces the voltage on the ITO pixel electrode. Because of the slow decay time of the gate pulse, the TFTs at the end of the row are not sufficiently turned OFF before the data voltage changes for the next pixel on the column. Then, there is a potential for partial recharging of the pixel to the next pixel's data voltage, as shown in Fig. 6.38.

Incorrect pixel charging leads to gray scale errors and/or residual DC voltage on the LC (and therefore image retention).

Conventional select line metals such as Ta, Cr, and Mo have a relatively high resistivity of more than 12 μΩcm (see Table 6.3 and Sec. 3.3 in Chapter 3). A high gate line resistance can show up in the display as a brightness gradient from the driven side to the undriven side or as an increase in flicker and image retention in sections of the viewing area. The RC delay is most severe when the storage capacitor is connected to the gate

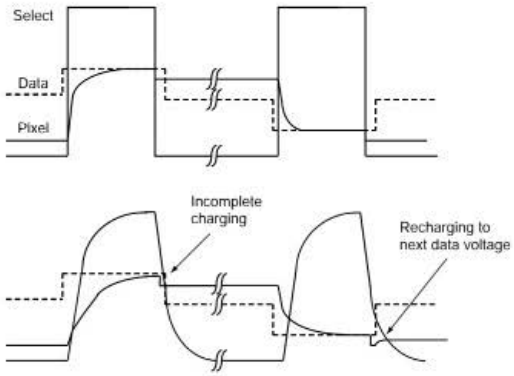

Figure 6.38: Pixel wave forms at beginning (top) and end (bottom) of gate line with RC delay.

line because it increases the capacitive load on the gate line. When the Cs-on-common pixel configuration (see Fig. 2.20 in Chapter 2) is used, this problem is somewhat alleviated. For very large displays there is also the option to drive the gate lines from both left and right side, so that the worst-case RC delay occurs in the center pixels. Twice the number of row drivers will be required. In this configuration, both R and C are reduced by a factor of two, resulting in a 4× reduction in the worst-case RC propagation delay. RC delays on the data buslines are also important, although not as critical for performance as RC delays on the gate lines.

Most large and high-resolution AMLCDs use Al as the busline material for both select and data lines and some use Cu (see Table 6.3).

Al and Cu have a much lower resistivity of around 4 and 2.5 μΩcm, respectively. Unfortunately, pure Al grows hillocks during high-temperature processing such as the PECVD step for the gate nitride and a-Si. This can cause shorts and yield problems. To prevent hillock formation, the Al layer can be anodized, encapsulated, or covered by a cap layer such as Mo or Ti (Fig. 6.39). Alternatively, an Al alloy with, for example, Nd can be used (Fig. 6.39). Since anodization and encapsulation require extra patterning steps, they are used less frequently than cap layers or Al alloys.

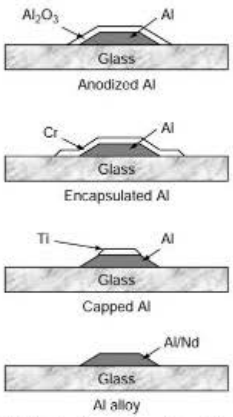

Figure 6.39: Methods to employ Al gate buslines.

Figure 6.40: Photograph of a 57-in. TFT LCD developed by Samsung Electronics.

The largest reported a-Si TFT LCDs are an 82-in. HDTV by Samsung Electronics, a 65-in. HDTV by Sharp and a 57-in. HDTV by Samsung Electronics [10]. The 57-in. display shown in Fig. 6.40 has a resolution of 1080×1920 pixels and utilizes dual-sided row drive to reduce both resistance and capacitance of the select lines by 2× for a reduction in RC delay of 4×. Viewing angle is enhanced by the PVA (patterned vertical alignment) mode. Response time is improved for television applications by overdrive.

The application of large TFT LCDs beyond 30 in. is mostly in enhanced-definition and high-definition television and in digital signage. In both markets they compete with plasma displays.

References

1. W. den Boer, J.Z.Z. Zhong, T. Gu, Y.H. Byun, and M. Friends, "High Aperture TFT LCD Using Polymer Interlevel Dielectric," *Proc. Eurodisplay* '96, pp.53–56 (1996).
2. J.Z.Z. Zhong, W. den Boer, Y.H. Byun, and S.V. Thomsen, "New AMLCD Structure—Color Filter Passivated a-Si TFT," *Proc. Asia Display* '98, pp. 113–116 (1998).

3. B.W. Lee, C. Park, S. Kim, T. Kim, Y. Yang, J. Oh, J. Choi, M. Hong, D. Sokong, and K. Chung, "TFT LCD with RGBW Color System," *SID 2003 Digest*, pp. 1212–1215 (2003).
4. Search the Internet for "3M Optical Films" (with the Vikuity™ trade name)
5. H. Mori and P.J. Bos, "Designing Concepts of the Discotic Negative Birefringence Compensation Films," *SID 1998 Digest*, pp. 830–833 (1998).
6. K. Kondo, K. Kinugawa, N. Konishi, and K. Kawakami, "Wide-Viewing-Angle Displays with In-Plane Switching Mode of Nematic LCs Addressed by 13.3-in. XGA TFTs," *SID 1996 Digest*, pp. 81–84 (1996).
7. Z. Tajima, "IPS Technology Trends," *Asia Display/IMID '04 Digest*, pp. 15–18 (2004).
8. A. Takeda, S. Kataoka, T. Sasaki, H. Chida, H. Tsuda, K. Ohmuro, T. Sasabayashi, Y. Koike, and K. Okamoto, "A Super-High Image Quality Multi-domain Vertical Alignment LCD by New Rubbing-Less Technology," *SID 1998 Digest*, pp. 1077–1080 (1998).
9. K.H. Kim, N.D. Kim, D.G. Kim, S.Y. Kim, J.H. Park, S.S. Seomun, B. Berkeley, and S.S. Kim, "A 57-in. Wide UXGA TFT-LCD for HDTV Application," *SID 2004 Digest*, pp. 106–109 (2004).
10. H. Okumura and H. Fujiwara, "A New Low-Image-Lag Drive Method for Large-Sized LCTVs," *SID Digest 1992*, pp. 601–604 (1992).